PHOTOGRAPHIC FLUID VELOCITY MEASUREMENT IN A HYDROCYCLONE

PHOTOGRAPHIC FLUID VELOCITY MEASUREMENT IN A HYDROCYCLONE

by

Neils Stephen Richard Knowles
B.A.Sc. (U.O.)

A thesis submitted to the Faculty of Graduate Studies in partial fulfilment of the requirements for the degree of Master of Engineering.

McMaster University, Hamilton
March, 1971

McMASTER UNIVERSITY LIBRARY

MASTER OF ENGINEERING (1971) MCMASTER UNIVERSITY

HAMILTON, ONTARIO

TITLE: Photographic Fluid Velocity Measurement in a Hydrocyclone

AUTHOR: Stephen R. Knowles

SUPERVISOR: Professor D.R. Woods

NUMBER OF PAGES: vii, 144

SCOPE AND CONTENTS: The three dimensional flow patterns in a 3 inch diameter hydrocyclone operating without an air core were studied using tracer particles and high speed cine photography. The cyclone was constructed and operated according to present design criteria for the optimum separation of liquid-solid mixtures. Both cyclone geometry and operating conditions were the same throughout all experiments. Analysis of films posed at 55 locations inside the hydrocyclone provided data for 18 velocity profiles which described the three dimensional flow in the hydrocyclone. This data was then checked for consistency by material balance considerations and compared with the results of earlier investigators who operated their cyclones with air cores.

Acknowledgements

I would like to express my thanks to Dr. D.R. Woods for his direction and encouragement throughout this project.

All the technical staff have been most helpful. In particular, I would like to thank Mr. Joseph Newton for his help in designing the optical table and Mr. Uldis Goults for his help with the photography.

Dr. I. Feuerstein, A.J.S. Liem and Dr. K.A. Burrill have contributed many useful suggestions; these are gratefully acknowledged.

Financial assistance from the American Iron and Steel Institute and a scholarship from the National Research Council are sincerely appreciated.

Stephen R. Knowles

Hamilton, March 1971

Table of Contents

Appendicies

List of Tables

List of Figures

List of Figures(continued)

1 Introduction

1.1 Background

A cyclone separates particles or droplets from a liquid or a gas. There are two classes of cyclones: gas and liquid cyclones. In this work liquid cyclones or hydrocyclones are studied although the general term cyclone is often used in this thesis. Hydrocyclones are for separational problems in the steel and chemical industies, for the separation of concentrated mixtures and for the prevention of water pollution.

A side and plan veiw of a typical cyclone is shown in Figure-1. The cyclone is essentially a cone, however the upper section is usually cylindrical to make attachment of the tangential feed pipe simple. The feed fluid is injected at the top of the cyclone body at a tangent to the wall. The fluid spirals down toward the bottom exit or underflow where some fluid leaves the cyclone. Due to inward radial flow, some liquid is transported toward the central axis and an upward spiral carries this fluid out the overflow. The overflow pipe, or vortex finder, protrudes into the cyclone body below the feed pipe. If a density difference exists between particles(or droplets) in the feed and the carrier fluid, these particles will move relative to the fluid due to the high centrifugal forces generated in the cyclone. Heavier particles migrate toward the wall and lighter particles migrate toward the central axis. Heavier and lighter particles leave by the underflow and the overflow respectively. In general, this device can be used to classify or separate particles greater than three microns in diameter.

Hydrocyclones are widely used in industry because of their low initial cost, the small floor area requirements and the absence of moving parts. However, at present, procedures for the design of hydrocyclones are not based

Figure-1

Schematic Representation of Spiral Flow in a Hydrocyclone

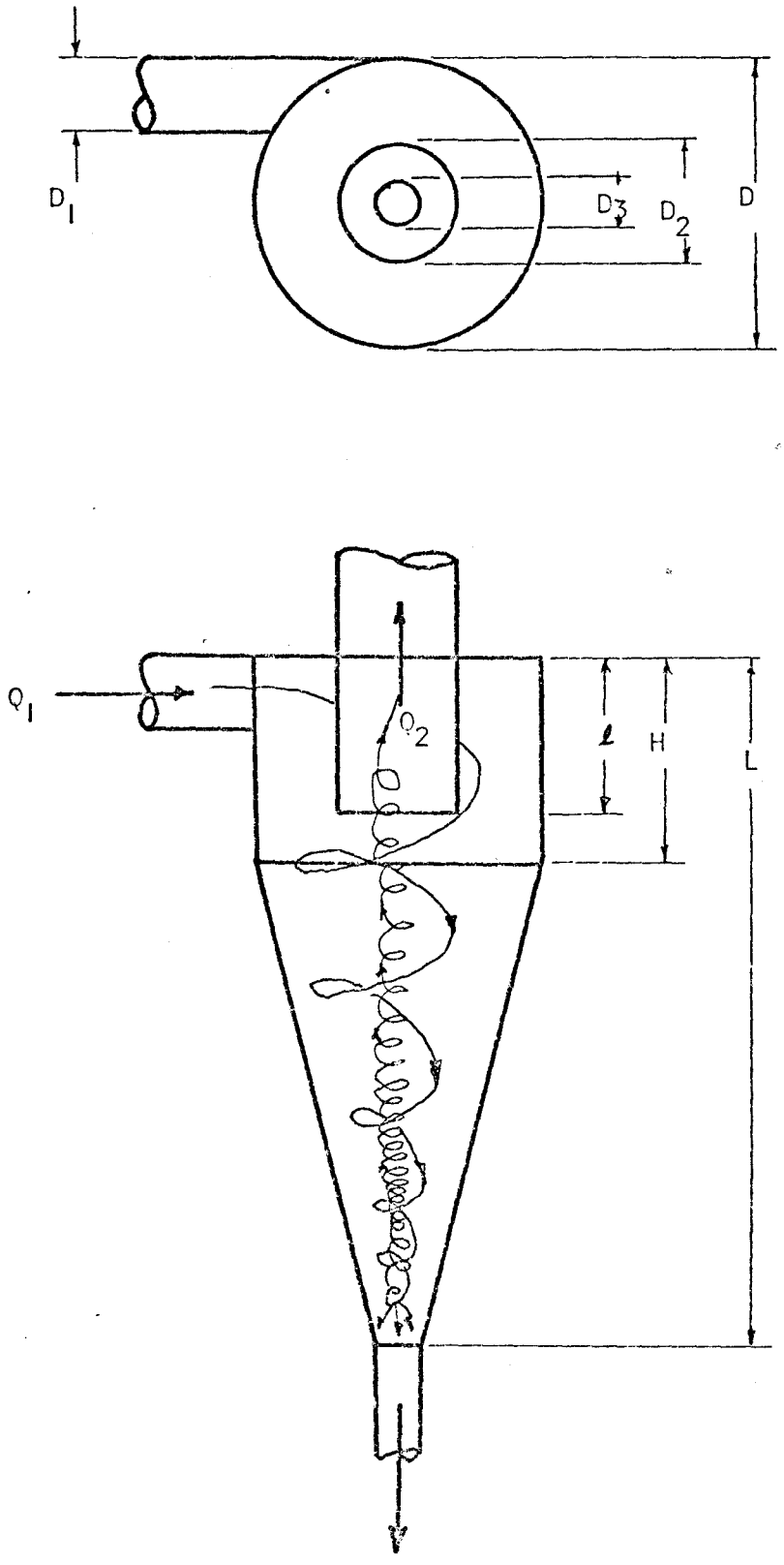

on fundamental concepts but on empirical correlations. The difficulty in obtaining a well designed hydrocyclone is a major drawback in the use of the device.

1.2 Design of Hydrocyclones

Many design procedures have been presented in the open literature. Perhaps the most notable works are those of Bradley[B-2], Kelsall[K-2], Lilge[L-1], Moder and Dahlstrom[M-2], Rietema[R-1] and Yoshioka and Hotta [Y-1]. Some of these design techniques are based on empirical considerations; others on relationships derived from hypothesized separation mechanisms.

The methods are limited by the narrow limits of applicability for each method and discrepancies resulting from the different methods. The effect of a gas(or vacuum) has yet to established quantitatively. There has been a problem in defining cyclone pressure drop and efficiency. The situation is not wholly negative. Many of the design techniques are very useful when applied within the limits for which they were formulated. Clearly, a more unified design approach, applicable over a wide range of operating conditions would be useful.

The purpose of this work is to develop a technique to observe fluid movement inside a hydrocyclone. Based on such knowledge, more generally applicable design techniques can be developed.

1.3 Description of Hydrocyclone Flow Patterns.

In the past, the qualitative description of the flow patterns was based on the work of Kelsall[K-2], Bradley[B-3,B-4], Ohasi and Maeda[O-1] and Fontein[F-2].

The cylindrical co-ordinate system shown in Figure-2 has been adopted because the major part of the cyclone is symmetrical with the central, z-axis. The fluid has three velocity components: the tangential component, v_θ, the axial or vertical component, v_z and the radial component, v_r. Each component

Figure-2

Hydrocyclone Co-ordinate System

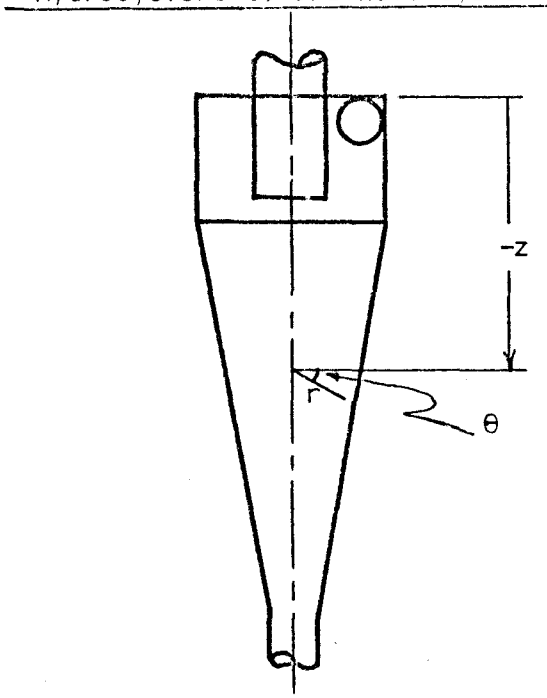

is discussed separately.

1.3.1 The Tangential Velocity Component

Two concentric tangential flow regimes form. Close to the central axis a forced vortex develops. This implies solid body rotation where the tangential velocity varies linearly with the radius. At a radius estimated by Kelsall[K-2] as 0.14R, a free vortex flow regime begins to form. in this region the tangential velocity, v_θ, varies with $1/r^n$, where the constant, n, is less than 1.0. Bradley[B-4] has compiled a table of n values for a wide range of geometries and operating conditions. All values of n are for cyclones operating with an air core.

For a mass to have a tangential velocity, it must rotate about an axis at a finite distance. For this reason, the tangential velocity at the central axis of a cyclone operating without an air core must be zero.

Because there is no slip at a solid-liquid interface, the the tangential velocity at the wall must be zero.

1.3.2 The Radial Velocity Component

Only Kelsall[K-2] and Ohasi and Maeda[O-1] have attempted to measure this velocity component in a hydrocyclone.

Kelsall's numerically derived values suggest that inward radial flow increases uniformly from zero, at the radius of the air core, to a maximum value close to the cyclone wall whereupon it drops to zero at the wall. there is also a suggestion of outward radial flow in the upper reaches of the cyclone where eddy flow may occur. The radial velocity profiles of Ohasi and Maeda suggest that inward and outward radial flow occurs at all levels.

In general, there is clearly ground for further investigation of this flow component. The effect of the radial velocity is most important in describing the mechanism by which particles are assisted or hindered in their radial migration across the cyclone.

1.3.3 The Vertical Velocity Component

The vertical flow patterns in the hydrocyclone are intimately related to the radial flow patterns. The relationship is shown schematically in Figure-3.

There are two axial flow regimes one up and one down. Flow down is considered negative. The two flow regimes suggest that there should be a surface or locus of zero vertical velocity. This has been confirmed by Kelsall [K-2] and Bradley[B-3]. When formulating design relationships, it is important to insure that particles heavier than the carrier fluid migrate to the outside of the surface and lighter particles migrate to the inside of the surface. In this way, heavy particles will leave by the underflow and lighter particles will leave by the overflow. The surface of zero vertical velocity is shown in Figure-3.

Figure-3

Schematic Representation of the Non-Tangential Flow in a Hydrocyclone

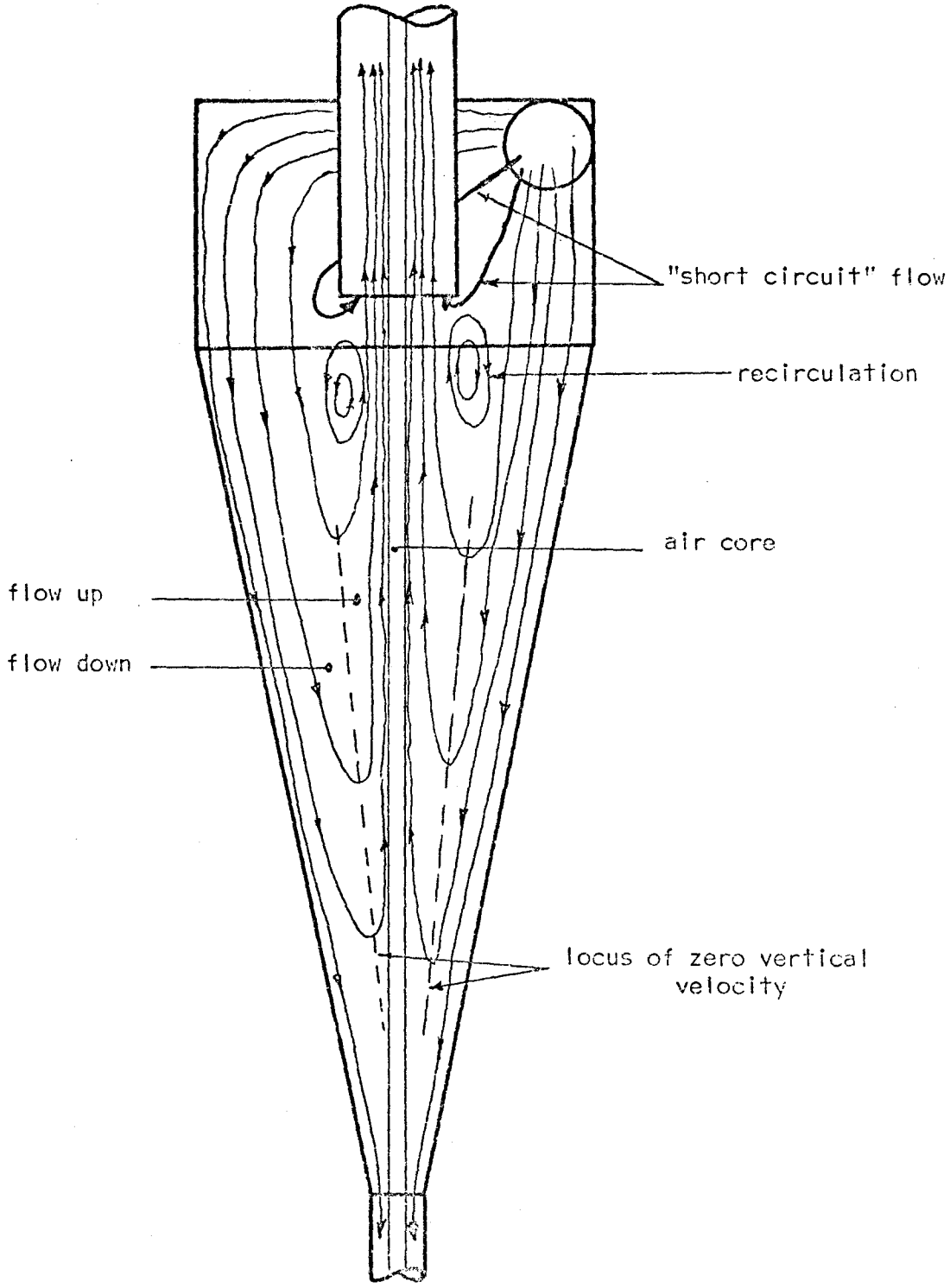

Due to the tangential feed arrangement, liquid spirals down through the cyclone. There is radial flow throughout. Inward radial flow feeds the upward spiralling flow which becomes the overflow. The underflow comes from the remaining portion of the downward stream. This is shown schematically in Figure-3,which also illustrates the possibility of re-circulation due to outward radial flow near the vortex finder.

"Short circuit" flow, indicated by heavy lines in Figure-3 can occur in cyclones. Feed liquid passes by the shortest possible route from the feed port to the vortex finder. This flow should be eliminated if possible or feed material can pass through the cyclone without being subjected to the device's separating power, with a resulting decrease in the net separation.

1.4 Review of Methods of Measuring Fluid Velocity in a Hydrocyclone

Many different methods have been used to measure the fluid velocity and/or its components. Probes or spinning objects have been immersed in the fluid in the hydrocyclone to measure the velocity directly. Some indirect methods include the measurement of the pressure profile along the wall of the cyclone and the optical study of moving particles or dyes.

Table-1 lists the methods and investigators.

1.4.1 Direct Methods

Direct methods have three serious drawbacks. First, they can be used only to measure the tangential velocity, and secondly the insertion of foreign objects causes an irreversible friction loss at the point of measurement, the effect of which on the fluid velocity is difficult to estimate. Finally, the use of spinning balls or rotating vanes requires very difficult experimental design and construction, and the presence of a gas core.

Table-I

Hydrocyclone Studies Involving Fluid Velocity Measurements

Direct Methods			
Investigator	Technique	Cyclone Geometry*	Reference
Baldina	pitot tube	cylindrical	B-1
Bradley	spinners	conventional	B-5
Fontein & Dijksman	rotating vanes	conventional	F-1
Kearsey & Hibberts	rotating vanes	cylindrical	K-1
Lilge	pitot tube	conventional	L-1
Peebles & Garber	pitot tube	spherical	P-1
Wilson	spinners	cylindrical	W-1
Yoshioka & Hotta	pitot tube	conventional	Y-1
Indirect Methods			
Bradley & Pulling	photography, dyes	conventional	B-3
Bradley & Pulling	pressure along wall	conventional	B-3
Kelsall	particle movement, microscopy	conventional	K-2
Ohasi & Maeda	particle movement, photography	conventional	O-1
Saito & Ito	particle movement, photography	cylindrical vortex chamber	S-1

*  conventional,  cylindrical,  spherical

1.4.2 Indirect or Tracer Methods

Bradley and Pulling[B-3] used the external pressure profile along the cyclone wall to infer the internal conditions.

Ohasi and Maeda[O-1] used a multiple exposure technique to follow the movement of perspex spheres(density 1.03 gm/cc) in water inside a 3.1 inch diameter cyclone operating with an air core. Tangential, vertical and radial velocities were measured for various geometries and flow arrangements.

Saito and Ito[S-1], using conventional cine photography, followed the movement of five millimetre gypsum and beeswax balls(density≈1.00 gm/cc) in a simple open vortex chamber. Only tangential velocities were measured.

Kelsall[K-2] viewed alumina particles(density 2.70 gm/cc) moving in a 3.0 inch diameter hydrocyclone operating with an air core by means of a microscope equipped with two rotating objective lenses. Only tangential and vertical velocities were measured. The particles were assumed to move identically with the water except in the radial direction. For this reason, radial velocities were calculated from continuity considerations.Kelsall used a longer vortex finder and larger cone angle than those recommended by later works[R-1,Y-1,B-3,H-1]. This does not affect the validity of his results, determined over a wide range of geometries, feed rates and flow splits, but rather their applicability.

With tracer techniques, the three velocity components can be measured without disturbing the cyclone flow patterns. The choice of tracer particles must be made with care.

1.5 Objectives of the Present Study

In summary, no work has been published in the open literature

on the velocity profiles within hydrocyclones operating without an air core. Such conditions are important for industrial applications.

The most attractive experimental technique is the photographic study of the three velocity components of a tracer. The tracer is selected so that it behaves like the fluid.

The objectives of the present study were:

(i) To develop the necessary photographic and tracer techniques and equipment for the indirect measurement of the three components of fluid velocity within a hydrocyclone. The cyclone would be designed based on the present design criteria for the optimum separation of liquid-solid systems. The design procedures are based on data collected from systems operating with an air core.

(ii) To measure the velocity distribution for one set of operating conditions.

(iii) To compare these results with those for operation with an air core.

2 Exnerimental Approach

2.1 Theoretical Considerations

In this work small droplets of an immiscible liquid are injected into the fluid and viewed from two mutually perpendicular directions. The motion is then recorded with high speed cine photography. The films of the droplet movement are analyzed to determine the tangential, vertical and radial velocity components of the droplets. A macroscopic material balance can be used as a consistency check on the data.

It would be ideal if the movement of a small parcel of fluid inside the hydrocyclone could be observed. However, if this small fluid parcel is replaced by adroplet of an immiscible liquid having the same density as the continuous phase and the refractive indicies differ sufficiently so that the two phases are visually distinguishable, then the small fluid parcel can be observed. The droplets will be referred to as tracer or marker particles.

For this study, water and anisole($C_6H_5OCH_3$) were chosen as the continuous and dispersed phases respectively. Anisole was dyed red by adding 0.2%(by weight) Flaming Red oil-soluble dye. This was done to increase the contrast for photographic work. Physical and optical properties of the two liquids are summarized in Table-2.

Consider now the resolution of the individual velocity components. If an object, moving in three dimensional space, is viewed from two mutually perpendicular directions, each view shows the projections of two velocity components. In this way, four projections of velocity components can be seen. One of the velocity components will be the same in each view.

Table-2

Density and Refractive Index of Anisole and Water

	anisole	water	temperature (^{o}C)	reference
density (gm/cc)	0.99327	0.99823	20	I-1, P-2
refractive index	1.51791	1.33299	20	H-2

Invariably, the path of a droplet inside the hydrocyclone is a vertical spiral about the central axis. The viewing directions used in this work define a horizontal plane as shown in Figure-4. One view shows the droplets moving horizontally and vertically while the other view shows the droplet spiralling up or down about the central axis.

The resolution of tangential and vertical components of velocity from view A is straightforward. The vertical velocity can be measured simply from recordings of droplet movement in view B while measurement of the radial velocity from this view is more complicated.

Two methods of calculating the radial velocity from view B recordings were developed. The first method involves using tangential velocity data determined from view A recordings, while the second method gives values of the radial velocity which are not dependent on previous measurements.

The approach in the first method is illustrated in Figure-5, which shows a plan view of a droplet moving in the cyclone. Timing is known from measuring the film speed. The distance of importance is $(r-r_2)$. If it assumed that v_θ is constant over a short arc length , then r_2 can be calculated from the relationship,

$$r_2=[(r-d_2)^2+(v_\theta \Delta t)^2]^{\frac{1}{2}}. \qquad (1)$$

The radial velocity is

$$v_r=\frac{(r-r_2)}{\Delta t}. \qquad (2)$$

Inward radial velocity is considered positive to follow the convention of earlier workers. Combinations of equations (1) and (2) gives

$$v_r=\frac{r-[(r-d_2)^2+(v_\theta \Delta t)^2]^{\frac{1}{2}}}{\Delta t}. \qquad (3)$$

This method was not used because:

(i) Values of v_θ, which are subject to experimental er-

Figure-4

Viewing Droplet Movement in the Hydrocyclone

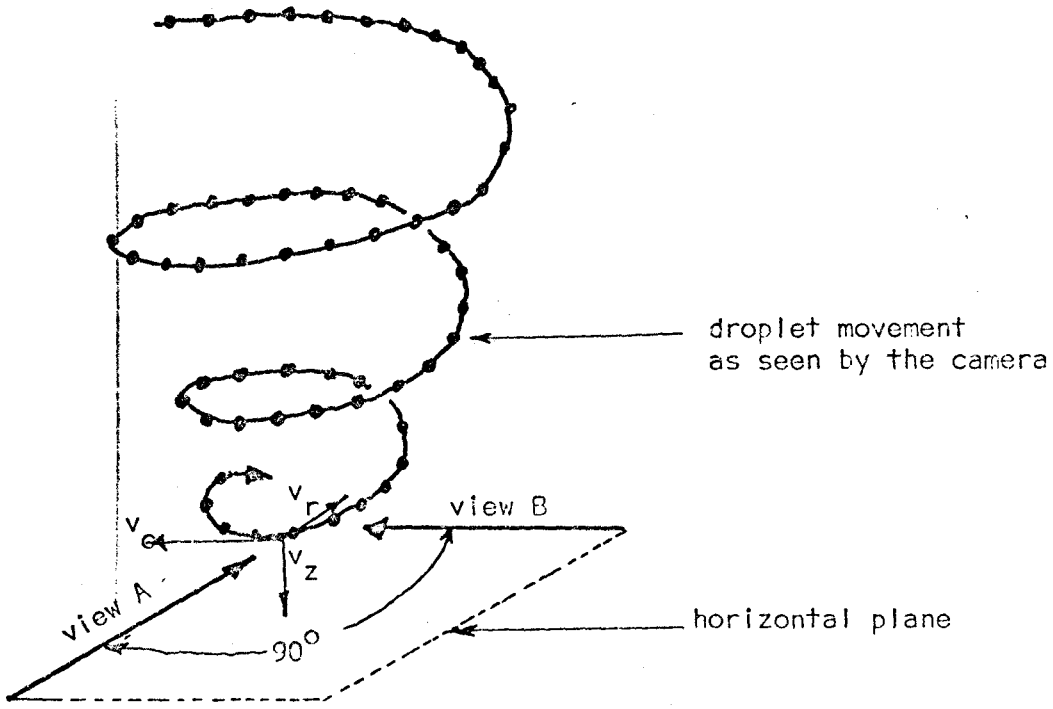

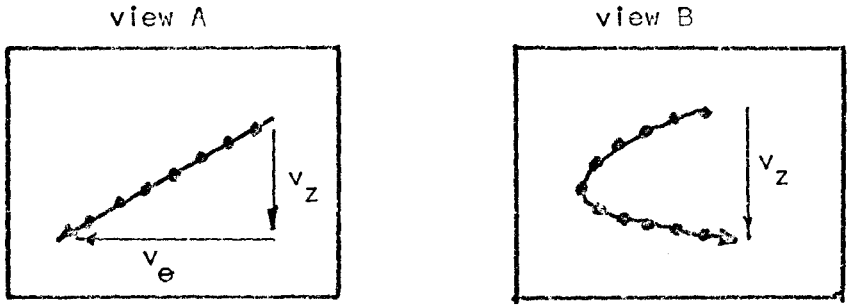

Figure-5

First Method of Measuring Radial Velocities

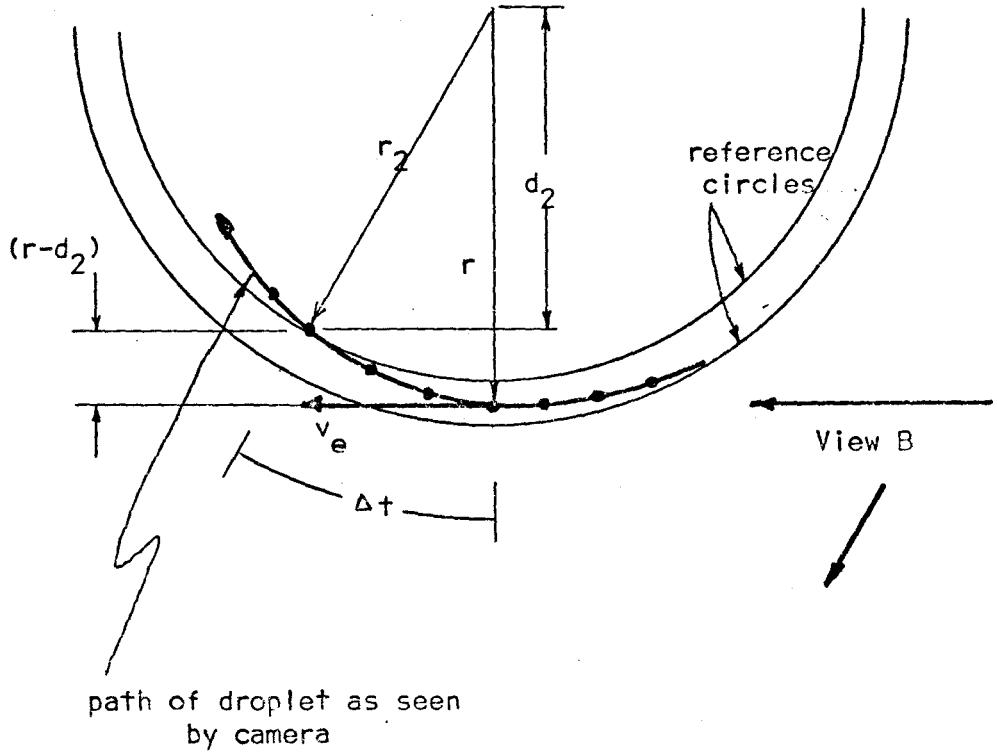

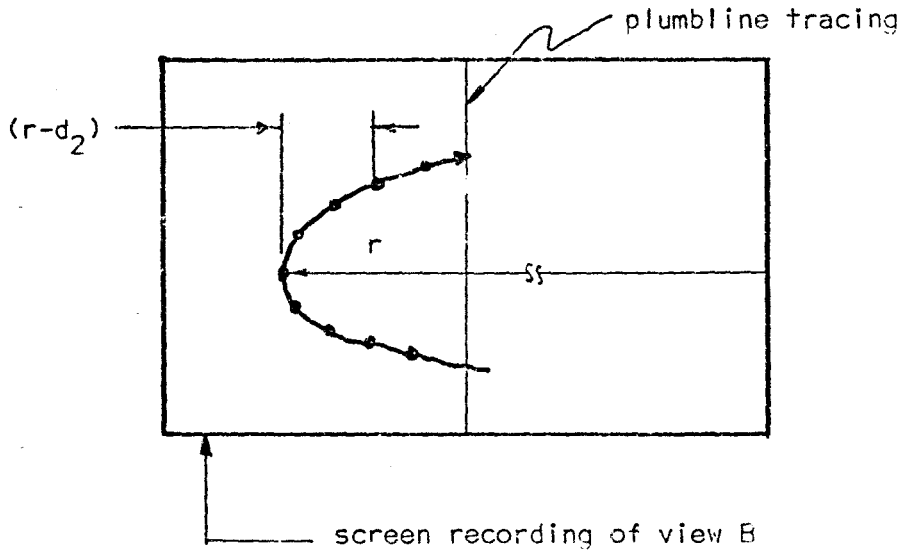

ror, had to be used which compound the total possible error in v_r.

(ii) Values of v_θ had to be interpolated often.

(iii) Unreasonable values of v_r were calculated close to the central axis.

The second method is illustrated in Figure-6. As before, timing is determined from measuring the film speed. If it is assumed that the vertical velocity is constant over a short vertical distance, then the vertical dispalcement about the "r" position is equal for equal short time intervals (or equal numbers of frames as film speed is constant over about 50 frames). Using this criterion the projected radius difference, (d_1-d_2) can be measured, and the angles, θ_1 and θ_2 set equal.

The distance required is (r_1-r_2). From an inspection of the three similar triangles in Figure-6, it can be seen that if

$$\theta = \theta_1 = \theta_2, \qquad \text{----------(4)}$$

then

$$\cos\theta = \frac{d_1}{r_1} = \frac{d_2}{r_2}, \qquad \text{----------(5)}$$

so that

$$r_1 - r_2 = \frac{d_1 - d_2}{\cos\theta}. \qquad \text{----------(6)}$$

Since only r is known and the total arc length considered is very small, $\cos\theta$ is estimated as

$$\cos\theta \approx \frac{(d_1+d_2)/2}{r} = \frac{\bar{d}}{r}. \qquad \text{----------(7)}$$

Thus,

$$v_r = \frac{r_1 - r_2}{\Delta t} \approx \left[\frac{d_1 - d_2}{\Delta t \bar{d}}\right] . r. \qquad \text{----------(8)}$$

In order to estimate the error in using equation (8), the values of $\bar{d}/r$ were calculated for each value of v_r. The values were observed to

Figure-6

Second Method of Measuring Radial Velocities

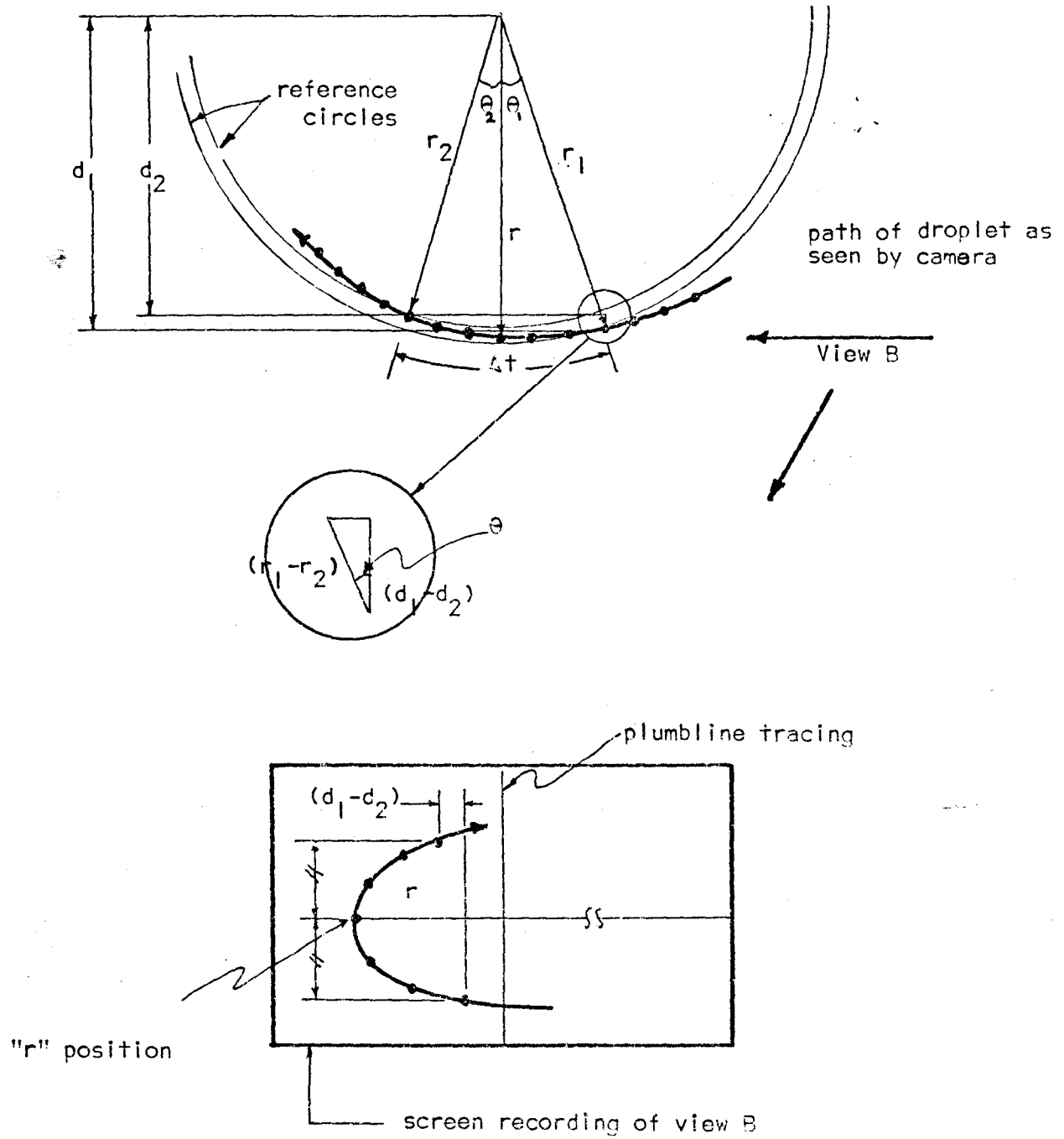

approach 1.0 within 5 per cent. In other words, there is only a small error involved in assuming that (d_1-d_2) is equal to (r_1-r_2).

The latter method(equation (8)) gave more reasonable values of v_r toward the central axis and had the advantage of requiring no previous data. This method was used to calculate all radial velocities in this study.

More details of film analysis and the calculations involved are in the appendix, section A3.1.

The material balance can be used to check the consistency of the data. External and internal material balances are shown in Figure-7. The overall material balance using envelope 1, is

$$Q_1 = Q_2 + Q_3. \text{----------(9)}$$

Quantities Q_1 and Q_2 are obtained from calibrated flow meters, hence Q_3 is also known. A material balance around envelope 2 yields the relationship,

$$Q_1 + Q_2 = Q_1' + Q_2' \text{ .----------(10)}$$

The net flow down, Q_3, is constant throughout the cyclone. Q_1' and Q_2' can be calculated by an integration of a vertical velocity profile. Q_3 is then calculated and compared with the actual value.

Figure-8 illustrates how the vertical velocity profiles can be used to calculate Q_1' and Q_2'. The flow up, Q_2' is

$$Q_2' = \int_0^{R'} 2\pi r v_z dr, \text{----------(11)}$$

and the flow down, Q_1' is

$$Q_1' = \int_{R'}^{R_w} 2\pi r v_z dr. \text{----------(12)}$$

Figure-7

Hydrocyclone Material Balances

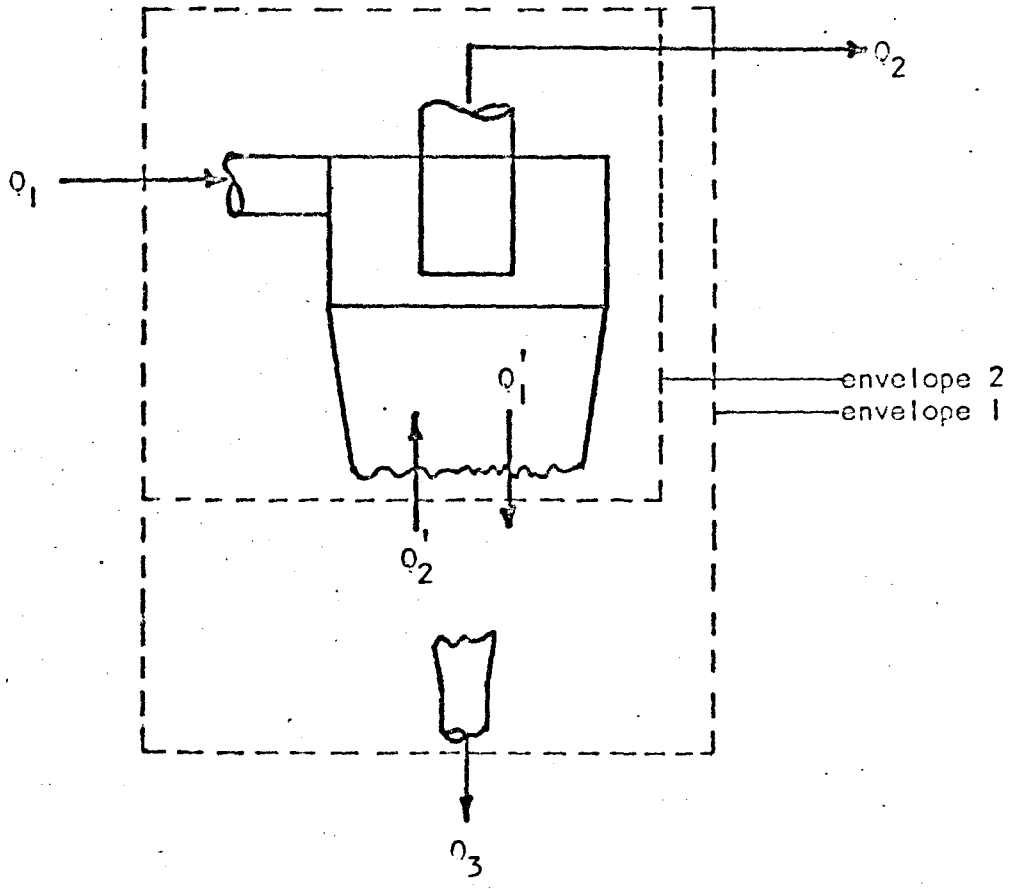

Figure-8

Integration of a Vertical Velocity Profile

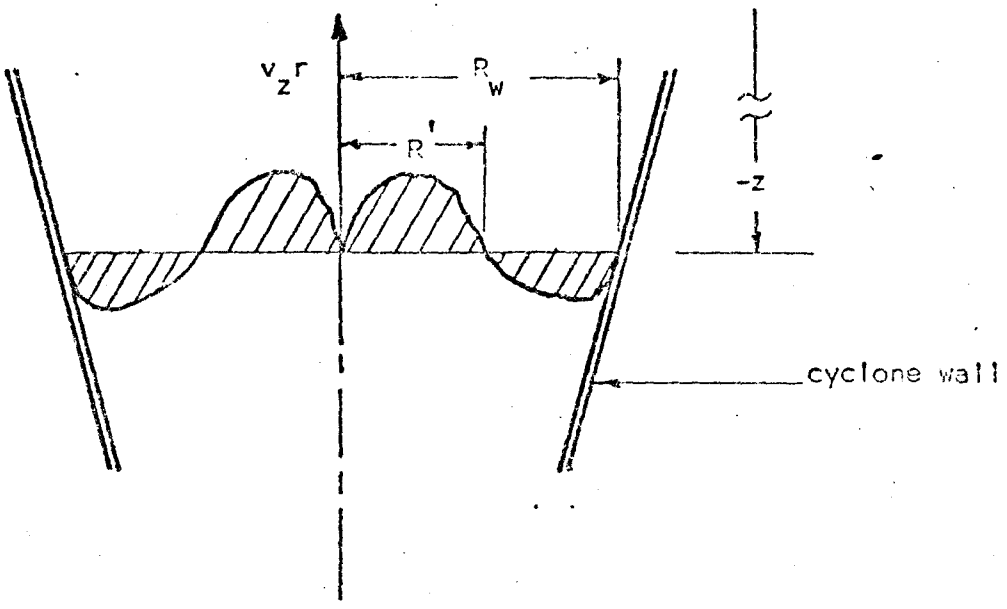

R' is the radius at which the vertical velocity is zero and R_w is the wall radius at the elevation considered. Equations (11) and (12) are only applied at levels below the vortex finder. In this region, the vertical velocity is assumed to be symmetric about the central axis. At levels above the vortex finder, several velocity profiles,at different angular positions would be required to integrate correctly.

Thus, if the calculated net flow based on vertical velocity measurements does not agree with the actual underflow, Q_3, within $\pm$ 10 per cent, then the velocity measurements are incorrect. The tolerance of $\pm$ 10 per cent is based on the accuracy of overall flow measurements.

2.2 Equipment Design, Construction and Operation

The equipment employed in this work can be divided into four categories: the hydrocyclone, the peripheral flow system, the optical arrangement and the high speed cine camera. The procedures for operating the above equipment and for analyzing the final films are also discussed.

2.2.1 The Hydrocyclone

The cyclone geometry was based on design procedures recommended by Rietema[R-1] together with the suggestions of Bradley and Pulling[B-3] for the diameter of the underflow and Haas et al[H-1] for the cylinder height. The internal cyclone diameter chosen was 3 inches. This size cyclone is common in industrial practice and also allows easy comparison with the results of Kelsall[K-2] and Ohasi and Maeda[O-1].

The actual dimensions of the cyclone used in this study are shown in Figure-9. For safety, the cyclone was constructed of thick-wall glass throughout. The inlet and over flow pipe were tapered to allow coupling with metal fittings employing teflon seals. The geometries used in this study study and those used by Kelsall and Ohasi and Maeda are summarized in

Figure-9

Cyclone Dimensions *

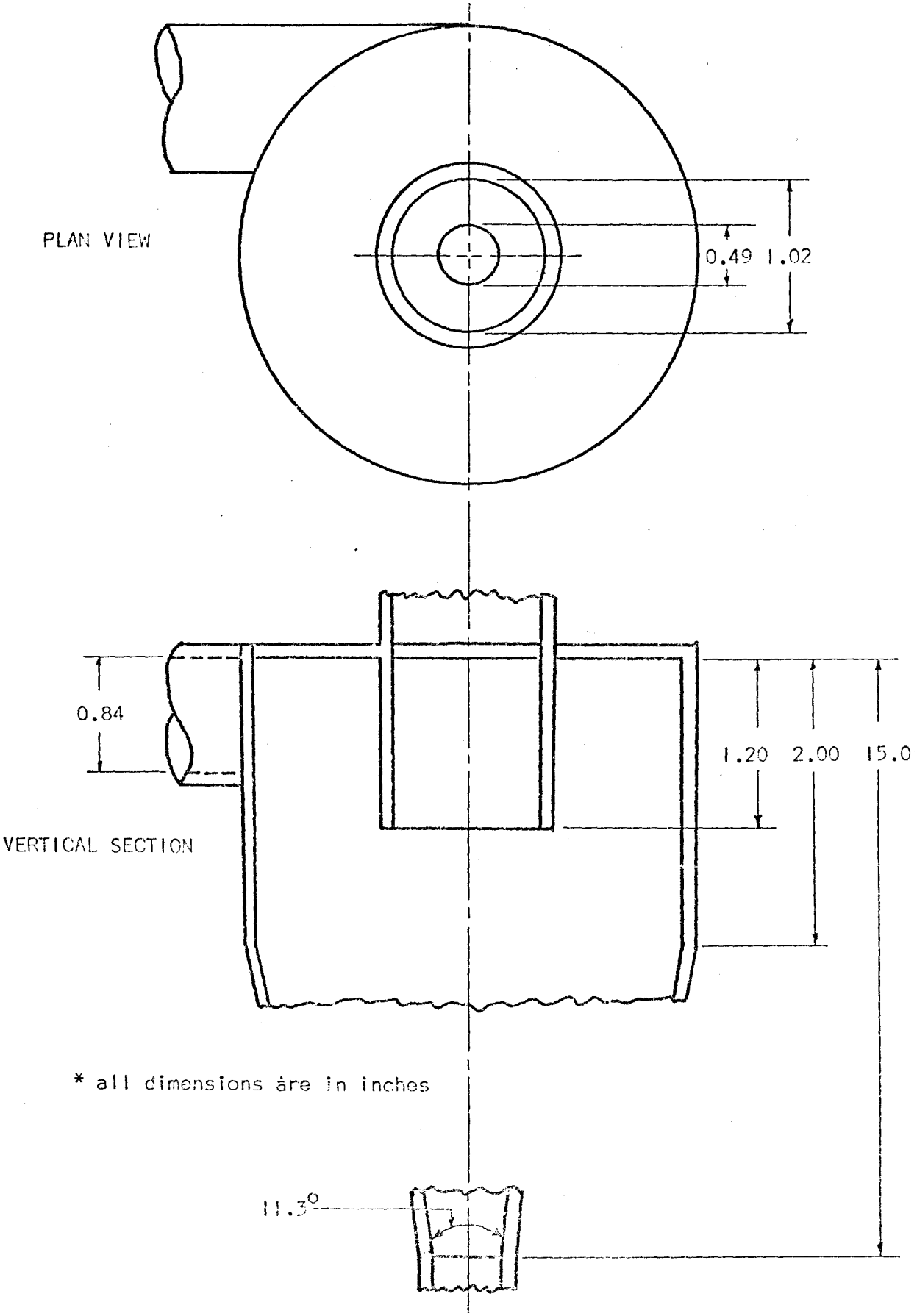

* all dimensions are in inches

Table-3.

The operating conditions selected for this study, as well as those used by Kelsall and Ohasi and Maeda are listed in Table-4. The operating conditions were chosen to be within the range of the velocity measuring technique and of industrial practice. Details of the selection of operating conditions are given in the appendix, section A1.3.

2.2.2 The Peripheral Flow System

The peripheral flow system is shown in Figure-10. The reservoir supplies two centrifugal pumps in parallel with the cyclone. Anisole is injected from a pressure reservoir into the feed pipe where the turbulence disperses this immiscible fluid. The overflow is recycled and the underflow drained. The make-up water feed rate is set equal to the underflow rate to maintain steady state.

Flowrates and pressures were measured on calibrated rotameters and pressures gauges, respectively. The underflow rate was checked by weighing an amount of water collected in a known time.

2.2.3 The Optical Arrangement

A small volume inside the hydrocyclone is viewed from two mutually perpendicular directions, so that the three velocity components can be resolved.

Figure-11 shows the optical arrangement. Two concentrated arc lamps were matched by eye to give equal intensity, by using a variable transformer on one of the lamp power supplies. Converging lenses and collimators gave two narrow beams of parallel light which produced the two silhouetted views of droplets moving in the hydrocyclone. The light was then directed by prisms to a half-silvered mirror which superimposes the two views and transmits then to the high speed cine camera. A half-silver-

Table-3

Comparison of Cyclone Geometries

Dimension	This Study	Kelsall*	Ohasi and Maeda*
D (in.)	3.00	3.00	3.1
D_1	0.28D	0.21D	0.24D
D_2	0.34D	0.17D	0.32D
D_3	0.16D	0.17D	0.076D
ℓ	0.40D	1.33D	0.75D
H	0.67D**	?	1.96D
L	5D	2.8D***	4.84D***
θ (degrees)	11.3	20	15.3
feed entry 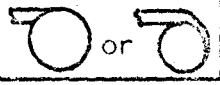			

*The geometries of Kelsall and Ohasi and Maeda listed above are those which are closest to the geometry used in this study and for which there is velocity profile data available in the open literature.

**A value of 0.5D was the suggested optimum but the value above was required for glass blowing.

***Estimated value.

Table-4

Comparison of Operating Conditions

Quantity	This Study	Kelsall*	Ohasi and Maeda*
Q_1 (USGPM)	7.5	15.8	17.3
Q_2 (USGPM)	6.0	7.0	14.4
Q_3 (USGPM)	1.5	8.8	2.9
P_1 (PSIG)	15.7	40	14.4
P_2 (PSIG)	10.5	?	?
P_3 (PSIG)	11.9	?	?
$\langle v_\theta \rangle_1$ (FEET/SEC)	4.34	25.9	9.67
$\langle v_z \rangle_2$ (FEET/SEC)	2.37	11.5	5.90
Air Core (YES or NO)	NO	YES	YES
Temperature (^{o}C)	18	?	?

* The operating conditions of Kelsall and Ohasi and Maeda listed above are those which are closest to those used in this study and for which there is velocity profile data available in the open literature.

Figure-10

Peripheral Flow System

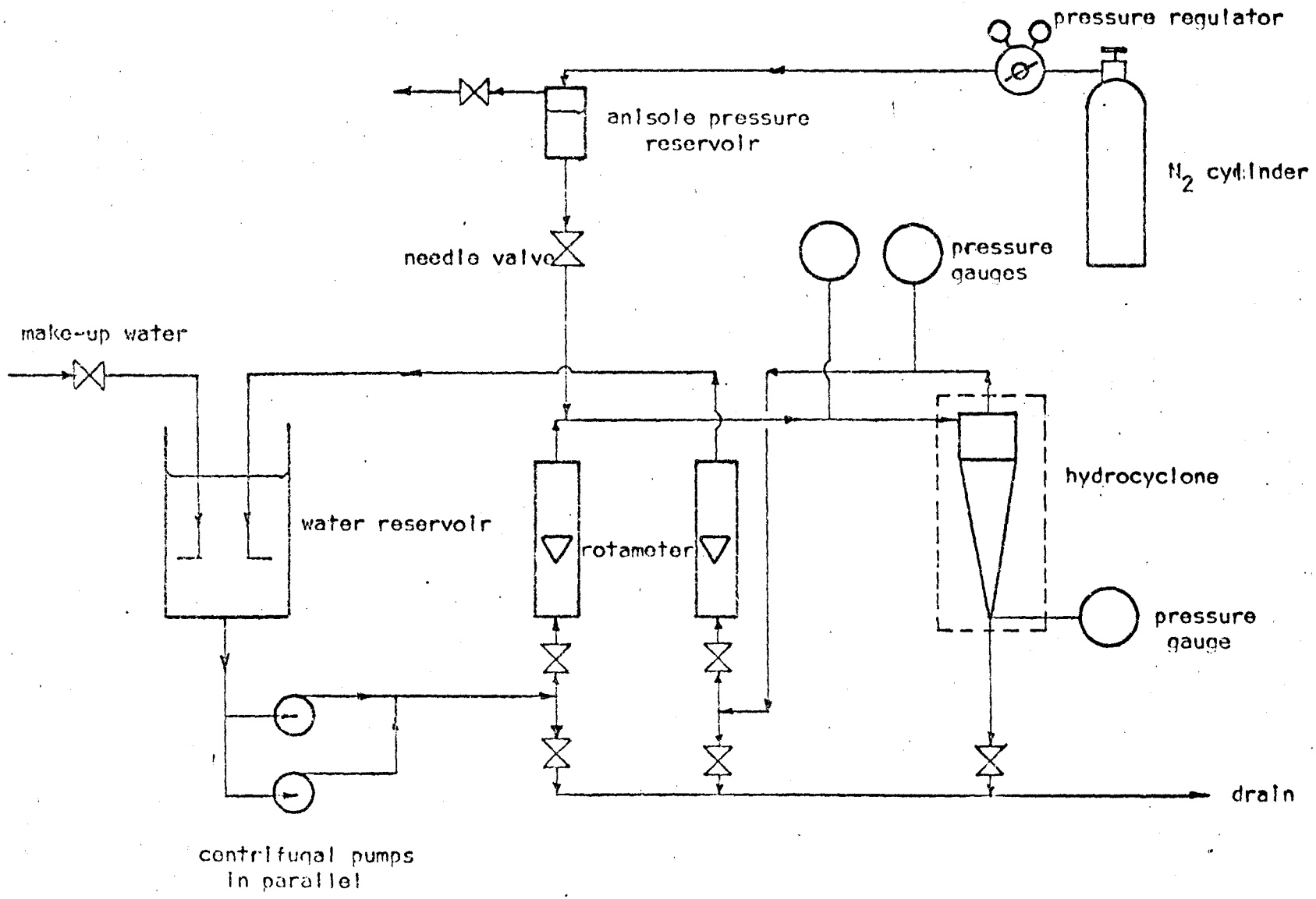

Figure-11

Schematic Optical Arrangement

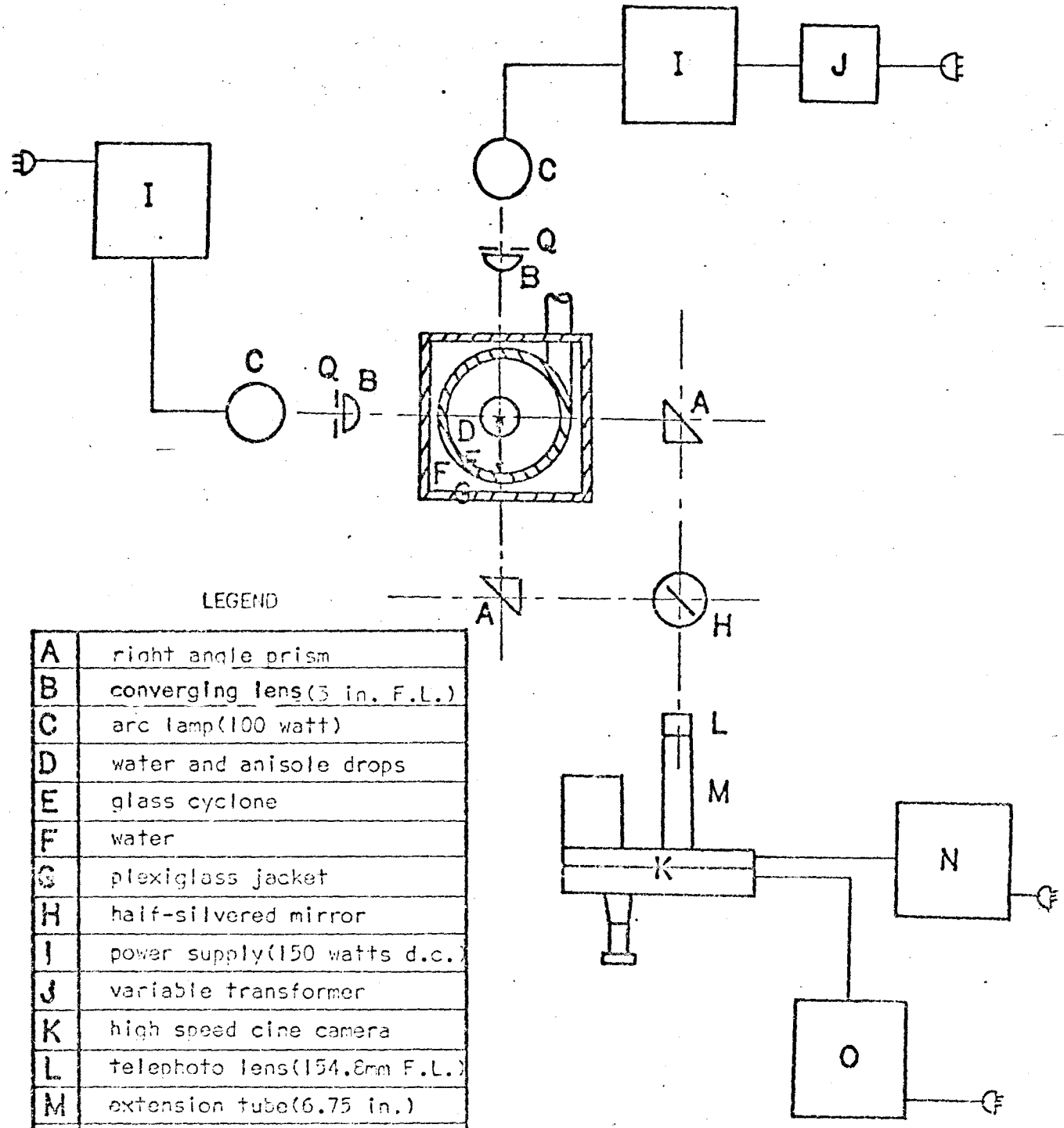

LEGEND

A	right angle prism
B	converging lens(3 in. F.L.)
C	arc lamp(100 watt)
D	water and anisole drops
E	glass cyclone
F	water
G	plexiglass jacket
H	half-silvered mirror
I	power supply(150 watts d.c.)
J	variable transformer
K	high speed cine camera
L	telephoto lens(154.8mm F.L.)
M	extension tube(6.75 in.)
N	pulse generator
O	power supply(a.c.)
P	plane of study
Q	collimator

ed mirror reflects half the incident light while the remaining half is transmitted in the incident direction.

In Figure-II, the cyclone is shown with a transparent jacket. This machined plexiglass jacket, enclosing the cyclone, is filled with water. The presence of the water reduces the distortion due to the curved surface of the cyclone. The surfaces of the jacket presented to incident parallel light are flat and perpendicular to the light's direction, eliminating distortion at this interface. Since water is on both sides of the cyclone wall, distortion due to the curved wall of the cyclone is lateral, that is, light is shifted horizontally but not obliquely. Some oblique distortion is enevitable in view B as the focal plane moves close to the cyclone wall.

The lamps, lenses, collimators, prisms, the half-silvered mirror and the camera were attached to a steel plate machined to a tolerance of $\pm$ 0.0005 inch. This plate could be moved vertically and horizontally relative to the jacketted cyclone. Horizontal(radial) measurements were made using a sliding scale arrangement accurate to $\pm$ 0.01 inch. Vertical measurements were made with a leveled cathetometer accurate to $\pm$ 0.005 cm.

The plane of investigation, shown in Figure-II, was chosen for two reasons. First, throughout most of the cyclone body the flow can be assumed to be axi-symmetric so that point fluid velocities measured on any r-z plane can be assumed identical. This assumption can be verified. Second, provision for a third direction of movement presents many constructional difficulties.

The cyclone was mounted on a large, angle steel table equipped with leveling screws. The table was leveled prior to cyclone installation.

Then, the jacketted cyclone was mounted on the table and a 0.003 inch thick copper plumb line was hung through the overflow and underflow pipes and the cyclone's position adjusted until the plumbline was suspended through the center of each outlet pipe. This procedure ensured that the central axis of the cyclone was vertical.

All devices used for viewing the system were aligned and fixed in position. The arc lamps, which are effectively point light sources, were positioned one focal length away from the lenses. The lenses' flat faces were set parallel to the face of the cyclone jacket using a machinist's square. The prisms' faces were also set parallel to the face of the cyclone jacket in the same way. The camera was subsequently positioned on the centerline of the half-silvered mirror at the focal length of the lens—extension tube arrangement and a plumbline hung co-incident with the cyclone's central axis. Then, viewing through the camera's eyepiece, the half-silvered mirror was rotated until both images were superimposed. The mirror was then fixed in position.

A detailed drawing of the optical table, showing the mechanical details and actual dimensions, appears in the appendix, section A1.2.

2.2.4 High Speed Photography

A rotating prism cine camera(Hycam model number K20S1BE) with a maximum exposure rate of 36,000 quarter frames per second was used. A speed of approximately 20,000 quarter frames per second was used throughout all the experimental runs.

The shutter speed at the selected exposure rate is 1/50,000 of a second. This shutter speed required 400ASA Eastman Kodak 4-X Negative type 7224 16 mm film(in 100 ft. rolls). Concentrated arc lamps(Sylvania K100 d.c.) were selected as light sources.

Since the camera accelerated to the desired speed relatively slowly, true film speed was established by using a calibrated pulse generator which powered a small neon bulb in the camera. The bulb puts tiny dots or blips of light on the film; the time between each is known from the frequency of the pulse generator, which was set at 1,000 cycles per second throughout all runs. The acceleration characteristics of the camera, provided by the manufacturer, are included in the appendix, section A4.4.

Various lens-extension tube arrangements were tried to reduce the depth of field as much as possible. The arrangement shown in Figure-11 was finally selected and the depth of field estimated as 2 to 3 mm. The implications of this are discussed later in section 3.2.

2.2.5 Experimental Procedure

The discussion below is, of necessity, general. Details are given in the appendix, section A2.1. In this section all the positions at which rolls of film were exposed are tabulated.

An experimental run is defined as a number of films exposed at various radial positions at one vertical elevation. Six runs were carried out.

To conduct a run, the optical plate was placed at the desired elevation and the vertical distance from the inside top of the cyclone to the center of the camera lens was measured with the leveled cathetometer. The plumbline was then hung through the cyclone and adjusted until it was co-incident with the cyclone central axis. The optical plate was then moved radially until, viewing through the camera, the two images were exactly superimposed. The scale reading was then taken for later radial positioning. The plumbline was susequently photographed from each direction, separately. One 100 ft. roll of film was sufficient for this if the film speed was maintained at about 5,000 quarter frames per second.

The plumbline was then withdrawn and the cyclone coupled into the flow system. The operating conditions mentioned previously were set and the entire system allowed to run for approximately 15 minutes. The temperature in the reservoir and the feed, overflow and underflow pressures were recorded. Then, a small amount of dyed anisole, sufficient so that it could just be seen with the naked eye, was injected continuously. Rolls of film were then exposed at various predetermined radial positions. At the end of a run the underflow rate was checked by collecting and weighing an amount of water colected in a known time.

A list of the filming positions used in this project's six runs is given in Table- 5.

2.2.6 Film Analysis

The movement of anisole droplets in the cyclone was recorded on tracing paper attached to a backprojection screen. Details of the backprojection apparatus are in the appendix, section A1.2.

By photographing a rotating scale hung on the cyclone's central axis, droplet movement in the cyclone could be related to image movement on the screen. Details of the calibration are in the appendix, section A4.1.

Image velocity on the screen was determined by counting the number of frames between timing dots. Angle measurements could be made using the tracing of the plumbline as a reference.

The films were analyzed for droplet movement in view A to determine tangential and vertical velocities. The films were then reanalyzed to record droplet movement in view B so that vertical and radial velocities could be calculated.

The entire detailed analysis procedure and the calculations for reducing screen data to the final velocities is given in the appendix, sections A2.2 and A3.1.

Table-5

Filming Positions Inside the Hydrocyclone

z (in.)	r (in.)	z (in.)	r (in.)	z (in.)	r (in.)
-1.00	0.64 0.80 1.00 1.20 1.40 1.50*	-1.51	0.10 0.20 0.30 0.30** 0.50 0.70 0.70** 0.90 1.10 1.30 1.30** 1.50*	-2.02	0.05 0.10 0.17 0.20 0.30 0.50 0.75 1.00 1.33 1.45 1.50*
z (in.)	r (in.)	z (in.)	r (in.)	z (in.)	r (in.)
-2.49	0.10 0.20 0.30 0.50 0.75 1.00 1.25	-3.00	0.05 0.10 0.15 0.20 0.25 0.50 1.00 1.25 1.35 1.40*	-3.51	0.05 0.10 0.15 0.25 0.50 0.75 1.00 1.25 1.35*

* wall radius

** replicates for reproducibility study

3. Results and Discussion

From the 55 rolls of film recording the movement of anisole droplets in the cyclone at various points, 18 velocity profiles have been prepared, depicting the flow patterns near the vortex finder in a hyrdocyclone operating without an air core.

3.1 Comparison of the Results with those of Kelsall and Ohasi and Maeda

The results of this study and those of the above-mentioned investigators were put in dimensionless form to provide a simple basis for comparison.

The following dimensionless quantities were defined:

$$r^+ = \frac{r}{R} \qquad \text{----------(13)}$$

$$z^+ = \frac{z}{L} \qquad \text{----------(14)}$$

$$v_\theta^+ = \frac{v_\theta}{\langle v_\theta \rangle_i} \qquad \text{----------(15)}$$

$$v_z^+ = \frac{v_z}{\langle v_z \rangle_2} \qquad \text{----------(16)}$$

$$v_r^+ = \frac{v_r}{\langle v_\theta \rangle_i} \qquad \text{----------(17)}$$

The average inlet velocity $\langle v_\theta \rangle_i$ and the average velocity in the overflow pipe have been chosen to calculate v_θ^+, v_z^+ and v_r^+. Quantities R,L, $\langle v_\theta \rangle_i$ and $\langle v_z \rangle_2$ can befound in Tables-3 and 4.

Before comparing the results of the three studies, the overall differences in operation and investigation should be made clear.

In this study, no air core was allowed to form because of back pressure maintained at both underflow and overflow. Investigation was concentrated in the region near the vortex finder as this region had not been

considered in detail experimentally. Kelsall worked with an air core produced by free discharge of the underflow. Also, the vortex finder was unusually long. He did this to stabilize the flow. Investigation as in the case of Ohasi and Maeda, was directed toward the cyclone as a whole. Ohasi and Maeda unlike Kelsall, used a flooded underflow which produced air cores of much smaller diameter.

Comparison of the various works is considered possible. The inlet Reynolds number in this work was 2.7×10^4 while Kelsall's was 7×10^4 and Ohasi and Maeda's value was 6×10^4. The proximity of these values indicates comparison of the various results is reasonable. Also, Kelsall's large number of results showed that they were relatively independent of total pressure drop and flow split so that comparison of his results with those of this study is possible. The fact that Ohasi and Maeda's pressure drop and flow split were close to those in this work is another justification for comparison of their results with those of this study.

The tangential velocities shown in Figure-12 indicate that the transition from forced to free vortex is not so well marked in a cyclone operating without an air core. The extent of tangential velocity fall-off with radius is not as great as with cyclones operating with an air core. This is also reflected in the values of n determined by fitting each worker's results to the relationship,

$$v_e = K/r^n, \qquad (18)$$

which has been proposed for free vortex flow in a hydrocyclone. The relationship has no fundamental basis only empirical. In this study n was determined to be 0.122, 0.229, 0.334, 0.300 and 0.217 at the levels of z^+ equal to -0.101, -0.134, -0.166, -0.200 and -0.234 respectively. Kelsall and Ohasi and Maeda found (average) values of n of 0.77 and 0.74

Figure-12

COMPARISON OF TANGENTIAL VELOCITY PROFILES

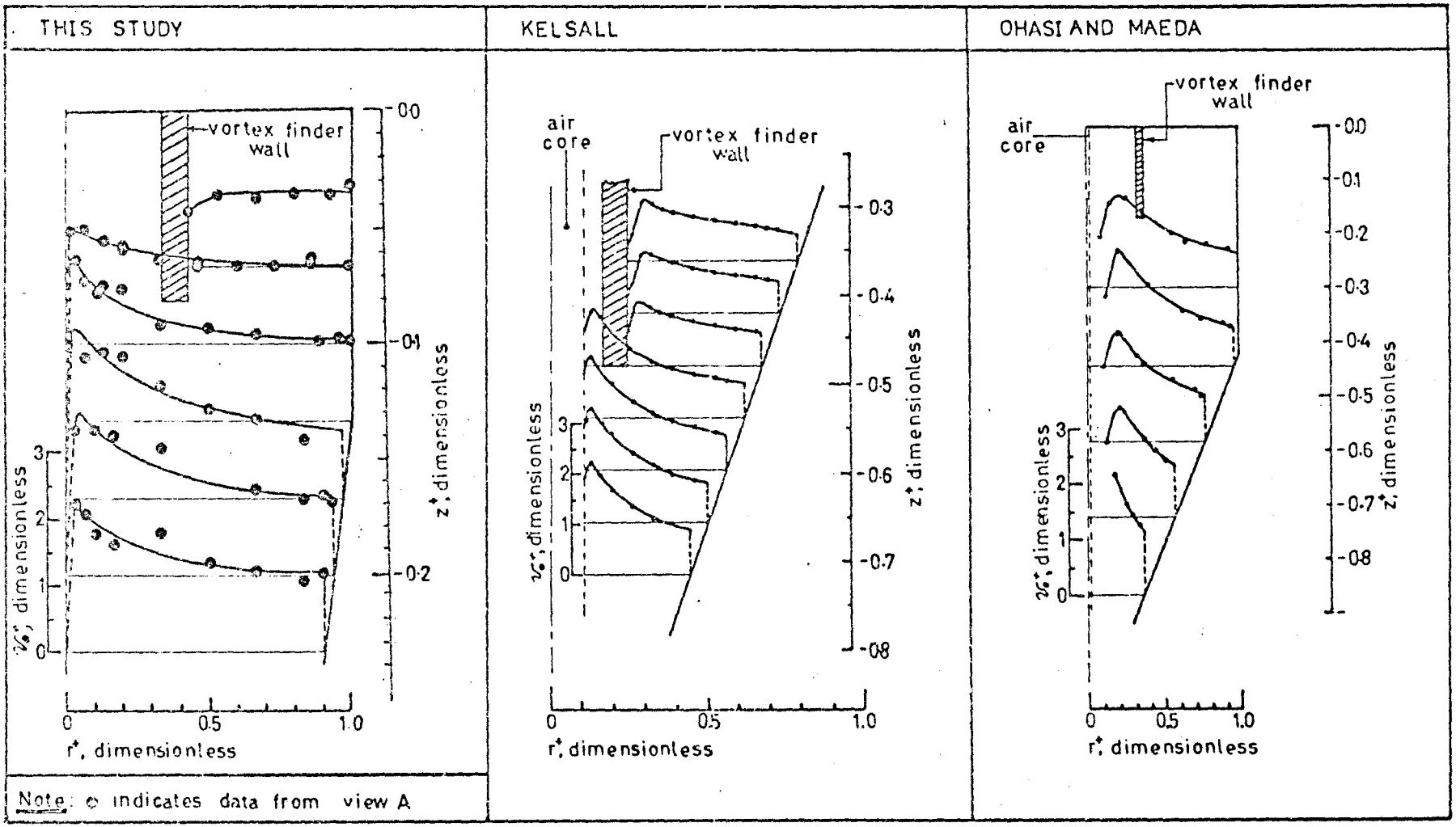

respectively for the operating conditions cited in Table-4.

The vertical velocities determined in this study are shown in Figures 13 and 14. View A data are determined by averaging anywhere from 2 to 12 individual measurements taken from a single roll of film. The averaging was required because of the depth of field problem. For the sake of clarity, only the average measurements are shown except in Figure-13 for v_z^+ versus r^+ at $z^+ = -0.134$. In this plot, to illustrate the range of the individual measurements, all points have been plotted. Averaging of view B measurements was not necessary as droplets invariably crossed the focal plane of this view at right angles. The agreement of the data from the two views is considered satisfactory. The depth of field problem is discussed in more detail in section 3.2.

The curves shown in Figure-15 were determined by drawing the smoothest curves possible through the data in Figures 13 and 14.

Comparison of the three sets of vertical velocities indicates an important difference in the three studies. Perhaps because Kelsall had an unusually long vortex finder and because Ohasi and Maeda determined their profiles at large vertical displacements, short circuit flow was not detected. Such a flow pattern was found in this study at elevation $z^+ = -0.101$. This is illustrated by the "hump" in Figure-15. The flow produced by this part of the profile has been estimated as 5.7% of the feed flow, which being quite small reinforces Rietema's[R-1] suggestions for optimum geometry.

The locus of zero vertical velocity in Figure-15 suggests that in both modes operation, i.e., with or without an air core, the locus of zero vertical velocity reflects the shape of the cyclone.

Figure-13

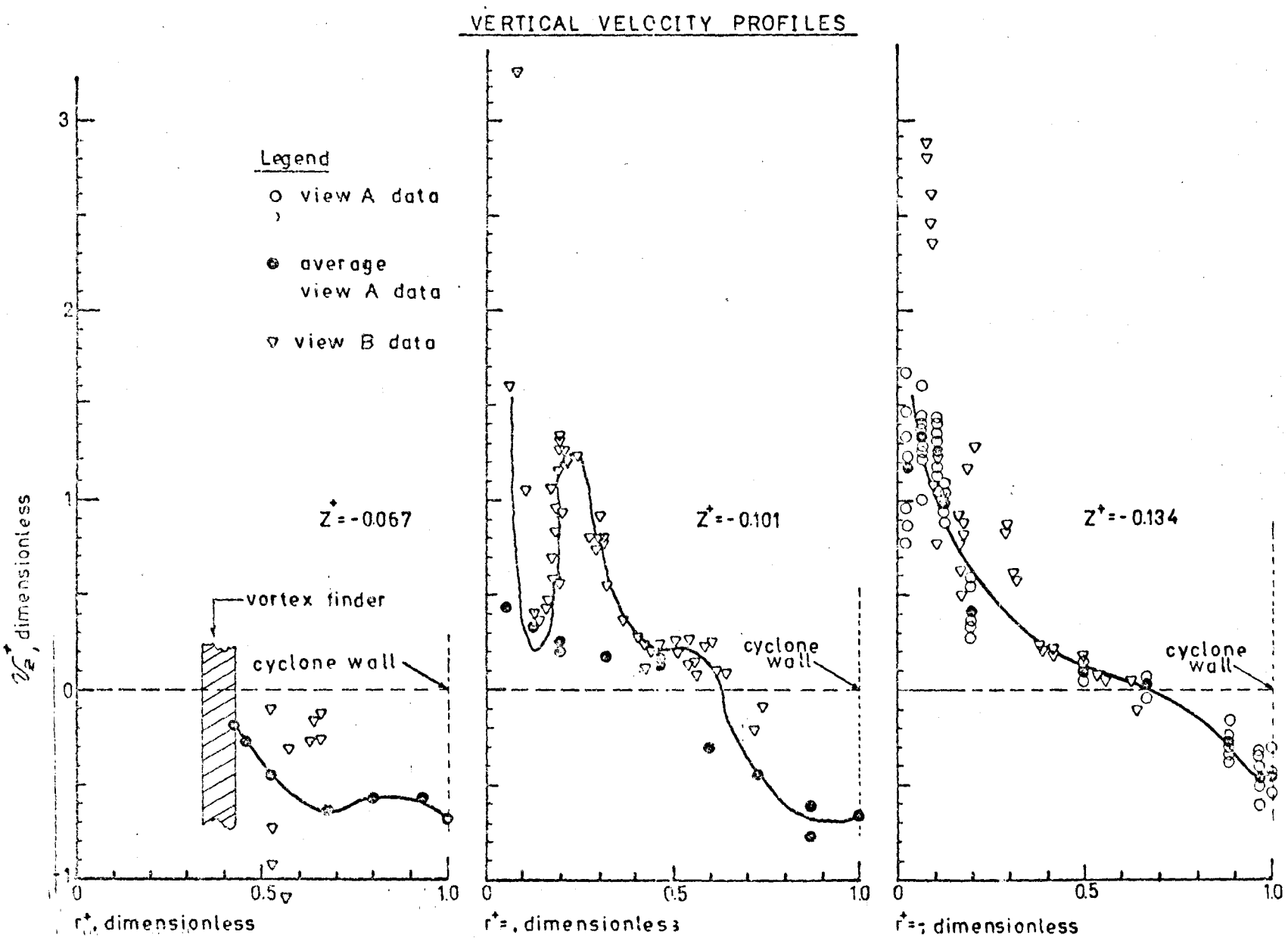
VERTICAL VELOCITY PROFILES
Legend
view A data
average view A data
view B data
$Z^+ = -0.067$
$Z^+ = -0.101$
$Z^+ = -0.134$
vortex finder
cyclone wall
cyclone wall
cyclone wall
v_z^+, dimensionless
r^+, dimensionless
r^+, dimensionless
r^+, dimensionless
3
2
1
0
-1
0
0.5
1.0

Figure-14

VERTICAL VELOCITY PROFILES

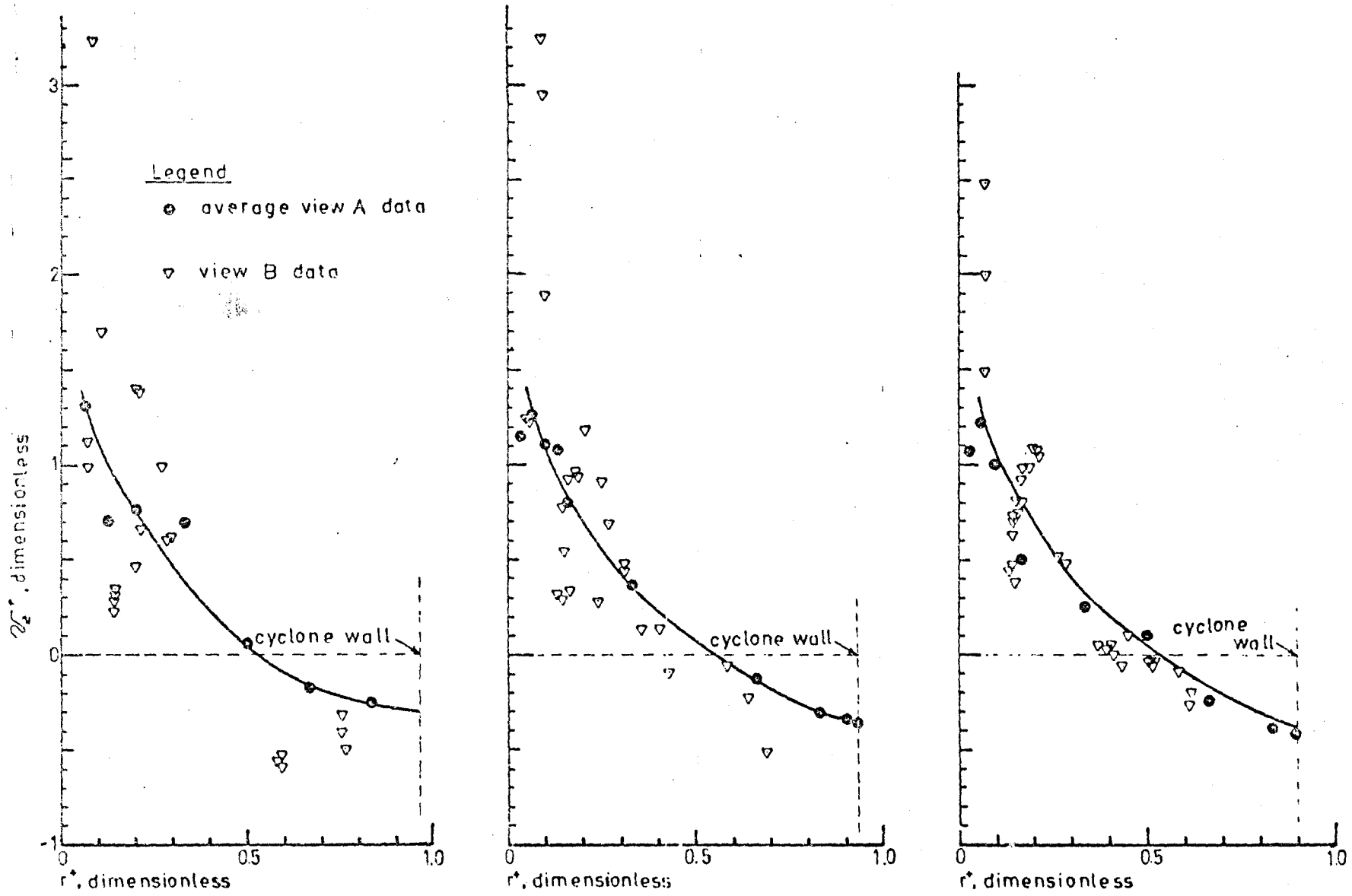

Figure-15

COMPARISON OF VERTICAL VELOCITY PROFILES

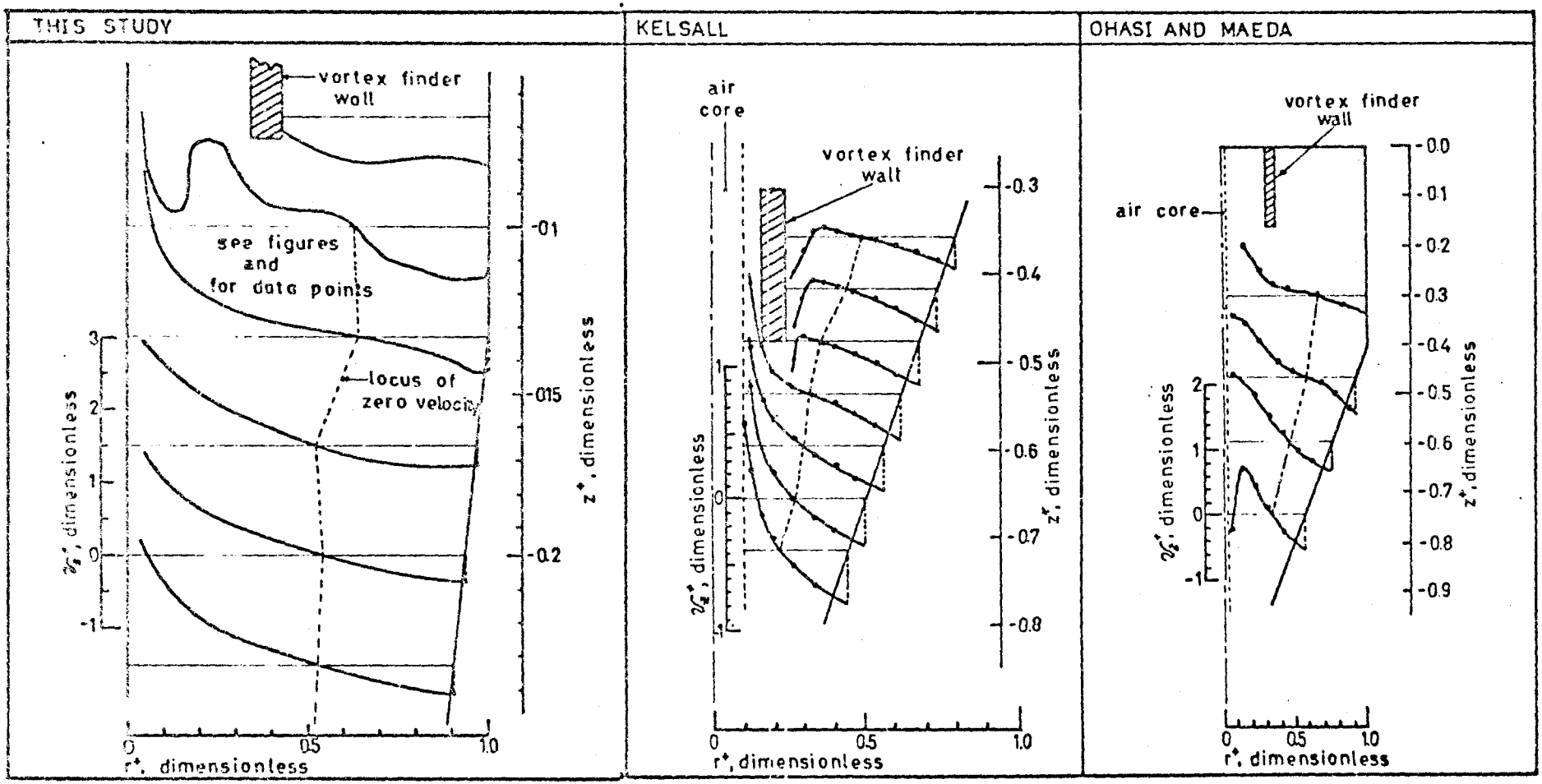

In general, it would seem that vertical transport of fluid in a hydrocyclone is quite similar whether or not an air core is present.

To check the consistency of the data, vertical velocity integrations were carried out as described in section 2.1. The results, determined graphically, as described in section A3.3, are shown in Table-6.

At the top elevation, no velocities were determined in the vortex finder pipe. Hence, at this position Q_3 was not calculated. The value of Q_1' at this position is however much higher than Q_1 indicating that circular flow symmetry does not exist at this position. This is also indicated at the level, $z^+ = -0.101$, where there is most likely assymetric flow conditions also since at the remaining four elevations, the calculated and actual values of Q_3 agree satisfactorily.

In general, in Table-6 Q_1' decreases down the cyclone while Q_2' increases up the cyclone. This trend is in agreement with the discussion on vertical and radial flow given in section 1.3.3.

A further data consistency check is provided in Figure-16 where calculated and experimental values of the radial velocity are compared. The experimental values are observered to be in modest ageement with the v_r^+ values calculated from r-z internal material balances assuming axial symmetry. Details of this calculation are given in the appendix in section A3.4.

The radial velocities determined in this study are outward toward the central axis and inward toward the wall. Large gradients in the radial velocity profiles as evident in those of Kelsall and Ohasi and Maeda, were not observed in this study. Rather, the radial velocity appears to be constant over most of the distance between the central axis and the wall.

Table-6

Vertical Velocity Integrations

z^+	Q_1' (USGPM)	Q_2' (USGPM)	calculated Q_3 (USGPM)	actual Q_3 (USGPM)
-0.067	23.6	-------	--------	1.50*
-0.101	17.3	8.30	9.00	1.50*
-0.134	7.02	5.70	1.32	1.55**
-0.166	7.36	5.77	1.59	1.47**
-0.200	6.77	5.27	1.50	1.51**
-0.234	6.42	5.02	1.40	1.58**

* determined from feed and overflow rotameter readings

** determined by weight-time measurements

Figure-16

COMPARISON OF RADIAL VELOCITY PROFILES

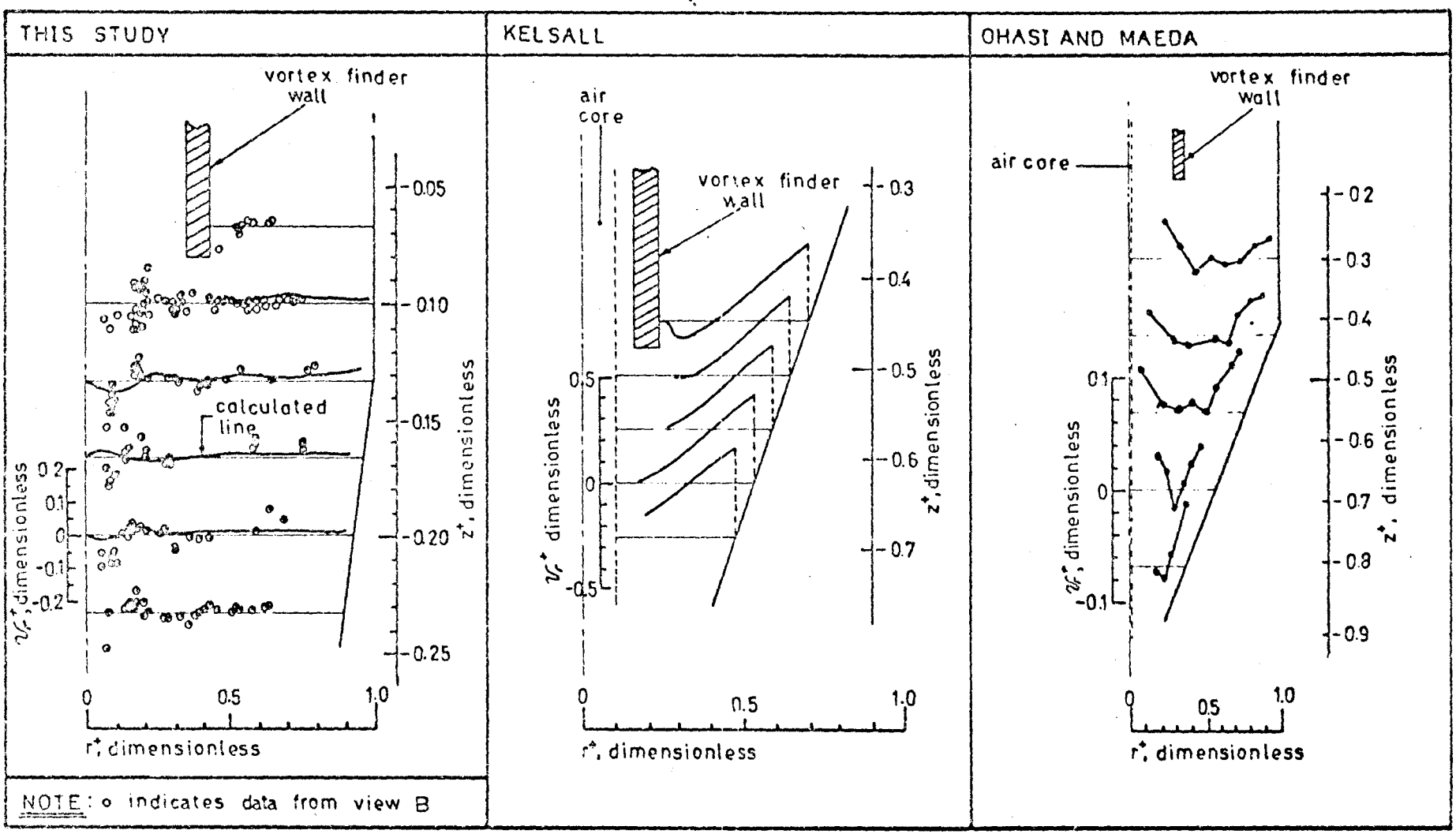

The behaviour of the radial velocity at elevations below those considered may of course be different as the effect of the cyclone taper becomes more important. Both Kelsall and Ohasi and Maeda used tracer particles which were heavier than water; this may have caused the radial velocities to be exaggerated somewhat.

A listing of all the measured values of v_θ^+, v_z^+, and v_r^+ is given in the appendix in section A3.1.

3.2 Error Analysis

For determining tangential and vertical velocities, the error in fluid metering(5%), film speed measurement(0.5%), screen calibration(0.5%), screen distance measurement(1%) and angle measurement($\pm$ 0.5°) are far overshadowed by the depth of field problem in view A which was produced by the lens-extension tube arrangement adopted in this study. The problem is illustrated in Figure-17.

The depth of field has been estimated as 2 mm, by moving an illuminated target. Reduction of the depth of field beyond the present value would require a much longer lens-extension tube combination than the 10 inch combination used in this study. A longer arrangement, when combined with the camera would make the photographic section of the equipment unwieldy and difficult to align with the other optical devices.

The depth of field is only a problem when view A droplet behaviour is observed. In this view anisole droplets moved almost parallel to the focal plane, which due to the depth of field had a finite thickness. To overcome this problem, the behaviour was observed and averaged. The mean value was assigned the radial position at the center of the focal plane.

When measuring distances on a tracing paper recording, an absolute error of 0.02 screen units has been estimated. This is acceptable

Figure-17

Depth of Field Problem Illustration

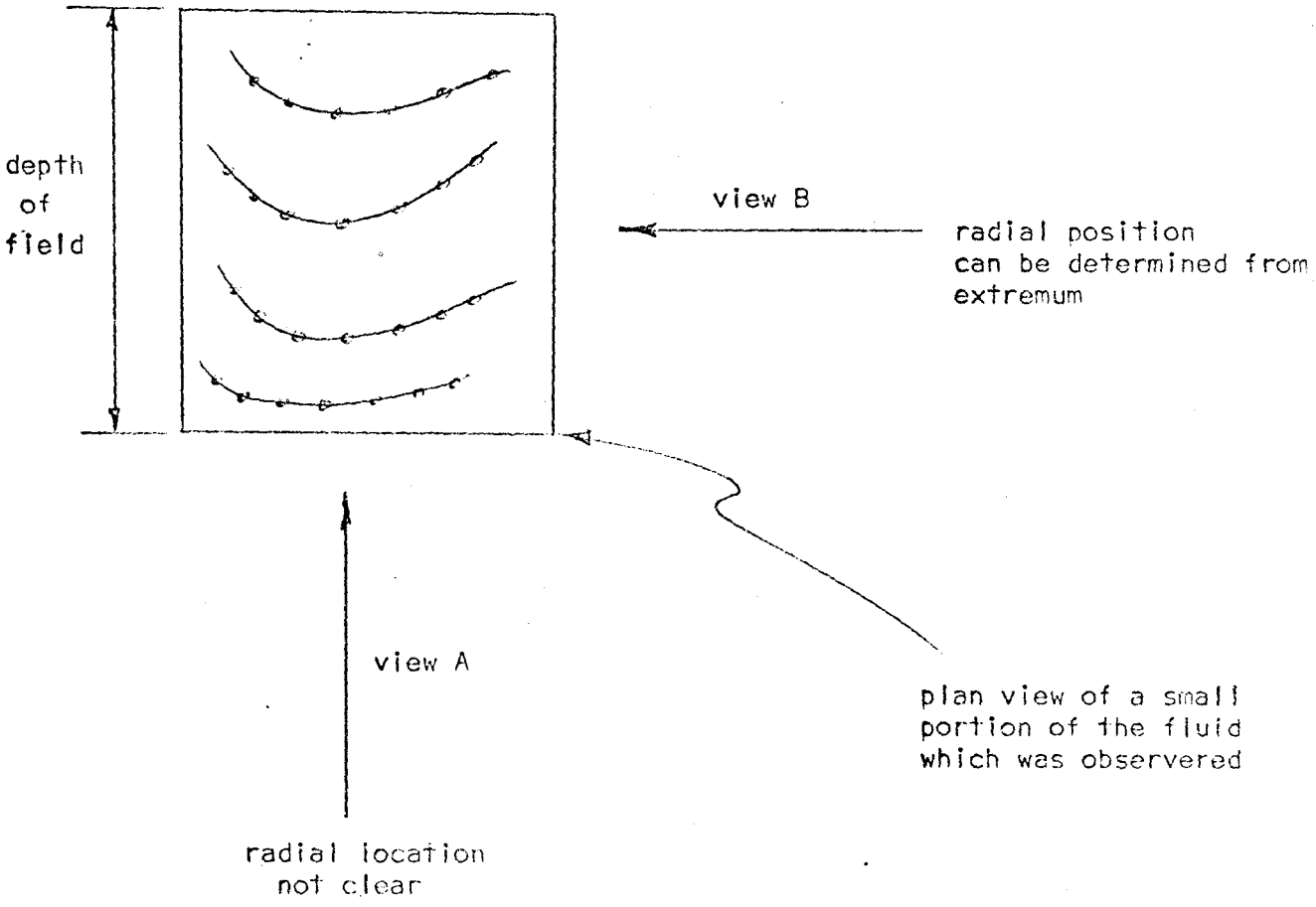

when measuring distances of the order of 2.00 screen units or greater which was the case for the majority of measurements made to determine v_θ^+ and v_z^+. However, as described in section 2.1, the determination of v_r^+ values from screen recordings required measurements of the small horizontal difference, (d_1-d_2). Consequently, the relative error in this term may be as high as 60%. The calculated values of v_r^+ are considered more reliable. These latter values were calculated from small flow segment where the error has been estimated as 10% so that the calculated values of v_r^+ are considered accurate to within 20%.

At $z^+ = -0.101$, replicate measurements were made to study the reproducibility of the technique. The results are shown in Table-7. The velocities appear to be reproducible to within 4%.

3.3 General Discussion

The velocity profiles prepared in this work were determined by observing the behaviour of small anisole droplets dispersed in water. The character of these droplets bears further discussion.

As stated, the droplets were dispersed by the turbulence in the feed pipe at a "tee" joint. From visual observations, it was concluded that if the anisole reservoir pressure was maintained constant, the drop size and distribution was a function only of the total feed rate. Feed rate and reservoir pressure were maintained constant throughout all runs so that it is concluded that the drop size and distribution was identical for each run. The actual drop sizes ranged from about 50 to about 350 microns.

The density difference between anisole and water at 20°C is 0.00596 gm/cc. Thisimplies that anisole droplets behaved as neutrally buoyant spheres. Much information has been collected about the behaviour of neutrally buoyant spheres in Poiseuille flow in straight tubes.

Table-7

Reproducibility Measurements*

Film Roll No.	r^+	v_θ^+
SRK-87	0.200	1.48
SRK-88	0.200	1.43
SRK-90	0.467	1.24
SRK-91	0.467	1.23
SRK-94	0.867	1.26
SRK-95	0.867	1.28

* $z^+ = -0.101$

Lateral migration of such spheres has been found to be proportional to such parameters as drop to tube diameter (to about the power three) and tube Reynolds number and inversely proportional to the distance from the wall. Although the flow situations are decidedly different the implication is that no lateral migration occurs.

An inspection of all the velocities listed in the appendix for view A measurements shows there is no apparent relationship between droplet size and velocity.

During the six runs carried out in this study, the feed, overflow and underflow pressures were recorded as listed in Table-4. It is to be noted that the total pressure drop was much larger than that estimated in section A1.3, where a correlation based on air core operation was used.

Due to the great number of droplet images seen in both views, the uniformity of the drop size distribution and the problem caused by the depth of field, it was not possible to identify a given droplet in both views simultaneously. Had this been possible, the film analysis would have been simplified.

4 Conclusions

4.1 New Conclusions

(i) The tangential velocity profiles in a hydrocyclone operating without an air core are similar in character to those produced with air core operating although the exponent, n, in equation(18) is much reduced.

(ii) The vertical flow patterns in a hydrocyclone operating with and without an air core are very similar.

(iii) "Short circuit" exists in hydrocyclones operating without an air core.

(iv) There is outward radial flow near the central axis and inward radial flow toward the wall in a hydrocyclone operating without an air core. No large radial velocity gradients were observed.

(v) Anisole droplets in the size range 50 to 350 microns can be used as tracer particles to measure water velocities.

(vi) Mass balances based on v_z^+ profiles closed to within an average of 9.2% for profiles produced in this work.

(vii) The method devised in this study is a reasonable method for obtaining fluid velocity data, but the technique would be much improved by a combination of reduction of the depth of field and compaction of the equipment. Although difficult film analysis is involved, any other arrangement of the views would require viewing from the top which would be hampered by the presence of the vortex finder.

4.2 Confirmation of Earlier Findings

(i) The major part of the tangential flow regime can be described as free vortex flow and equation (18) models this physical behaviour satisfactorily.

(ii) The locus of zero vertical velocity reflects the shape of the cyclone.

(iii) Inward radial flow occurs at radii greater than 0.4R.

(iv) Outward radial flow occurs near the central axis.

(v) The vertical and tangential velocity profiles indicate that there is effectively slip flow at the cyclone wall.

5 Recommendations

(i) A more complete analysis of the hydrocyclone encorporating more angular and radial positions could be initiated.

(ii) The effect of feed rate, flow split and air core absence or presence on point fluid velocities could be studied.

(iii) Observation of the behaviour of particles heavier or lighter than water could be studied.

(iv) Reduction of the depth of field by using a microscope would be a significant improvement to the technique.

(v) Various mechanical improvements to the equipment could be made, such as: flow measurement of the anisole, temperature control on the water reservoir and manometers to replace pressure gauges.

6 Nomenclature

6.1 Latin alphabet

A_i cross sectional area of cyclone inlet pipe, ft^2

A_z dimensionless area proportional to small vertical flow segment, dimensionless

d radial distance projected into view B, ft

D inside diameter of cylindrical section of cyclone, ft

D_p droplet diameter, ft

$D_{p_{50}}$ droplet diameter(see section A1.3), ft

D_1 inlet diameter, ft

D_2 overflow diameter, ft

D_3 underflow diameter, ft

g gravitational acceleration, ft/sec^2

H vortex finder height, ft

K proportionality constant, ft^{n+1}/sec

l height of cylindrical section of cyclone, ft

L overall cyclone height, ft

n exponent, dimensionless

$(\Delta P)_t$ cyclone pressure drop(see section A1.3), lb/ft^2

Q_1 feed rate, ft^3/sec

Q_1' flow down at elevation z, ft^3/sec

Q_2 overflow rate, ft^3/sec

Q_2' flow up at elevation z, ft^3/sec

Q_3 underflow rate, ft^3/sec

r radius, ft

r^+ radius, dimensionless

R cyclone cylindrical section radius, ft

R' radius at which vertical velocity is zero, ft

R_w wall radius at elevation z, ft

$(Re)_i$ inlet pipe Reynolds number, dimensionless

Δt time interval, sec

v_r radial velocity, ft/sec

v_r^+ radial velocity, dimensionless

v_z vertical velocity, ft/sec

v_z^+ vertical velocity, dimensionless

v_θ tangential velocity, ft/sec

v_θ^+ tangential velocity, dimensionless

$\langle v_\theta \rangle_1$ area average inlet velocity, ft/sec

$\langle v_z \rangle_2$ area average overflow velocity, ft/sec

z vertical distance, ft

z^+ vertical distance, dimensionless

6.2 Greek Alphabet

η continuous phase viscosity, ft/lb.sec

π universal constant, dimensionless

θ angle, degrees

ρ continuous phase density, lb/ft^3

ρ_s solid density, lb/ft^3

7 References

A-1 Anon., Eng. Mining. J. 158(6),87(1957).

B-1 Baldina, O.M., Energemaschinostroanie, 10,13(1961).

B-2 Bradley, D., Ind. Chemist. 34,473(1958).

B-3 Bradley, D., and D.J. Pulling, Trans. Inst. Chem. Engrs., 37,34(1959)

B-4 Bradley, D., "The Hydrocyclone", Pergammon Press, 1st ed., (1965).

B-5 Bradley, D., AERE-4027(1967).

B-6 Brenner, H., Advances in Chemical Engineering, 6,287(1966)

F-1 Fontein, F.J. and C. Dijkman, Inst. Min. Met. Symp. on Recent Developments in Mineral Dressing, London,(1952), p.229.

F-2 Fontein, F.J., Eng. Mining J., 160(7),82(1959).

H-1 Haas, P.A. et al., Chem. Eng. Progr., 53,203(1957).

H-2 Hodgman, C.D.(ed.), "Handbook of Physics and Chemistry", 44th ed. p. 807.

H-3 Herkenhoff, E.C., Minig Engr., 9,873(1957).

H-4 Ibid, p.3073.

I-1 "International Critical Tables", McGraw-Hill, New York, 1926.

K-1 Kearsey, H.A. and N.S. Hibbert, Ind. Chemist, Aug.,371(1959).

K-2 Kelsall, D.F., Trans. Inst. Chem. Engrs., 30,87(1952)

L-1 Lilge, E.O., Trans. Inst. Mining Met., 71,285(1962).

M-1 Mitzmager, A. and J. Mizrahi, Trans. Inst. Chem. Engrs., 42,152(1964).

M-2 Modder, J.J. and D.A. Dahlstrom, Chem. Eng. Progr., 48(2),75(1952).

O-1 Ohasi, H. and S. Maeda, Chem. Eng.(Japan), 22,200(1958).

P-1 Peebles, F.N. and H.J. Garber, Ph.D. Thesis, Dept. Chem. Eng. Univ. Tennessee (Jan., 1956).

P-2 Perry, J.H.(ed.), "Chemical Engineers' Handbook", 4th ed., p. 3-70.

R-1 Rietema, K., Chem. Eng. Sci., 15,298(1961).

S-1 Saito, N. and K. Ito, Geophys. Mag. Tokyo, 22,283(1951).

S-2 Scott, P.P. and J.L. Lummus, Oil gas J., Oct.,188(1956).

S-3 Smith, J.L. Jr, Trans. ASME, Dec.,602(1962).

T-1 Tangel, O.F. and R.J. brison, Chem. Eng., 62,234(1953).

W-1 Wilson, R.H., ORNL 1598(1953).

Y-1 Yoshioka, N. and Y. Hotta, Chem. Eng.(Japan), 19,632(1955).

APPENDICIES

Appendix A1

Experimental Equipment

AI.1 Backprojection Apparatus

A backprojection device was made to simplify the analysis of the films.

This apparatus was designed to maintain the full frame projector at a fixed distance from the screen and to provide sufficient magnification so that simple graphical analysis of screen recordings could be carried out on a conventional drawing board directly.

The frame was constructed of one inch square tubular steel. The screen and projector supports were constructed of 0.5 inch plywood and set at 30 and 60 degrees to the vertical respectively. The screen was a piece of 0.25 inch plate glass 20 inches by 10 inches.

Figure AI-1 shows a side and plan view of the apparatus.

An extension control was used with the projector so that it could be controlled while viewing the screen.

Figure AI-1

Backprojection Apparatus

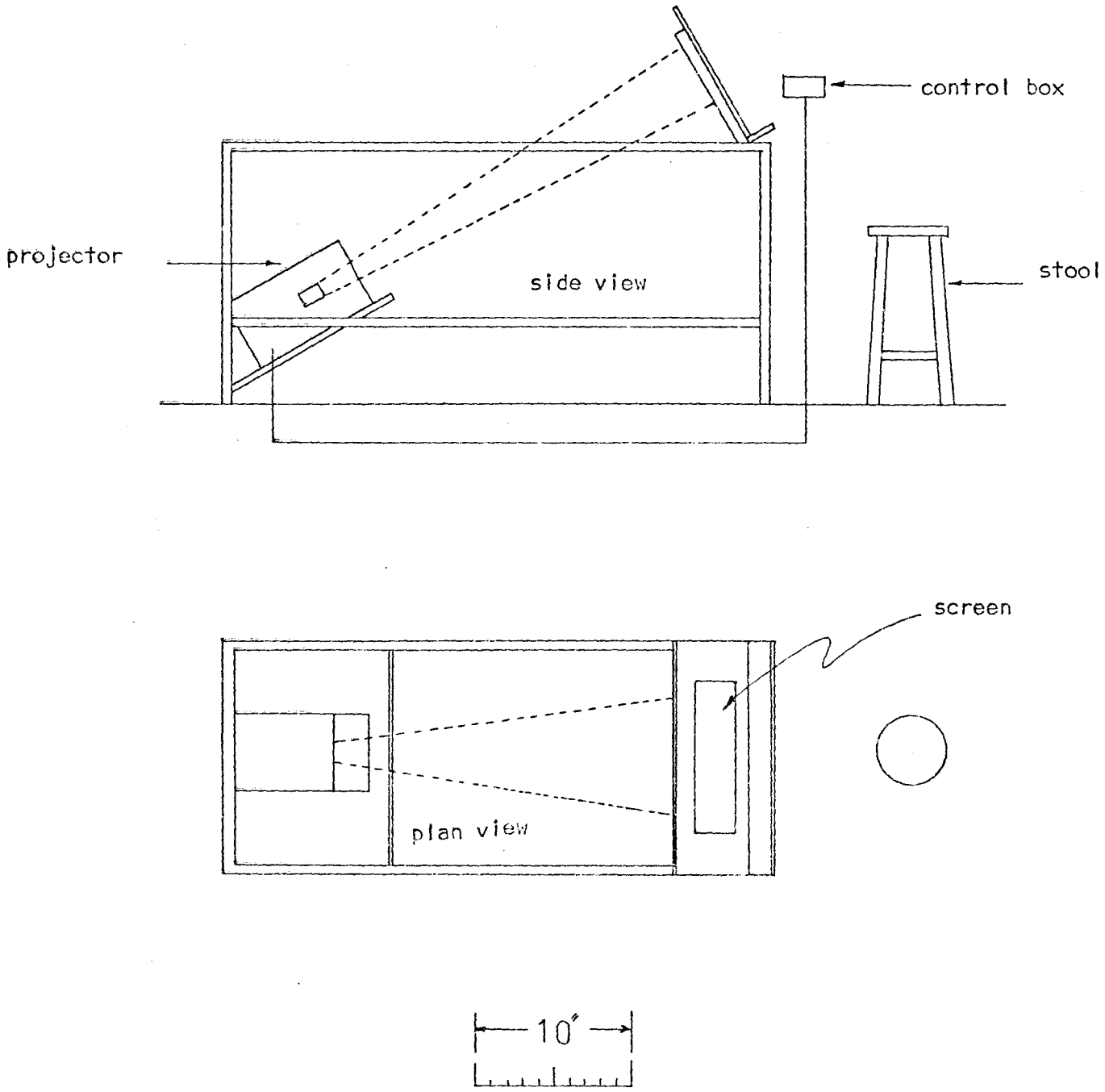

AI.2 Optical Table Assembly

A simplified drawing of the optical table assembly is shown in Figure-AI-3. The four upright poles which govern the vertical movement of the optical plate, are notched as illustrated in Figure-AI-2. It is in these notches that the swing-in latches, shown in Figure-AI-3, are engaged to position the optical plate.A detailed drawing of the optical plate is given in Figure-AI-4.

All plates shown in Figures AI-3 and AI-4 were machined to a tolerance of $\pm$ 0.005 inch. The bushings were brass. Steel roller bearings were installed in the set of bushings guiding the vertical movement of the optical plate.

Figure-AI-2

Detail of Notched Upright Poles

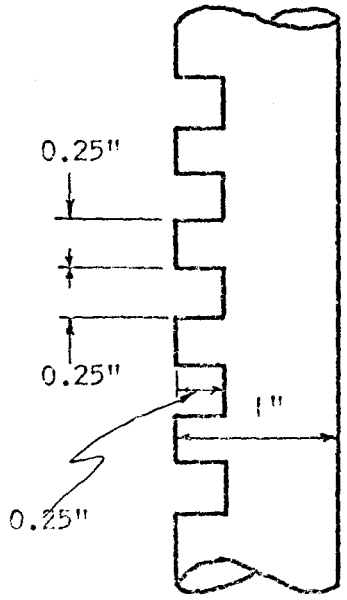

Figure-A1-3

Optical Table Assembly

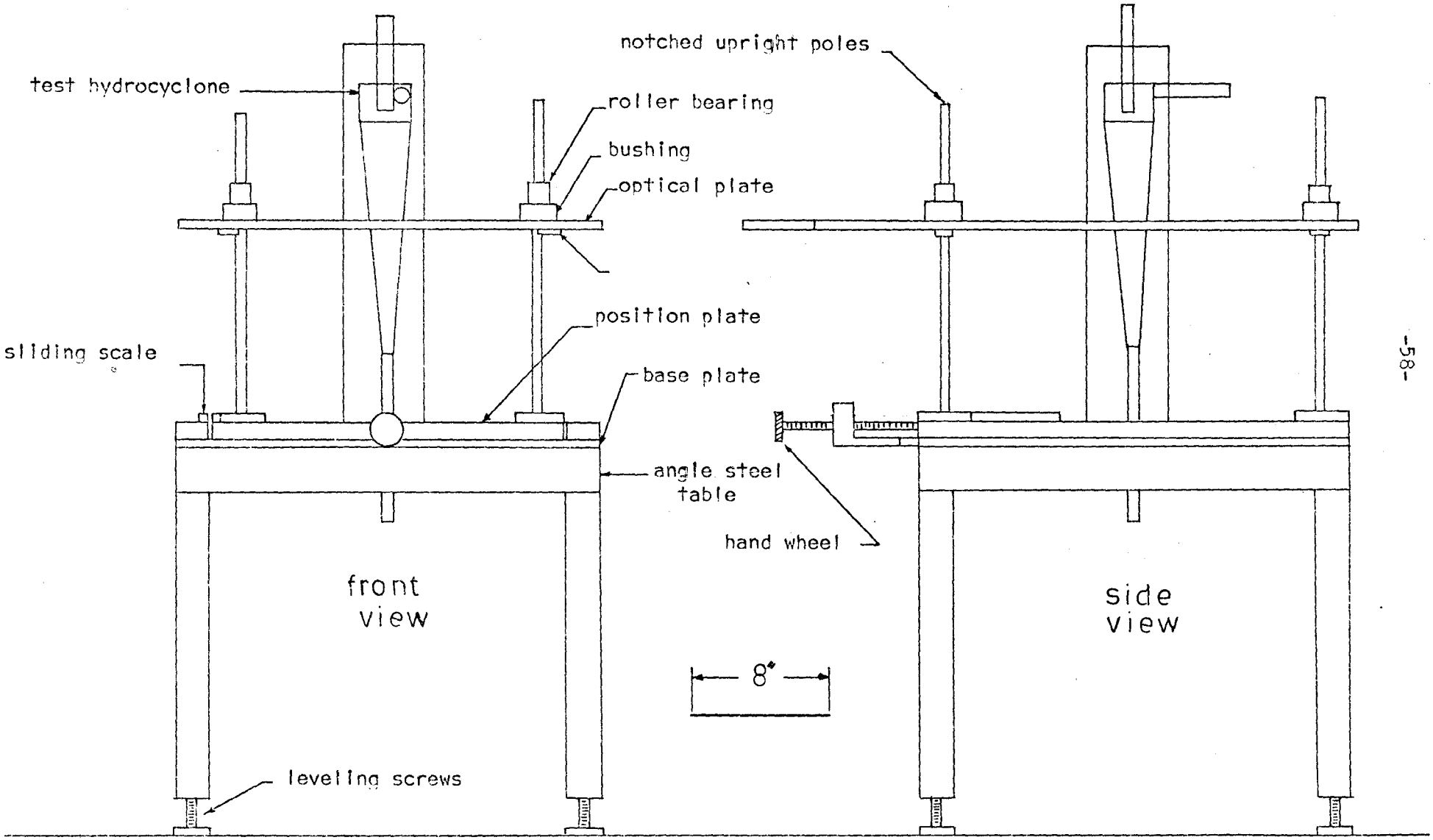

Figure-A1-4

Plan View of Optical Plate

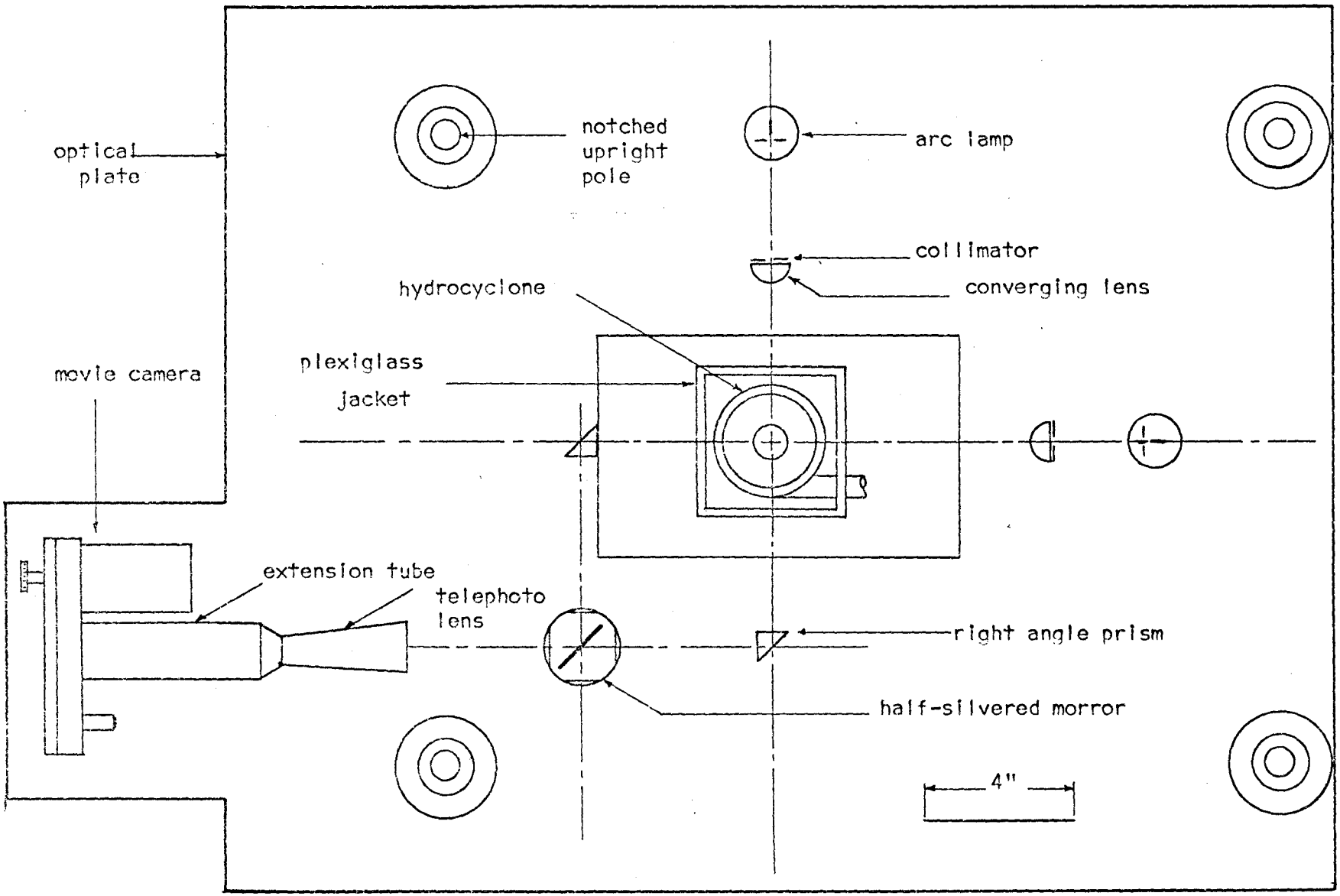

AI.3 Selection of Operating Conditions

Given the cyclone described in this work, what are reasonable operating conditions?

Exploratory experiments showed that a feed rate of 7.5 USGPM was a reasonable flow rate at which to employ the optical technique devised in this study. The flow split was selected arbitrarily as 4 to 1 so that 80% of the feed was directed to the overflow and 20 % directed to the underflow. This split is within the range of industrial application.

To insure that the chosen operating conditions approached those used in industrial practice, the cut diameter(diameter of a particle which has an equal chance of exiting by the underflow or overflow), $D_{p_{50}}$, and the pressure drop across the cyclone, $(\Delta P)_t$, were calculated for a hypothetical mineral dressing problem.

The problem details and solution are described below.

Mineral Dressing Problem

Statement of The Problem

A cyclone is fed a feed mixture of less than 1% solids and water at a rate of 7.5 USGPM. The ore to be separated has a specific gravity of 1.5. The flow split is set at 4 to 1. All physical properties are to be evaluated at 20°C.

Solution

Method: Rietema[R-1(paper IV)]

Restrictions: (i) Rietema's method of design has been developed for cyclones opersting with an air core.

(ii) Rietema's method of design has been developed for an optimum geometry that he has proposed.

Solution Details

The first restriction will be dealt with later while it is noted that the first restriction has been met. The physical dimensions of the cyclone used in this work were determined using Rietema's suggestions for optimum geometry.

The required physical properties are listed below.

$$\eta = 7.06\times10^{-4} \text{ lb/ft.sec}$$

$$\rho = 62.5 \text{ lb/ft}^3$$

$$\rho_s = 93.8 \text{ lb/ft}^3$$

Also,

$$Q_i = 7.5 \text{ USGPM or } 1.67\times10^{-2} \text{ ft}^3/\text{sec}.$$

The average inlet velocity is

$$\langle v_\theta \rangle_i = Q_i / A_i$$

where A_i is the cross sectional area of the feed port.

$$A_i = \frac{\pi D_i^2}{4} = \frac{(3.14)(0.84/12)^2}{4} = 3.85\times10^{-3} \text{ ft}^2.$$

Thus

$$\langle v_\theta \rangle_i = \frac{1.67\times10^{-2}}{3.85\times10^{-3}} = 4.35 \text{ ft/sec}.$$

The inlet Reynolds number is

$$(Re)_i = \frac{4\rho Q_i}{\pi D_i \eta} = \frac{(4)(62.5)(1.67\times10^{-2})}{(3.14)(0.84/12)(7.06\times10^{-4})} = 2.68\times10^{-4}.$$

From Figure-2 in the above mentioned reference,

$$\frac{(\Delta P)_t}{(0.5)\rho\langle v_\theta \rangle_i^2} = 4.0 ,$$

where $(\Delta P)_t$ is the pressure drop between the feed and overflow pipes.

$$(\Delta P)_t = \frac{(4.8)(0.5)\rho\langle v_\theta \rangle_i^2}{(144)(g_c)} = \frac{(4.0)(0.5)(62.5)(4.35)^2}{(32.2)(144)} = 0.51 \text{ psig}.$$

Refering again to Rietema's work,

$$(Re)_i = \frac{(6.5)D_{p_{50}}^2 \Delta\rho\,(\Delta P)_t}{\eta^2}$$

where $\Delta\rho$ is the density difference between the ore and the water. $D_{p_{50}}$ can now be computed.

$$D_{p_{50}} = \left[\frac{(Re)_i^{\,2}\,\eta^2}{(6.5)\Delta\rho\,(\Delta P)_t}\right]^{0.5}$$

$$D_{p_{50}} = \left[\frac{(2.68\times10^{4})(7.06\times10^{-4})^2}{(6.5)(31.3)(0.51)(32.2)(144)}\right]^{0.5} = 1.67\times10^{-4}\ \text{ft}$$

or

$$D_{p_{50}} = 51 \text{ microns}$$

The two desired quantities $D_{p_{50}}$ and $(\Delta P)_t$ have been estimated but must be considered in light of the fact that the above design method has been developed for cyclones operating with an air core. The effect of the presence of an air core on $D_{p_{50}}$ has yet to be determined while it has been observed that if the air core is not present the pressure drop increases. For this reason, the value of $(\Delta P)_t$ estimated above must be considered conservative. The observed pressure distribution is given in Table-4.

In general, the values of $D_{p_{50}}$ and $(\Delta P)_t$ calculated above are representative of those encountered in industrial practice. See for example the following operating reports: A-1, H-3, S-2, and T-1.

AI.4 Equipment Suppliers

A list of all equipment suppliers is given in Table-AI-I along with their addresses and brief specifications of the various items.

Table-AI-I

List of Equipment Suppliers

ITEM	SPECIFICATIONS	SUPPLIER
anisole and flaming red dye	reagent grade	Fisher Scientific 184 Railside Rd. Don Mills, Ont.
camera power supply and projector	- 0 to 320 v. (A.C.) - 0 to 32 frames/sec	Photographic Analysis 8 Brian Cliffe Dr. Don Mills, Ont.
cine camera	model no. K20SIBE (see also Section 2.2.4)	Photographic Analysis 8 Brian Cliffe Dr. Don Mills, Ont.
cyclone	see Section 2.2.i	Glass Blowing Shop McMaster University Hamilton, Ont.
cyclone jacket	0.25" plexiglass see also Figure-AI-3	Chem. Eng. Mach. Shop McMaster University Hamilton. Ont.
feed rotameter	tube no. R-13A-25-3 float no. 13-RV-310 316 SS with teflon packing	Brooks Instrument Division Emerson Electric Box 150, Markham, Ont.
half-silvered mirror		Ealing Scientific 719 Lajoie Ave. Dorval 760, P.Q.
lamps	100 watts D.C. Xenon-filled	Sylvania Electric Products Inc. Salem Mass. U.S.A.

Table-AI-1 (continued)

ITEM	SPECIFICATIONS	SUPPLIER
lamp power supplies	150 watts D.C.	George W. Gates Inc. Franklin Sq. L.I.,N.Y. U.S.A.
lenses	3 inch focal length converging lens	Hamilton Photographic Repair, 30 Market St. Hamilton, Ont.
optical table	see Section AI.2	Engineering Mach. Shop Mcmaster University Hamilton, Ont.
overflow rotameter	tube no. FP-1-35-G-10/83 float no. 1-GSVGT-69-(T60)	Fischer Porter 1110 Wilson Ave. Downsview, Ont.
pressure gauges	0 to 30 psig 0 to 15 psig	Brian Engineering 45 Shaft Rd. Rexdale 603, Ont.
prisms	45°-45°-90° 1 in. on the side	Ealing Scientific 719 Lajoie Ave. Dorval 760, P.Q.
puise generator	100 or 1000 cycles/sec	Potter Instrument Co. Plainview, N.Y. U.S.A.
pumps	10 USGPM @ 80 ft. head, 3450 RPM, 316 SS	Hayward Gordon 50 Chauncey Ave. Toronto 18, Ont.
tubing and fittings	0.75" and 0.625" 316 SS and teflon	Niagara Valve and Fittings Ltd., 174 Parkdale Ave. N.,Ham.
valves	0.5" globe and gate 0.25" needle valve 316 SS	Niagara Vavle and Fittings Ltd., 174 Parkdale Ave. N., Ham.
valves(other)	1" gate and globe brass	Neo Metals Ltd. 76 Mead Ave. Hamilton, Ont.

Appendix A2

Experimental and Film Analysis Procedures

A2.1 Detailed Experimental Run Procedure

a. The optical plate was set in the desired position. This was accomplished by swinging out the four latches and raising or lowering the plate as required, and then swinging the latches in.

b. The cathetometer was leveled and the distance from the inside top of the cyclone to the center of the camera lens was measured.

c. The copper wire plumb line was hung through the cyclone's exit ports and adjusted until it hung coincident with the central axis of the cyclone.

d. The optical plate was moved radially with the handwheel until, viewing through the eyepiece of the camera, the two images of the plumb line were superimposed exactly.

e. The reading on the sliding scale arrangement was recorded. This was the reading for r = 0.00. Other radial positions were related to this measurement.

f. The plumb line was photographed with each prism, separately, at a film speed of approximately 5000 quarter frames per second.

g. The plumb was withdrawn and the cyclone coupled into the flow system.

h. The make-up water valve was opened and the reservoir filled to about 80% of its capacity.

i. The anisole reservoir pressure was set at 40 psig using the pressure regulator.

j. The pumps were started and the feed rate adjusted to 7.5 USGPM.

k. The overflow rate was adjusted to 6.0 USGPM by throttling the underflow.

l. The make-up water flowrate was adjusted so that the level in the reservoir was constant and then the system was allowed to run about 20 minutes. The three pressures and the reservoir temperature were then recorded.

m. The optical assembly was then set at the first predetermined radial position and the arc lamps switched on and the intensities matched, by viewing each separately through the eyepiece of the camera and adjusting the intensity of one with a variable transformer.

n. The pulse generator was switched on and the signal sent to the camera. The voltage supply for the camera was then set at 156 volts (A.C.). This voltage gives a film speed of approximately 20,000 quarter frames per second.

o. Enough anisole was continuously injected so that it could be just seen with the naked eye.

p. A 100 ft. roll of film was then threaded into the camera and the film exposed by switching on the camera power supply.

q. The film was subsequently taken out of the camera and returned to a sealed film tin. The camera was then inspected for film chips and cleaned if necessary.

r. Steps p. to q. were repeated at predetermined radial positions.

s. After all the films had been exposed, the system was stopped and drained.

A2.2 Film Analysis

Two views of the droplets' movements inside the cyclone are recorded on each roll of film. Each film was viewed first to record the movements of droplets in view A and then re-examined to record droplet movement in view B. Each set of recordings were then analyzed on a conventional drawing board to yield the numerical data used to calculate the final velocities.

The procedure for transcribing the information from the films to tracing paper is given for views A and B.

A2.2.1 Recording Droplet Movement in View A

The procedure for view A is as follows:

a. A piece of tracing paper(17" x 11") was fixed to the backprojection screen with masking tape.
b. The image of the plumbline was then traced onto the paper.
c. The first data film was threaded into the projector and run at 16 full frames per second.
d. A droplet in clear focus was selected and the projector stopped.
e. The outline of the droplet was traced.
f. The position of the center of the droplet was recorded with dots as it was moved one full frame at a time across the screen.
g. The projector was reversed and the droplet image returned to its original position.
h. The image was then moved forward frame by frame until a timing dot was seen at the side of the film. The image and timing dot position were then marked with the same letter of the Latin alphabet. This procedure was carried out (alphabetically) until the image was out of view.

i. The sequence of letters along an image's path was used to identify the direction of the droplet's and the film's movement.

j. Steps c. to i. were repeated with new droplets until the film was run through or the tracing paper became too crowded.

k. A second sheet of tracing paper was placed on top of the old and the plumb line tracing transferred from one sheet to the other.

l. The first tracing paper recording was removed from under the new one.

m. Steps c. to l. were then repeated for all the remaining films.

A typical recording of droplets moving in view A is shown in Figure-A2-1. This figure is a photoreduced copy of a recording used in this study.

A2.2.2 Recording Droplet Movement in View B

The procedure for view B is as follows:

a. Tracing paper was attached to the screen and the plumbline traced as before.

b. A film was threaded into the projector and run at 16 full frames per second.

c. A droplet in clear focus was selected and the projector stopped.

d. The image was recorded as described above.

e. The positioning of the plumbline and the Latin lettters with reference to image and timing dot positions was carried out as described in section A2.2.1.

f. Steps b. to e. above were repeated for the entire film.

g. Steps b. to f. were repeated for all the films.

A typical recording of droplet movement in view B is shown in Figure-A2-2. This figure is a photoreduced copy of a recording used in this study.

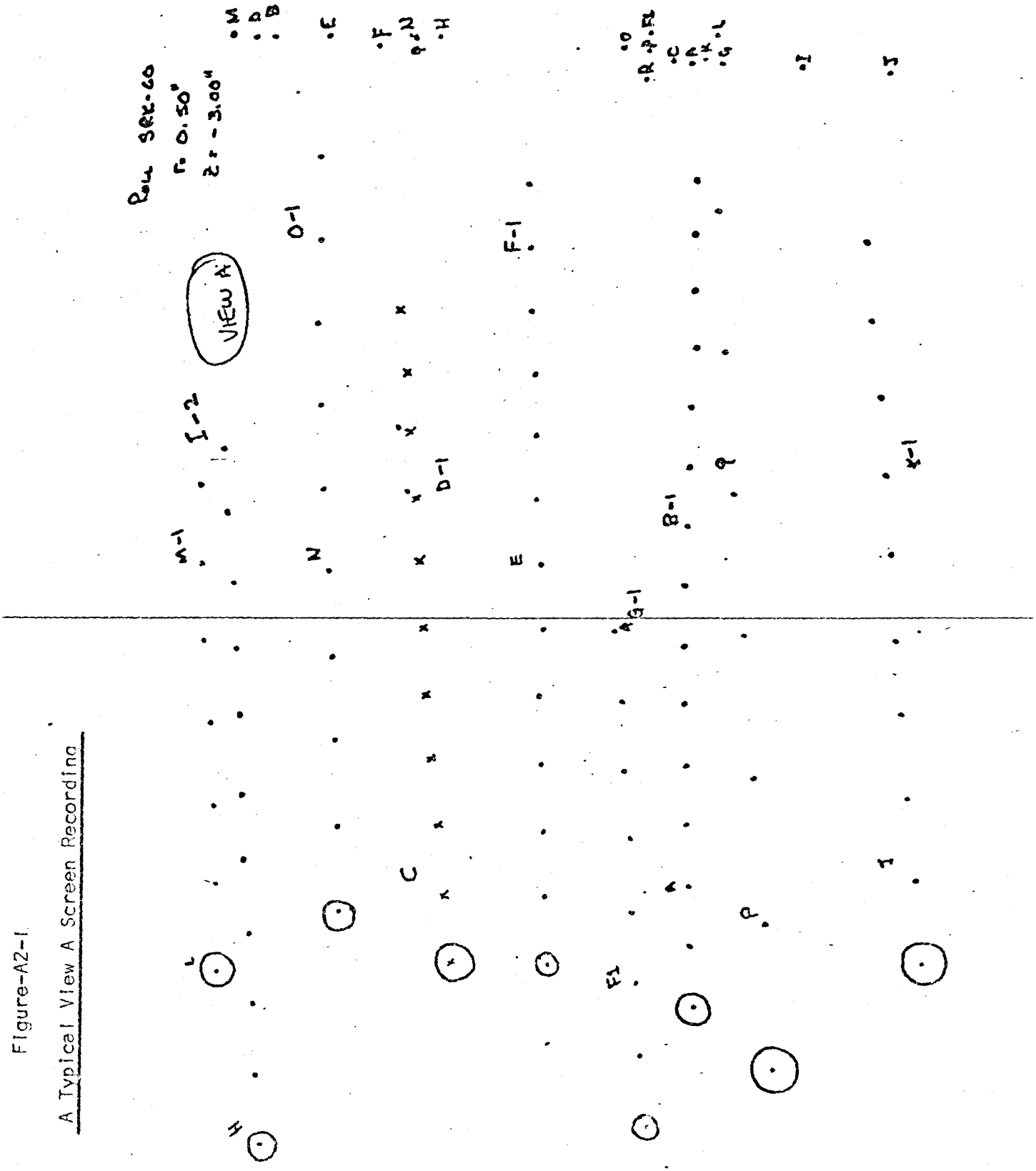

Figure-A2-1

A Typical View A Screen Recording

Figure-A2-2

A Typical View B Screen Recording

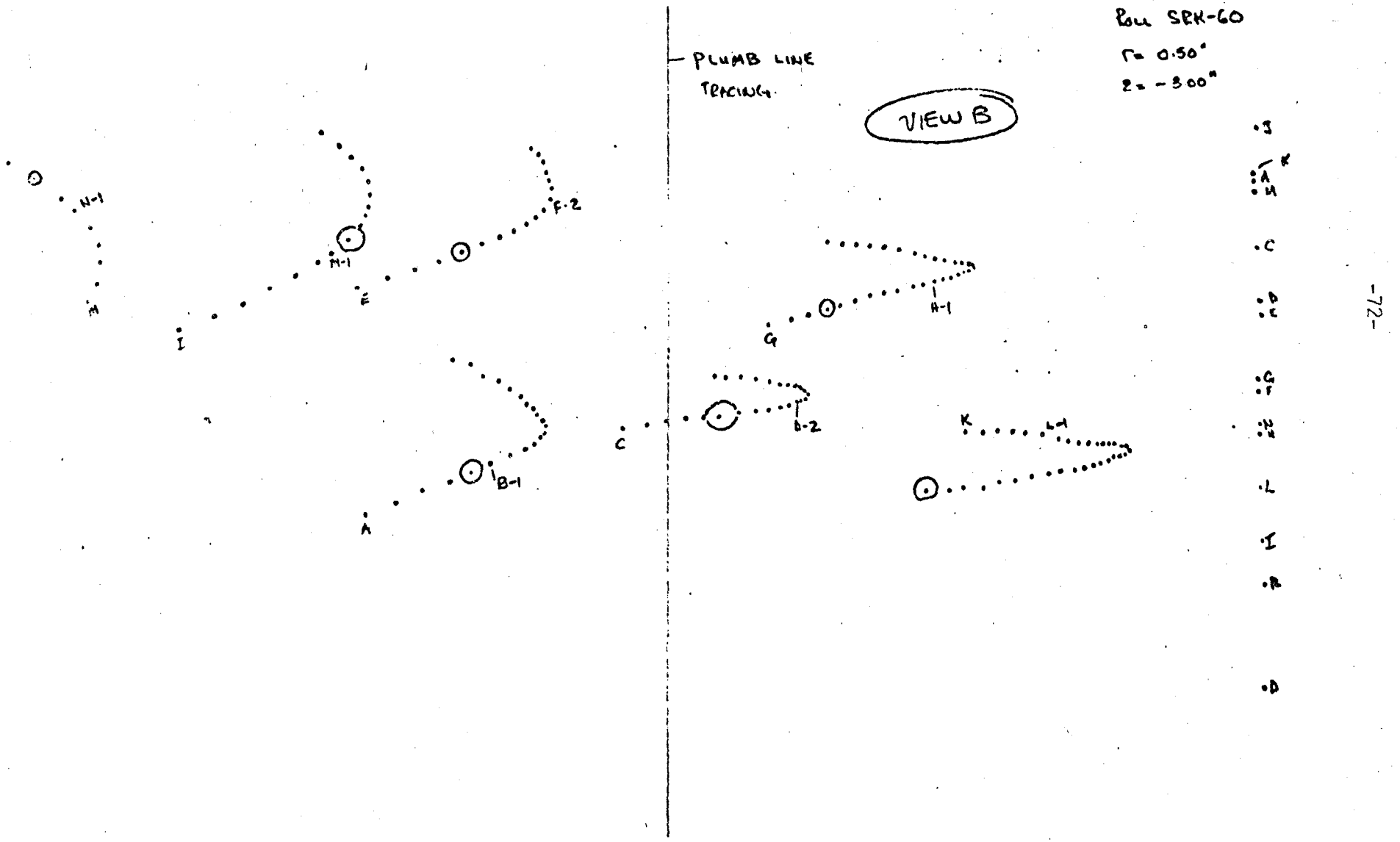

A2.3 Screen Recording Analysis

In general, this section describes measurement of horizontal and vertical distances and time intervals based on ideas discussed in Section 2.1.

A2.3.1 Analysis of View A Recordings

The analysis of view A screen data is illustrated in Figure-A2-3. This recording is for one roll of film exposed at one position in the cyclone. It is a simplified representation of how a recording such as that shown in Figure-A2-1 was analyzed.

All distances which were measured in screen units were assigned FORTRAN names for later programming requirements. The distances VECT, VERT, PARSIZ, HORIZ and FRACT were measured with a divider and a ruler. The number of full frames for an image to progress from a code letter to a successive code letter was counted and multiplied by 4 to give the number of quarter frames. A quarter frame is 4.31 screen units high on the screen so that dividing the quantity FRACT by 4.31 gave the additional fraction of a quarter frame between the successive code letters. The time between the timing dots was 0.001 second. After the second code letter of a pair of letters, the number of 0.001 second time intervals was recorded. This number was assigned the name BLIP.

The above procedure was carried out for all recordings of droplets moving in view A. Table-A2-1 gives a listing of all data. The term screen units(S.U.) is discussed in more detail in section A4.1.

A2.3.2 Analysis of View B Recordings

The analysis of view B screen data is illustrated in Figure-A2-4, which is a simplified representation of how a recording such as that

Figure-A2-3

Analysis of View A Recordings

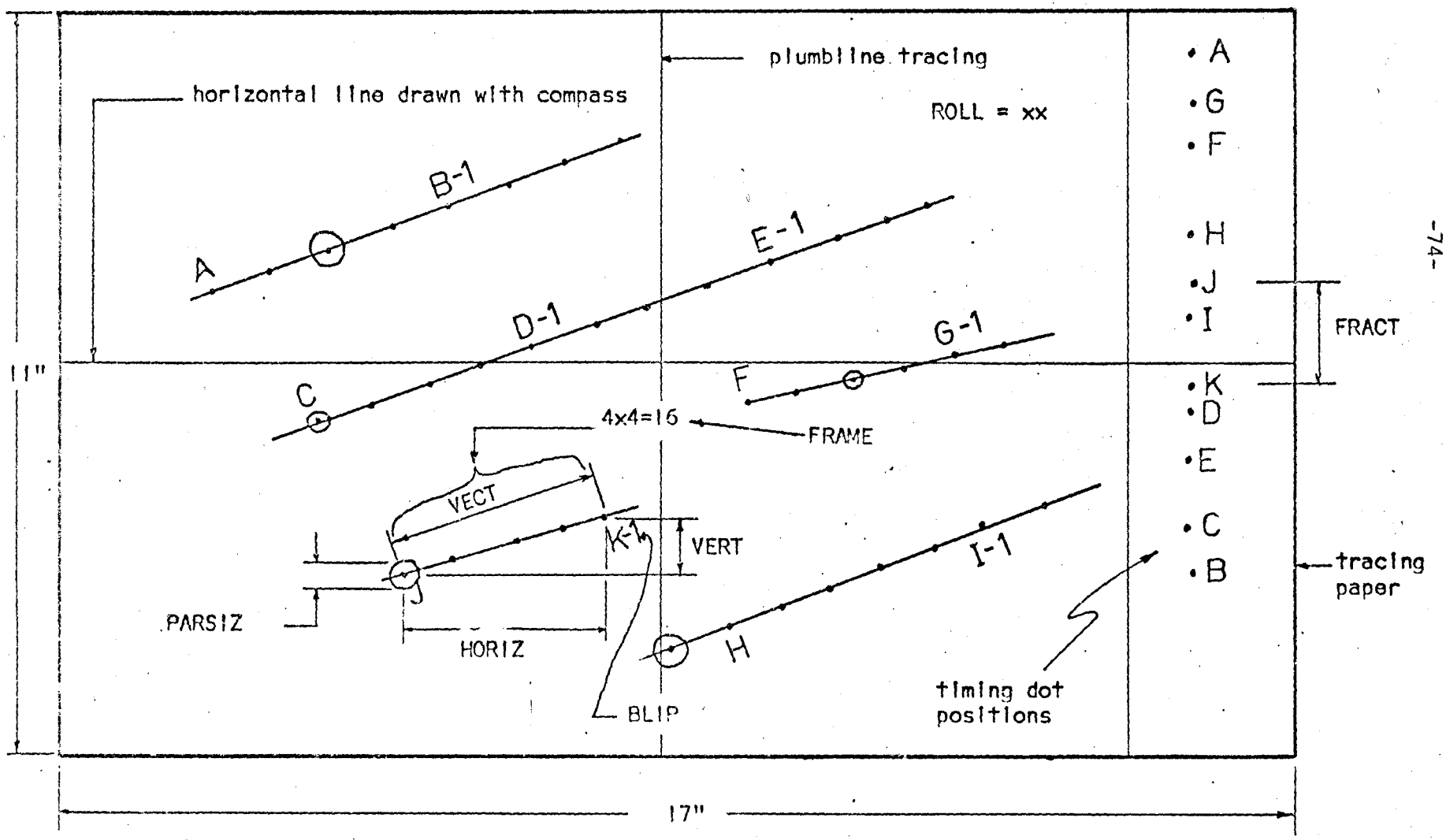

TABLE-A2-1

DATA FROM VIEW A SCREEN RECORDINGS

ROLL	PARSIZ	HEIGHT	RADIUS	VERT	HORIZ	VECT	FRAME	FRACT	BLIP
--	S.U.	IN	IN	S.U.	S.U.	S.U.	--	S.U.	--
33.0	0.32	2.49	0.10	+2.41	6.87	7.25	18.0	+5.50	1.0
33.0	0.79	2.49	0.10	+2.02	6.49	6.81	20.0	+9.62	1.0
33.0	0.55	2.49	0.10	+4.79	11.91	12.88	36.0	+11.53	2.0
34.0									
34.0	0.55	2.49	0.20	+1.92	12.68	12.80	36.0	+4.20	2.0
34.0	0.51	2.49	0.20	+1.60	8.70	8.82	20.0	-1.62	1.0
34.0	0.51	2.49	0.20	+1.59	7.60	7.80	20.0	-2.10	1.0
34.0	0.51	2.49	0.20	+1.14	6.52	6.66	20.0	+4.75	1.0
35.0									
35.0	0.86	2.49	0.30	+1.50	7.60	7.72	20.0	-1.60	1.0
35.0	0.86	2.49	0.30	+1.47	7.20	7.34	20.0	-1.72	1.0
35.0	0.67	2.49	0.30	+1.59	6.21	6.42	16.0	+10.91	1.0
35.0	0.78	2.49	0.30	+1.15	7.91	8.00	12.0	-5.82	1.0
35.0	0.50	2.49	0.30	+1.66	8.11	8.22	20.0	-1.72	1.0
36.0									
36.0	0.51	2.49	0.50	+2.98	15.18	15.44	44.0	-13.50	2.0
36.0	0.48	2.49	0.50	+2.50	3.78	4.01	44.0	-2.20	2.0
36.0	0.70	2.49	0.50	+3.17	14.32	14.68	44.0	-1.10	2.0
36.0	0.29	2.49	0.50	+0.95	6.03	6.10	16.0	+9.30	1.0
37.0									
37.0	0.45	2.49	0.75	+0.13	4.22	4.22	20.0	+7.32	1.0
37.0	0.52	2.49	0.75	+0.13	4.22	4.22	20.0	+4.45	1.0
37.0	0.52	2.49	0.75	+0.13	4.16	4.16	20.0	+4.96	1.0
37.0	0.52	2.49	0.75	+0.29	9.29	9.29	44.0	-8.60	2.0
37.0	0.49	2.49	0.75	+0.11	4.35	4.35	20.0	-1.71	1.0
37.0	0.49	2.49	0.75	+0.09	4.36	4.36	20.0	-2.21	1.0
37.0	0.40	2.49	0.75	+0.17	9.26	9.26	36.0	-5.21	2.0
37.0	0.40	2.49	0.75	+0.12	5.08	5.08	16.0	+6.36	1.0
37.0	0.64	2.49	0.75	+0.18	10.37	10.37	40.0	-3.70	2.0
38.0									
38.0	0.29	2.49	1.00	-0.41	3.89	3.95	20.0	+5.52	1.0
38.0	0.29	2.49	1.00	-0.76	8.96	9.04	44.0	-4.60	2.0
38.0	0.78	2.49	1.00	-0.16	4.28	4.28	20.0	-6.60	1.0
38.0	0.78	2.49	1.00	-0.50	8.21	8.21	36.0	+3.98	2.0
38.0	0.69	2.49	1.00	-0.45	4.10	4.10	20.0	+0.00	1.0
38.0	0.69	2.49	1.00	-0.37	4.04	4.08	20.0	+0.67	1.0
38.0	0.48	2.49	1.00	-0.20	3.65	3.67	20.0	+7.88	1.0
38.0	0.48	2.49	1.00	-0.24	4.26	4.28	24.0	-9.42	1.0
38.0	0.39	2.49	1.00	-0.36	3.70	3.73	20.0	+8.11	1.0
38.0	0.39	2.49	1.00	-0.28	4.38	4.39	24.0	-9.71	1.0
38.0	0.39	2.49	1.00	-0.61	8.16	8.21	44.0	-1.58	2.0
39.0									
39.0	0.85	2.49	1.25	-0.52	3.80	3.88	16.0	+0.88	1.0
39.0	0.85	2.49	1.25	-0.52	3.86	3.98	32.0	+2.91	2.0
39.0	0.30	2.49	1.25	-0.61	3.29	3.35	16.0	+2.89	1.0
39.0	0.30	2.49	1.25	-0.62	3.46	3.51	32.0	+5.25	2.0
39.0	0.40	2.49	1.25	-0.53	3.45	3.48	16.0	+10.30	1.0
43.0									

43.0	0.48	2.02	0.05	+2.04	7.10	7.39	12.0	+4.03	1.0
43.0	0.49	2.02	0.05	+2.02	8.55	9.02	20.0	-4.31	1.0
43.0	0.45	2.02	0.05	+2.30	8.37	8.70	20.0	+7.40	1.0
43.0	0.40	2.02	0.05	+2.15	7.30	7.60	12.0	+1.08	1.0
43.0	0.90	2.02	0.05	+3.20	12.35	12.78	24.0	-1.02	1.0
43.0	1.02	2.02	0.05	+2.18	7.14	7.49	16.0	+4.17	1.0
43.0	0.55	2.02	0.05	+1.40	6.73	6.91	12.0	+3.21	1.0
43.0	0.82	2.02	0.05	+3.70	14.50	14.96	28.0	-1.66	2.0
43.0	0.61	2.02	0.05	+1.74	8.92	9.09	20.0	-4.70	1.0
44.0									
44.0	0.81	2.02	0.10	+2.41	7.35	7.75	16.0	-2.30	1.0
44.0	0.80	2.02	0.10	+2.61	7.69	8.09	20.0	+0.97	1.0
44.0	0.78	2.02	0.10	+2.32	5.72	6.10	16.0	+3.02	1.0
44.0	0.35	2.02	0.10	+2.65	7.98	8.40	20.0	-0.80	1.0
44.0	0.38	2.02	0.10	+2.70	6.99	7.31	12.0	+3.85	1.0
44.0	0.37	2.02	0.10	+2.89	8.11	8.60	20.0	-4.61	1.0
44.0	0.41	2.02	0.10	+2.62	6.30	6.81	12.0	+7.83	1.0
44.0	0.60	2.02	0.10	+1.95	6.99	7.27	16.0	-1.02	1.0
45.0									
45.0	0.50	2.02	0.17	+2.31	7.32	7.50	20.0	-6.79	1.0
45.0	0.60	2.02	0.17	+1.92	6.81	7.04	16.0	+2.99	1.0
45.0	0.65	2.02	0.17	+2.70	7.84	8.21	20.0	-1.95	1.0
45.0	0.68	2.02	0.17	+2.44	6.93	7.36	16.0	+2.81	1.0
45.0	0.73	2.02	0.17	+2.74	7.13	7.60	16.0	-6.91	1.0
45.0	0.45	2.02	0.17	+2.84	6.02	6.69	16.0	-2.04	1.0
45.0	0.35	2.02	0.17	+1.89	5.60	5.90	16.0	+3.52	1.0
45.0	0.62	2.02	0.17	+2.63	6.71	7.17	20.0	+2.00	1.0
46.0									
46.0	0.61	2.02	0.20	+1.80	6.48	6.73	20.0	-7.11	1.0
46.0	0.50	2.02	0.20	+1.75	6.40	6.65	12.0	+6.21	1.0
46.0	0.21	2.02	0.20	+1.54	6.65	6.91	12.0	+5.80	1.0
46.0	0.46	2.02	0.20	+1.72	6.82	7.05	12.0	+1.52	1.0
46.0	0.52	2.02	0.20	+1.90	8.49	8.76	20.0	-4.43	1.0
46.0	0.50	2.02	0.20	+1.95	5.89	6.20	16.0	+3.90	1.0
47.0									
47.0	0.65	2.02	0.30	+0.66	5.00	5.02	20.0	+1.60	1.0
47.0	0.70	2.02	0.30	+1.11	8.40	8.45	16.0	+8.80	2.0
47.0	0.68	2.02	0.30	+0.65	4.82	4.86	20.0	+3.75	1.0
47.0	0.92	2.02	0.30	+0.75	5.69	5.70	12.0	-6.46	1.0
47.0	0.72	2.02	0.30	+1.08	10.21	10.38	24.0	-0.72	2.0
47.0	0.36	2.02	0.30	+1.07	5.02	5.14	20.0	-2.25	1.0
47.0	0.72	2.02	0.30	+1.20	6.64	6.75	20.0	-6.34	1.0
48.0									
48.0	0.99	2.02	0.50	+1.19	5.85	5.99	16.0	+13.70	1.0
48.0	0.99	2.02	0.50	+1.52	7.20	7.36	20.0	-1.05	1.0
48.0	0.56	2.02	0.50	+0.90	5.91	6.00	12.0	+10.04	1.0
48.0	0.71	2.02	0.50	+1.02	6.39	6.44	16.0	+5.60	1.0
48.0	0.76	2.02	0.50	+0.52	5.80	5.80	16.0	+6.20	1.0
48.0	0.76	2.02	0.50	+0.88	7.39	7.43	20.0	-8.65	1.0
49.0									
49.0	0.70	2.02	0.75	+0.20	4.48	4.49	12.0	+0.91	1.0
49.0	0.42	2.02	0.75	+0.14	5.12	5.12	16.0	+0.36	1.0
49.0	0.50	2.02	0.75	+0.16	4.40	4.40	16.0	-5.05	1.0
49.0	0.55	2.02	0.75	+0.10	5.28	5.29	16.0	+1.92	1.0
49.0	0.32	2.02	0.75	+0.29	5.39	5.40	16.0	-6.26	1.0
50.0									
50.0	0.40	2.02	1.00	+0.09	3.99	3.99	8.0	+5.91	1.0

50.0	0.40	2.02	1.00	+0.11	4.08	4.08	8.0	+4.62	1.0
50.0	0.49	2.02	1.00	-0.07	4.40	4.40	16.0	-1.19	1.0
50.0	0.55	2.02	1.00	+0.10	4.78	4.78	12.0	+2.82	1.0
50.0	0.61	2.02	1.00	+0.09	4.41	4.41	12.0	+6.40	1.0
50.0	0.43	2.02	1.00	+0.10	5.13	5.13	12.0	-4.38	1.0
50.0	0.48	2.02	1.00	-0.09	4.79	4.79	12.0	+7.69	1.0
50.0	0.29	2.02	1.00	+0.11	4.58	4.58	12.0	+0.91	1.0
51.0									
51.0	0.80	2.02	1.33	-0.48	4.72	4.74	20.0	-6.21	1.0
51.0	0.46	2.02	1.33	-1.39	8.40	8.56	36.0	-0.19	2.0
51.0	0.99	2.02	1.33	-1.32	0.17	0.25	36.0	-4.82	2.0
51.0	1.00	2.02	1.33	-0.58	4.20	4.21	16.0	+5.28	1.0
51.0	0.46	2.02	1.33	-0.72	7.82	7.83	36.0	-0.19	2.0
51.0	0.56	2.02	1.33	-0.31	4.64	4.66	12.0	-0.52	1.0
51.0	0.38	2.02	1.33	-0.81	3.59	3.69	16.0	-9.26	1.0
51.0	0.38	2.02	1.33	-0.51	2.71	2.76	12.0	+7.02	1.0
51.0	0.38	2.02	1.33	-0.96	6.46	6.50	28.0	-1.83	2.0
52.0									
52.0	0.94	2.02	1.45	-1.87	8.02	8.30	36.0	+3.05	2.0
52.0	0.48	2.02	1.45	-2.12	8.12	8.38	36.0	+7.19	2.0
52.0	0.58	2.02	1.45	-1.61	7.72	7.88	36.0	+5.01	2.0
52.0	0.87	2.02	1.45	-1.22	5.08	5.21	20.0	-4.66	1.0
52.0	0.41	2.02	1.45	-1.51	9.19	9.32	28.0	-1.32	2.0
52.0	0.41	2.02	1.45	-1.71	13.04	13.19	44.0	+3.59	3.0
52.0	0.58	2.02	1.45	-1.49	7.96	8.11	36.0	+3.50	2.0
52.0	0.48	2.02	1.45	-0.88	3.99	4.09	16.0	+3.14	1.0
53.0									
53.0	0.52	2.02	1.50	-1.60	7.55	7.72	36.0	+0.06	2.0
53.0	0.92	2.02	1.50	-1.06	3.92	4.02	20.0	+3.71	1.0
53.0	0.39	2.02	1.50	-0.77	3.96	4.04	20.0	+3.91	1.0
53.0	0.55	2.02	1.50	-0.80	3.92	4.00	20.0	+3.35	1.0
53.0	0.71	2.02	1.50	-0.51	4.18	4.18	16.0	+6.15	1.0
53.0	0.38	2.02	1.50	-1.08	4.23	4.38	20.0	-3.50	1.0
53.0	0.60	2.02	1.50	-0.99	4.24	4.38	20.0	+4.40	1.0
55.0									
55.0	0.70	3.00	0.05	+1.82	7.69	7.90	20.0	-5.35	1.0
55.0	0.38	3.00	0.05	+2.48	7.90	8.30	16.0	-0.38	1.0
55.0	0.38	3.00	0.05	+2.38	7.29	7.61	20.0	+5.50	1.0
55.0	0.82	3.00	0.05	+2.21	7.89	8.21	20.0	-5.39	1.0
55.0	0.52	3.00	0.05	+1.88	7.46	7.71	20.0	-2.65	1.0
55.0	0.43	3.00	0.05	+2.95	8.05	8.61	16.0	-5.62	1.0
55.0	0.56	3.00	0.05	+1.42	6.60	6.75	16.0	-8.49	1.0
55.0	0.95	3.00	0.05	+2.55	7.55	8.00	20.0	+5.30	1.0
55.0	0.60	3.00	0.05	+2.25	7.60	7.92	20.0	+2.50	1.0
56.0									
56.0	0.66	3.00	0.10	+2.00	7.71	8.00	20.0	+6.80	1.0
56.0	0.65	3.00	0.10	+2.15	6.59	6.91	20.0	+1.49	1.0
56.0	0.65	3.00	0.10	+2.55	8.29	8.71	24.0	-7.70	1.0
56.0	0.52	3.00	0.10	+2.21	7.50	7.83	16.0	+3.08	1.0
56.0	0.79	3.00	0.10	+2.13	6.88	7.21	20.0	+5.10	1.0
56.0	0.45	3.00	0.10	+2.47	7.56	7.96	20.0	+7.35	1.0
56.0	0.51	3.00	0.10	+2.13	7.09	7.40	20.0	+10.00	1.0
56.0	0.56	3.00	0.10	+2.80	9.02	9.49	24.0	-8.00	1.0
57.0									
57.0	0.49	3.00	0.15	+2.10	7.31	7.52	16.0	+3.89	1.0
57.0	0.68	3.00	0.15	+2.29	6.41	6.81	16.0	+9.40	1.0
57.0	0.69	3.00	0.15	+2.38	7.40	7.76	16.0	-0.65	1.0

57.0	0.73	3.00	0.15	+2.21	7.99	8.35	16.0	+4.32	1.0
57.0	1.10	3.00	0.15	+1.44	7.47	7.60	20.0	-0.47	1.0
57.0	0.56	3.00	0.15	+1.92	7.70	7.91	20.0	+1.25	1.0
57.0	0.68	3.00	0.15	+1.05	6.98	7.29	20.0	-8.40	1.0
58.0									
58.0	0.68	3.00	0.20	+1.74	6.34	6.55	20.0	+0.41	1.0
58.0	0.75	3.00	0.20	+2.10	7.70	8.02	16.0	+0.00	1.0
58.0	0.36	3.00	0.20	+1.35	7.08	7.21	20.0	+4.28	1.0
58.0	0.64	3.00	0.20	+2.15	7.35	7.66	20.0	+7.21	1.0
58.0	0.48	3.00	0.20	+4.71	11.83	14.38	44.0	+0.82	2.0
58.0	0.58	3.00	0.20	+1.96	6.31	6.61	20.0	+4.89	1.0
58.0	0.68	3.00	0.20	+1.91	6.12	6.44	20.0	+3.20	1.0
59.0									
59.0	0.68	3.00	0.25	+1.12	5.92	6.02	20.0	-8.32	1.0
59.0	0.42	3.00	0.25	+1.92	7.58	7.81	20.0	+6.91	1.0
59.0	0.60	3.00	0.25	+1.85	8.34	8.54	20.0	+1.72	1.0
59.0	0.74	3.00	0.25	+1.67	7.45	7.66	20.0	+2.80	1.0
59.0	0.72	3.00	0.25	+1.05	7.55	7.62	20.0	+0.03	1.0
59.0	0.65	3.00	0.25	+1.96	7.90	8.15	20.0	+2.02	1.0
59.0	0.69	3.00	0.25	+1.00	5.19	5.30	12.0	-3.11	1.0
59.0	0.45	3.00	0.25	+1.00	5.16	5.28	16.0	+2.62	1.0
60.0									
60.0	0.60	3.00	0.50	+0.72	7.73	7.80	20.0	-9.11	1.0
60.0	0.55	3.00	0.50	+1.42	13.22	13.32	40.0	+6.85	2.0
60.0	0.55	3.00	0.50	+0.49	6.22	6.30	16.0	+3.97	2.0
60.0	0.70	3.00	0.50	+0.99	7.51	7.55	24.0	-7.90	1.0
60.0	0.42	3.00	0.50	+0.50	6.00	6.03	20.0	+1.00	1.0
60.0	0.50	3.00	0.50	+0.79	6.66	6.70	20.0	+1.42	1.0
60.0	0.60	3.00	0.50	+0.42	6.81	6.86	24.0	-7.82	1.0
60.0	0.83	3.00	0.50	+1.00	8.14	8.20	12.0	-4.45	1.0
60.0	0.79	3.00	0.50	+0.99	7.66	7.72	20.0	-3.50	1.0
61.0									
61.0	0.50	3.00	1.00	-0.42	8.70	8.71	44.0	-0.81	2.0
61.0	0.52	3.00	1.00	-0.29	2.92	2.94	20.0	+0.36	1.0
61.0	0.52	3.00	1.00	-0.20	4.69	4.70	24.0	-7.76	1.0
61.0	0.52	3.00	1.00	-0.35	4.30	4.36	16.0	+5.84	1.0
61.0	0.51	3.00	1.00	-0.18	4.48	4.48	24.0	-6.65	1.0
61.0	0.51	3.00	1.00	-0.19	3.85	3.85	20.0	+7.61	1.0
61.0	0.58	3.00	1.00	-0.24	4.60	4.60	16.0	-2.50	1.0
61.0	0.50	3.00	1.00	-0.20	4.51	4.53	24.0	-7.61	1.0
61.0	0.59	3.00	1.00	-0.21	3.95	3.96	20.0	+6.89	1.0
61.0	0.78	3.00	1.00	-0.59	8.55	8.56	36.0	+1.18	2.0
62.0									
62.0	0.86	3.00	1.25	-0.58	4.72	4.79	24.0	-7.88	1.0
62.0	0.65	3.00	1.25	-0.56	3.70	3.73	20.0	-6.22	1.0
62.0	0.55	3.00	1.25	-0.73	4.09	4.15	20.0	-1.92	1.0
62.0	0.48	3.00	1.25	-0.57	2.44	2.46	20.0	+0.69	1.0
62.0	0.69	3.00	1.25	-0.50	3.89	3.94	16.0	-1.88	1.0
62.0	0.68	3.00	1.25	-0.57	4.06	4.11	16.0	-2.36	1.0
62.0	0.68	3.00	1.25	-0.62	4.20	4.29	16.0	-1.96	1.0
62.0	0.76	3.00	1.25	-0.64	4.25	4.30	24.0	-11.92	1.0
63.0									
63.0	0.65	3.00	1.35	-0.69	4.20	4.26	16.0	+6.35	1.0
63.0	0.61	3.00	1.35	-1.35	9.01	9.14	44.0	+1.56	2.0
63.0	0.55	3.00	1.35	-0.46	3.65	3.71	20.0	+7.72	1.0
63.0	0.58	3.00	1.35	-1.17	7.50	7.58	44.0	-3.01	2.0
63.0	0.65	3.00	1.35	-0.58	3.41	3.42	20.0	-3.44	1.0

63.0	0.75	3.00	1.35	-0.47	3.45	3.50	20.0	+5.51	1.0
63.0	0.30	3.00	1.35	-0.55	3.70	3.72	20.0	+3.19	1.0
63.0	0.61	3.00	1.35	-0.80	4.03	4.15	20.0	+1.21	1.0
63.0	0.65	3.00	1.35	-0.80	4.65	4.71	20.0	-5.31	1.0
63.0	0.48	3.00	1.35	-0.71	4.45	4.55	16.0	-6.72	1.0
64.0									
64.0	0.78	3.00	1.40	-1.06	3.71	3.89	20.0	+5.97	1.0
64.0	0.66	3.00	1.40	-0.72	3.80	3.92	20.0	+0.00	1.0
64.0	0.80	3.00	1.40	-0.41	4.42	4.49	24.0	-0.68	1.0
64.0	0.60	3.00	1.40	-0.40	2.90	2.93	20.0	+0.62	1.0
64.0	0.51	3.00	1.40	-1.79	7.50	7.76	44.0	+0.000	2.0
64.0	0.50	3.00	1.40	-0.60	3.74	3.79	20.0	-6.50	1.0
64.0	0.72	3.00	1.40	-0.52	3.40	3.46	20.0	+5.48	1.0
64.0	0.53	3.00	1.40	-1.54	6.10	6.20	44.0	+1.14	2.0
64.0	0.60	3.00	1.40	-0.80	3.20	3.30	20.0	+2.72	1.0
64.0	0.58	3.00	1.40	-0.60	3.86	3.90	20.0	+7.38	1.0
64.0	0.79	3.00	1.40	-0.82	3.63	3.85	24.0	-7.70	1.0
66.0									
66.0	0.50	3.51	0.05	+2.21	8.28	8.61	24.0	-8.06	1.0
66.0	0.64	3.51	0.05	+2.32	8.28	8.69	20.0	-2.82	1.0
66.0	0.50	3.51	0.05	+1.61	7.58	7.82	16.0	+2.30	1.0
66.0	0.00	3.51	0.05	+1.00	8.48	8.69	24.0	-7.81	1.0
66.0	0.85	3.51	0.05	+1.06	6.69	7.01	20.0	+7.34	1.0
67.0									
67.0	0.60	3.51	0.10	+2.12	7.51	7.83	20.0	+6.00	1.0
67.0	0.52	3.51	0.10	+2.32	7.12	7.51	16.0	+3.36	1.0
67.0	0.96	3.51	0.10	+2.21	6.21	6.64	20.0	+6.82	1.0
67.0	0.60	3.51	0.10	+2.45	6.63	7.10	12.0	-1.44	1.0
67.0	0.60	3.51	0.10	+1.80	6.50	6.76	20.0	+8.21	1.0
67.0	0.70	3.51	0.10	+2.46	6.98	7.48	16.0	+0.24	1.0
67.0	0.40	3.51	0.10	+1.60	5.70	5.92	20.0	+7.89	1.0
67.0	0.96	3.51	0.10	+2.11	7.29	7.61	20.0	+5.52	1.0
67.0	0.68	3.51	0.10	+2.50	7.61	8.08	20.0	-0.99	1.0
67.0	0.89	3.51	0.10	+2.22	6.52	6.97	20.0	+7.37	1.0
68.0									
68.0	0.40	3.51	0.15	+2.50	6.91	7.38	24.0	-10.78	1.0
68.0	0.51	3.51	0.15	+1.88	5.31	5.71	20.0	-5.58	1.0
68.0	0.60	3.51	0.15	+1.61	7.30	7.30	16.0	-0.32	1.0
68.0	0.52	3.51	0.15	+1.98	5.60	5.98	20.0	+8.76	1.0
68.0	0.56	3.51	0.15	+1.81	5.86	6.09	20.0	+3.07	1.0
68.0	0.58	3.51	0.15	+2.21	7.20	7.58	24.0	-8.05	1.0
68.0	0.62	3.51	0.15	+1.22	6.22	6.32	20.0	+5.55	1.0
68.0	0.38	3.51	0.15	+2.12	6.18	6.58	20.0	-2.57	1.0
70.0									
70.0	0.61	3.51	0.25	+1.49	11.01	11.11	44.0	+1.11	2.0
70.0	0.55	3.51	0.25	+0.81	5.61	5.65	20.0	+1.05	1.0
70.0	0.38	3.51	0.25	+0.40	4.32	4.35	20.0	+8.60	1.0
70.0	0.70	3.51	0.25	+1.20	5.47	5.63	20.0	+8.42	1.0
70.0	0.72	3.51	0.25	+1.51	6.92	7.12	24.0	-7.48	1.0
70.0	0.48	3.51	0.25	+1.45	10.30	10.40	28.0	-7.32	2.0
71.0									
71.0	0.59	3.51	0.50	+1.58	7.99	8.17	24.0	-11.00	1.0
71.0	0.77	3.51	0.50	+0.52	6.72	6.79	20.0	-4.40	1.0
71.0	0.47	3.51	0.50	+0.60	6.95	6.97	20.0	-3.18	1.0
71.0	0.00	3.51	0.50	+0.71	0.52	0.55	40.0	-1.38	2.0
71.0	0.50	3.51	0.50	+0.48	6.40	6.44	20.0	+1.30	1.0
71.0	0.60	3.51	0.50	+0.00	5.40	5.40	20.0	+7.27	1.0

71.0	0.55	3.51	0.50	+0.16	5.41	5.41	20.0	+0.52	1.0
71.0	0.35	3.51	0.50	+0.37	6.12	6.13	20.0	+3.20	1.0
71.0	0.35	3.51	0.50	+0.26	6.02	6.05	20.0	+2.80	1.0
72.0									
72.0	0.40	3.51	0.75	+0.11	4.80	4.80	20.0	0.35	1.0
72.0	0.40	3.51	0.75	+0.29	4.71	4.71	20.0	+0.28	1.0
72.0	0.45	3.51	0.75	+0.25	5.10	5.10	20.0	-0.85	1.0
72.0	0.45	3.51	0.75	+0.18	4.13	4.13	16.0	+7.80	1.0
72.0	0.69	3.51	0.75	+0.09	9.20	9.20	44.0	-5.56	2.0
72.0	0.80	3.51	0.75	+0.10	5.40	5.40	24.0	-0.21	1.0
72.0	0.40	3.51	0.75	+0.28	9.00	9.00	44.0	-0.60	2.0
72.0	0.45	3.51	0.75	+0.26	9.21	9.25	44.0	-0.72	2.0
72.0	0.43	3.51	0.75	+0.20	4.31	4.31	20.0	-0.85	1.0
72.0	0.43	3.51	0.75	+0.27	4.38	4.38	20.0	+1.19	1.0
72.0	0.60	3.51	0.75	+0.19	4.08	4.08	20.0	+7.27	1.0
73.0									
73.0	0.49	3.51	1.00	-1.29	8.42	8.50	44.0	+1.25	2.0
73.0	0.51	3.51	1.00	-1.18	8.06	8.16	44.0	+1.39	2.0
73.0	0.55	3.51	1.00	-0.48	4.30	4.33	24.0	-7.70	1.0
73.0	0.55	3.51	1.00	-0.31	3.49	3.51	20.0	+0.49	1.0
73.0	0.55	3.51	1.00	-0.29	4.41	4.41	24.0	-7.66	1.0
73.0	0.67	3.51	1.00	-0.40	4.40	4.44	24.0	-0.04	1.0
73.0	0.67	3.51	1.00	-0.40	3.90	3.95	20.0	+8.99	1.0
73.0	0.62	3.51	1.00	-0.55	3.72	3.79	20.0	+9.11	1.0
73.0	0.80	3.51	1.00	-1.39	8.11	8.25	44.0	+0.30	2.0
73.0	0.40	3.51	1.00	-1.00	7.94	7.93	44.0	+1.70	2.0
73.0	0.48	3.51	1.00	-0.66	8.50	8.55	44.0	-1.30	2.0
73.0	0.61	3.51	1.00	-1.05	12.15	12.30	68.0	-8.06	3.0
73.0	0.59	3.51	1.00	-0.50	4.46	4.49	24.0	-0.50	1.0
74.0									
74.0	0.42	3.51	1.25	-1.08	7.60	7.74	44.0	+2.26	2.0
74.0	0.45	3.51	1.25	-0.66	4.02	4.10	20.0	+6.69	1.0
74.0	0.51	3.51	1.25	-0.69	3.62	3.71	20.0	+0.30	1.0
74.0	0.51	3.51	1.25	-0.71	3.52	3.61	20.0	+8.12	1.0
74.0	0.62	3.51	1.25	-0.59	4.40	4.42	24.0	-8.20	1.0
74.0	0.55	3.51	1.25	-1.62	6.01	6.15	44.0	+0.34	2.0
74.0	0.55	3.51	1.25	-0.86	3.28	3.29	24.0	-0.32	1.0
74.0	0.40	3.51	1.25	-0.53	3.64	3.70	20.0	+6.58	1.0
74.0	0.55	3.51	1.25	-0.93	4.17	4.25	24.0	-7.70	1.0
74.0	0.55	3.51	1.25	-0.92	3.50	3.60	20.0	+0.40	1.0
74.0	0.81	3.51	1.25	-0.89	3.83	4.00	20.0	+7.71	1.0
74.0	0.59	3.51	1.25	-2.10	7.98	8.28	44.0	+1.61	2.0
74.0	0.70	3.51	1.25	-1.40	8.04	8.10	44.0	-0.74	2.0
75.0									
75.0	0.55	3.51	1.25	-0.85	3.46	3.58	16.0	-0.77	1.0
75.0	0.45	3.51	1.25	-0.85	3.71	3.80	20.0	+4.11	1.0
75.0	0.51	3.51	1.25	-0.68	4.35	4.41	20.0	-2.09	1.0
75.0	0.51	3.51	1.25	-0.79	4.29	4.37	20.0	-1.96	1.0
75.0	0.80	3.51	1.25	-0.64	3.75	3.80	20.0	+8.62	1.0
75.0	0.78	3.51	1.25	-0.71	4.32	4.40	24.0	-0.08	1.0
75.0	0.40	3.51	1.25	-0.76	4.35	4.46	24.0	-8.02	1.0
75.0	0.40	3.51	1.25	-0.73	3.68	3.75	20.0	+8.12	1.0
75.0	0.45	3.51	1.25	-0.86	4.62	4.70	24.0	-0.16	1.0
75.0	0.55	3.51	1.25	-1.05	3.55	3.70	20.0	+7.90	1.0
75.0	0.55	3.51	1.25	-0.60	4.52	4.58	24.0	-8.65	1.0
75.0	0.42	3.51	1.25	-0.95	3.65	3.76	20.0	+7.70	1.0
75.0	0.56	3.51	1.25	-1.45	4.76	5.00	24.0	-10.30	1.0

75.0	0.55	3.51	1.25	-0.60	3.82	3.90	20.0	+0.15	1.0
94.0									
94.0	0.50	1.51	1.30	-1.40	3.61	3.96	2.00	-1.35	1.0
94.0	0.56	1.51	1.30	-1.90	5.52	5.86	16.0	-1.30	1.0
94.0	0.47	1.51	1.30	-2.10	4.92	5.41	24.0	-10.00	1.0
94.0	0.32	1.51	1.30	-1.75	4.14	4.50	16.0	-6.36	1.0
94.0	0.60	1.51	1.30	-2.28	4.10	4.80	24.0	-10.35	1.0
94.0	0.45	1.51	1.30	-2.31	4.59	5.10	12.0	+1.80	1.0
94.0	0.49	1.51	1.30	-1.17	4.02	4.21	20.0	+3.40	1.0
94.0	0.49	1.51	1.30	-1.40	4.95	5.11	12.0	-0.71	1.0
94.0	0.51	1.51	1.30	-1.35	5.30	5.50	20.0	+2.55	1.0
94.0	0.36	1.51	1.30	-0.87	4.26	4.41	12.0	+4.00	1.0
94.0	0.45	1.51	1.30	-0.72	3.85	3.95	20.0	-2.13	1.0
94.0	0.50	1.51	1.30	-0.76	3.61	3.72	12.0	+5.56	1.0
95.0									
95.0	0.51	1.51	1.30	-1.40	4.90	5.09	16.0	+0.00	1.0
95.0	0.57	1.51	1.30	-0.86	4.16	4.30	20.0	-2.71	1.0
95.0	0.58	1.51	1.30	-1.31	3.99	4.21	20.0	+7.10	1.0
95.0	0.59	1.51	1.30	-1.98	0.79	10.02	20.0	-0.81	2.0
95.0	0.60	1.51	1.30	-1.26	4.61	4.80	16.0	-0.51	1.0
95.0	0.52	1.51	1.30	-0.72	3.79	3.86	16.0	+7.15	1.0
95.0	0.64	1.51	1.30	-3.08	8.18	8.73	20.0	10.58	2.0
95.0	0.55	1.51	1.30	-1.08	4.81	4.96	24.0	-7.06	1.0
96.0									
96.0	0.61	1.51	1.50	-1.21	3.59	3.80	16.0	+0.65	1.0
96.0	0.71	1.51	1.50	-0.81	3.91	4.01	20.0	-1.12	1.0
96.0	0.44	1.51	1.50	-1.08	4.28	4.43	20.0	-3.07	1.0
96.0	0.50	1.51	1.50	-1.80	4.71	5.00	20.0	+2.75	1.0
96.0	0.60	1.51	1.50	-1.20	3.41	3.66	20.0	-0.47	1.0
96.0	0.59	1.51	1.50	-1.35	4.90	5.10	20.0	-3.07	1.0
96.0	0.55	1.51	1.50	-0.90	4.51	4.62	20.0	+1.50	1.0
78.0									
78.0	0.84	1.00	0.64	-0.30	2.79	2.80	24.0	-8.58	1.0
78.0	0.84	1.00	0.64	-0.19	2.51	2.52	20.0	+9.48	1.0
78.0	0.84	1.00	0.64	-0.21	2.39	2.41	24.0	-8.40	1.0
78.0	0.58	1.00	0.64	-0.18	2.45	2.48	20.0	+9.32	1.0
78.0	0.81	1.00	0.64	-0.43	2.81	2.86	20.0	+7.10	1.0
78.0	0.61	1.00	0.64	-0.55	2.98	3.02	20.0	+9.94	1.0
79.0									
79.0	0.56	1.00	0.80	-0.79	3.69	3.79	24.0	-8.59	1.0
79.0	0.56	1.00	0.80	-0.72	2.89	2.97	20.0	+9.25	1.0
79.0	0.64	1.00	0.80	-0.70	2.77	2.92	16.0	-5.02	1.0
79.0	0.64	1.00	0.80	-1.24	5.52	5.67	28.0	-7.62	2.0
79.0	1.02	1.00	0.80	-1.02	4.29	4.40	20.0	+2.10	1.0
79.0	1.02	1.00	0.80	-0.92	4.40	4.51	20.0	+2.21	1.0
79.0	1.02	1.00	0.80	-1.11	4.78	4.91	20.0	+2.00	1.0
80.0									
80.0	0.47	1.00	1.00	-1.20	3.69	3.88	20.0	+9.92	1.0
80.0	0.47	1.00	1.00	-1.11	4.21	4.38	24.0	-9.10	1.0
80.0	0.40	1.00	1.00	-1.68	7.60	7.78	28.0	+10.31	2.0
80.0	0.49	1.00	1.00	-1.29	3.69	3.91	12.0	+2.83	1.0
80.0	0.95	1.00	1.00	-0.85	3.22	3.34	8.0	+6.06	1.0
80.0	0.38	1.00	1.00	-1.42	3.93	4.17	20.0	+1.08	1.0
80.0	0.59	1.00	1.00	-0.97	3.72	3.85	16.0	-3.67	1.0
80.0	0.59	1.00	1.00	-0.67	2.88	2.95	12.0	+9.01	1.0
80.0	0.56	1.00	1.00	-1.38	3.29	3.58	20.0	+4.80	1.0
80.0	0.94	1.00	1.00	-1.68	3.50	3.90	20.0	-7.65	1.0

80.0	0.94	1.00	1.00	-1.11	2.98	3.17	16.0	+10.20	1.0
81.0									
81.0	0.81	1.00	1.20	-0.88	3.48	3.60	16.0	+2.19	1.0
81.0	0.84	1.00	1.20	-1.66	4.12	4.46	16.0	+5.74	1.0
81.0	0.39	1.00	1.20	-1.90	4.21	4.71	12.0	+2.78	1.0
81.0	0.56	1.00	1.20	-1.32	3.64	3.90	16.0	-6.10	1.0
81.0	0.81	1.00	1.20	-1.50	8.62	8.78	36.0	+8.00	2.0
81.0	0.72	1.00	1.20	-2.00	10.01	10.45	32.0	+11.10	2.0
81.0	0.76	1.00	1.20	-0.67	4.92	5.00	16.0	-1.81	1.0
81.0	0.79	1.00	1.20	-0.78	4.02	4.12	16.0	-1.64	1.0
81.0	0.79	1.00	1.20	-0.61	3.76	3.81	16.0	-1.90	1.0
81.0	0.76	1.00	1.20	-1.70	5.90	6.12	36.0	+7.98	2.0
82.0									
82.0	0.88	1.00	1.40	-1.18	4.79	4.92	24.0	-13.02	1.0
82.0	0.68	1.00	1.40	-0.70	3.80	3.90	16.0	+4.25	1.0
82.0	0.68	1.00	1.40	-0.97	3.61	3.72	16.0	+4.26	1.0
82.0	0.82	1.00	1.40	-0.97	3.09	3.21	12.0	+8.24	1.0
82.0	0.82	1.00	1.40	-1.20	3.65	3.80	16.0	-0.64	1.0
82.0	0.72	1.00	1.40	-1.06	4.01	4.18	16.0	+3.98	1.0
82.0	0.72	1.00	1.40	-1.16	3.90	4.09	16.0	+4.24	1.0
82.0	0.57	1.00	1.40	-0.82	3.64	3.74	20.0	-7.78	1.0
82.0	0.57	1.00	1.40	-0.51	2.80	2.82	16.0	+8.76	1.0
82.0	0.72	1.00	1.40	-1.20	4.01	4.21	16.0	+2.20	1.0
82.0	0.45	1.00	1.40	-1.80	4.34	4.70	16.0	-6.30	1.0
82.0	0.70	1.00	1.40	-1.28	4.14	4.40	16.0	+0.00	1.0
82.0	0.70	1.00	1.40	-1.24	4.02	4.22	16.0	+0.51	1.0
83.0									
83.0	0.64	1.00	1.50	-1.26	5.05	5.18	20.0	-13.22	1.0
83.0	0.52	1.00	1.50	-0.86	4.20	4.29	20.0	+4.79	1.0
83.0	0.59	1.00	1.50	-0.99	4.70	4.80	12.0	+6.20	1.0
83.0	0.61	1.00	1.50	-1.62	5.09	5.31	24.0	-7.61	1.0
83.0	0.71	1.00	1.50	-1.47	4.19	4.48	24.0	-8.06	1.0
83.0	0.60	1.00	1.50	-1.68	4.72	5.03	12.0	+4.96	1.0
85.0									
85.0	0.41	1.51	0.10	+0.61	5.36	5.40	12.0	+7.07	1.0
85.0	0.41	1.51	0.10	+0.60	6.96	7.03	16.0	-8.26	1.0
85.0	0.41	1.51	0.10	+0.37	4.90	4.95	12.0	+11.32	1.0
85.0	0.61	1.51	0.10	+0.70	5.29	5.32	12.0	+5.16	1.0
85.0	0.61	1.51	0.10	+0.70	5.68	5.71	12.0	+5.21	1.0
85.0	0.61	1.51	0.10	+1.00	7.22	7.84	16.0	-13.38	1.0
85.0	1.00	1.51	0.10	+2.39	7.78	8.15	16.0	-7.10	1.0
85.0	0.34	1.51	0.10	+0.53	5.16	5.22	20.0	+8.62	1.0
85.0	0.60	1.51	0.10	+0.50	5.55	5.60	12.0	-2.65	1.0
85.0	0.60	1.51	0.10	+0.41	6.00	6.02	12.0	-2.22	1.0
85.0	0.60	1.51	0.10	+0.43	5.94	5.98	12.0	-2.11	1.0
85.0	0.72	1.51	0.10	+0.62	5.62	5.63	16.0	+1.21	1.0
85.0	0.72	1.51	0.10	+0.64	5.02	5.00	16.0	+1.66	1.0
85.0	0.70	1.51	0.10	+1.62	5.90	6.12	16.0	+5.90	1.0
85.0	1.05	1.51	0.10	+1.31	6.12	6.27	20.0	+0.00	1.0
86.0									
86.0	0.69	1.51	0.20	+0.91	5.42	5.51	20.0	+7.48	1.0
86.0	0.75	1.51	0.20	+0.66	8.02	8.08	32.0	+5.01	2.0
86.0	0.75	1.51	0.20	+0.37	4.40	4.44	16.0	+2.70	1.0
86.0	0.75	1.51	0.20	+0.26	4.36	4.40	16.0	+3.22	1.0
86.0	0.72	1.51	0.20	+0.66	4.68	4.70	16.0	+2.02	1.0
86.0	0.72	1.51	0.20	+0.68	4.72	4.76	16.0	+2.85	1.0
86.0	0.30	1.51	0.20	+1.20	5.03	5.07	16.0	+1.80	1.0

86.0	0.30	1.51	0.20	+1.22	6.70	6.82	16.0	-1.62	1.0
86.0	0.50	1.51	0.20	+0.25	5.48	5.49	20.0	-1.90	1.0
86.0	0.50	1.51	0.20	+0.25	5.78	5.79	20.0	-1.70	1.0
86.0	0.60	1.51	0.20	+0.81	10.51	10.56	36.0	-7.91	2.0
86.0	0.50	1.51	0.20	+0.40	5.75	5.76	20.0	-2.44	1.0
86.0	0.50	1.51	0.20	+0.02	0.89	0.95	40.0	-10.70	2.0
86.0	0.50	1.51	0.20	+0.66	4.70	4.70	16.0	-3.72	1.0
86.0	0.50	1.51	0.20	+0.57	4.72	4.80	16.0	-3.52	1.0
86.0	0.30	1.51	0.20	+1.18	5.88	5.97	16.0	-0.14	1.0
87.0									
87.0	0.62	1.51	0.30	+0.39	4.54	4.56	12.0	+3.50	1.0
87.0	0.62	1.51	0.30	+0.36	4.65	4.66	12.0	+4.00	1.0
87.0	0.62	1.51	0.30	+0.31	4.61	4.62	12.0	+4.08	1.0
87.0	0.67	1.51	0.30	+0.40	5.75	5.77	20.0	-5.80	1.0
87.0	0.67	1.51	0.30	+0.54	6.29	6.31	20.0	-4.70	1.0
87.0	0.87	1.51	0.30	+0.12	4.50	4.50	12.0	+2.70	1.0
87.0	0.87	1.51	0.30	+0.10	4.50	4.50	12.0	+2.72	1.0
87.0	0.52	1.51	0.30	+0.32	5.60	5.60	20.0	-2.89	1.0
87.0	0.52	1.51	0.30	+0.32	5.91	5.95	20.0	-2.64	1.0
87.0	0.75	1.51	0.30	+0.61	4.51	4.59	16.0	-4.00	1.0
87.0	0.92	1.51	0.30	+0.58	8.30	8.31	20.0	+0.60	2.0
87.0	0.92	1.51	0.30	+0.50	5.17	5.20	12.0	-3.92	1.0
87.0	0.62	1.51	0.30	+0.62	10.89	10.95	32.0	-7.90	2.0
87.0	0.70	1.51	0.30	+0.41	5.86	5.87	20.0	-0.52	1.0
87.0	0.70	1.51	0.30	+0.53	6.24	6.25	20.0	-0.15	1.0
87.0	0.50	1.51	0.30	+0.46	5.16	5.17	20.0	-2.00	1.0
87.0	0.50	1.51	0.30	+0.37	4.22	4.29	16.0	+9.23	1.0
88.0									
88.0	0.70	1.51	0.30	+0.33	4.81	4.82	20.0	+1.12	1.0
88.0	0.70	1.51	0.30	+0.32	4.92	4.93	20.0	-0.20	1.0
88.0	0.70	1.51	0.30	+0.45	5.12	5.13	20.0	+0.10	1.0
88.0	0.46	1.51	0.30	+1.20	0.52	0.59	28.0	-5.91	2.0
88.0	0.70	1.51	0.30	+0.72	0.19	0.20	44.0	+2.14	2.0
88.0	0.52	1.51	0.30	+0.40	5.35	5.37	16.0	-2.76	1.0
88.0	0.52	1.51	0.30	+0.42	5.62	5.63	16.0	-2.39	1.0
88.0	0.52	1.51	0.30	+0.51	5.75	5.76	16.0	-1.75	1.0
88.0	0.80	1.51	0.30	+0.70	4.89	4.91	16.0	-3.66	1.0
88.0	0.80	1.51	0.30	+0.87	6.00	6.04	20.0	-21.34	1.0
88.0	0.80	1.51	0.30	+0.48	4.80	4.85	12.0	-3.90	1.0
88.0	0.80	1.51	0.30	+0.45	4.76	4.77	12.0	-3.80	1.0
88.0	0.80	1.51	0.30	+0.92	8.12	8.16	20.0	+11.12	2.0
88.0	0.68	1.51	0.30	+0.60	5.62	5.66	20.0	-1.90	1.0
88.0	0.68	1.51	0.30	+0.60	5.99	6.02	20.0	-1.50	1.0
88.0	0.50	1.51	0.30	+0.04	0.38	0.42	40.0	11.63	2.0
89.0									
89.0	0.58	1.51	0.50	+0.32	4.77	4.78	20.0	-6.58	1.0
89.0	0.58	1.51	0.50	+0.25	3.97	3.99	16.0	+11.73	1.0
89.0	0.58	1.51	0.50	+0.39	4.91	4.94	20.0	-6.62	1.0
89.0	0.58	1.51	0.50	+0.52	4.96	4.98	20.0	-6.30	1.0
89.0	0.66	1.51	0.50	+0.30	4.50	4.51	16.0	-1.88	1.0
89.0	0.66	1.51	0.50	+0.40	4.41	4.42	16.0	-1.92	1.0
89.0	0.66	1.51	0.50	+0.55	4.55	4.60	16.0	-1.84	1.0
89.0	0.76	1.51	0.50	+0.40	4.22	4.25	12.0	+2.68	1.0
89.0	0.76	1.51	0.50	+0.48	4.28	4.29	12.0	+2.10	1.0
89.0	0.39	1.51	0.50	+0.29	4.72	4.78	12.0	-2.92	1.0
89.0	0.39	1.51	0.50	+0.26	4.69	4.70	12.0	-2.52	1.0
89.0	0.38	1.51	0.50	+0.21	4.16	4.17	16.0	-5.00	1.0

89.0	0.62	1.51	0.50	+0.42	4.40	4.41	12.0	-0.66	1.0
89.0	0.62	1.51	0.50	+0.40	4.38	4.40	12.0	-0.55	1.0
89.0	0.62	1.51	0.50	+0.42	4.31	4.33	12.0	-0.61	1.0
89.0	0.62	1.51	0.50	+0.42	4.38	4.39	12.0	-0.55	1.0
89.0	0.73	1.51	0.50	+0.22	4.65	4.66	20.0	-7.50	1.0
89.0	0.73	1.51	0.50	+0.18	3.80	3.80	16.0	+10.42	1.0
89.0	0.73	1.51	0.50	+0.27	4.90	4.90	20.0	-7.68	1.0
89.0	0.41	1.51	0.50	+0.19	3.90	3.90	12.0	+3.85	1.0
89.0	0.41	1.51	0.50	+0.30	3.80	3.80	12.0	+3.62	1.0
89.0	0.41	1.51	0.50	+0.30	3.80	3.81	12.0	+4.52	1.0
89.0	0.41	1.51	0.50	+0.68	0.25	0.32	28.0	-0.71	2.0
90.0									
90.0	0.60	1.51	0.70	+0.06	4.01	4.01	16.0	+4.10	1.0
90.0	0.60	1.51	0.70	+0.00	0.21	0.21	36.0	-0.21	2.0
90.0	0.60	1.51	0.70	+0.08	3.94	3.94	16.0	+4.46	1.0
90.0	0.45	1.51	0.70	+0.23	4.01	4.01	16.0	+5.02	1.0
90.0	0.45	1.51	0.70	+0.26	5.10	5.11	20.0	-11.45	1.0
90.0	0.45	1.51	0.70	+0.41	3.89	3.90	16.0	+5.06	1.0
90.0	0.45	1.51	0.70	+0.40	4.01	4.02	16.0	+5.62	1.0
90.0	0.40	1.51	0.70	0.80	12.69	12.71	52.0	+3.69	3.0
90.0	0.40	1.51	0.70	+0.30	4.68	4.68	20.0	-11.12	1.0
90.0	0.52	1.51	0.70	+0.07	4.40	4.40	20.0	+3.66	1.0
90.0	0.52	1.51	0.70	+0.06	4.10	4.10	20.0	+3.40	1.0
90.0	0.52	1.51	0.70	+0.38	3.90	3.95	20.0	+8.69	1.0
90.0	0.86	1.51	0.70	+0.01	8.25	8.32	28.0	+2.30	2.0
90.0	0.41	1.51	0.70	+0.28	4.45	4.46	16.0	-3.90	1.0
90.0	0.41	1.51	0.70	+0.35	4.46	4.50	16.0	-4.15	1.0
90.0	0.41	1.51	0.70	+0.41	7.01	7.02	28.0	+0.10	2.0
91.0									
91.0	0.56	1.51	0.70	+0.40	8.11	8.11	36.0	+6.70	2.0
91.0	0.35	1.51	0.70	+0.24	4.45	4.48	16.0	-5.25	1.0
91.0	0.60	1.51	0.70	+0.20	4.01	4.03	20.0	+6.38	1.0
91.0	0.58	1.51	0.70	+0.41	3.87	3.89	16.0	+4.27	1.0
91.0	0.58	1.51	0.70	+0.29	3.79	3.80	20.0	+3.28	1.0
91.0	0.80	1.51	0.70	+0.20	2.04	2.04	12.0	+2.28	1.0
91.0	0.80	1.51	0.70	+0.21	2.08	2.09	12.0	+2.00	1.0
91.0	0.51	1.51	0.70	+0.31	4.50	4.51	20.0	-2.30	1.0
91.0	0.75	1.51	0.70	+0.48	4.45	4.47	20.0	+0.21	1.0
91.0	0.75	1.51	0.70	+0.49	4.26	4.30	20.0	-0.70	1.0
91.0	0.75	1.51	0.70	+0.61	4.34	4.39	20.0	+0.55	1.0
92.0									
92.0	0.31	1.51	0.90	-0.99	9.38	9.41	44.0	-3.20	2.0
92.0	0.60	1.51	0.90	-1.15	5.02	5.15	20.0	-7.98	1.0
92.0	0.33	1.51	0.90	-0.72	5.01	5.11	24.0	-9.22	1.0
92.0	0.41	1.51	0.90	-0.62	4.52	4.60	20.0	-10.12	1.0
92.0	0.63	1.51	0.90	-0.26	4.61	4.62	16.0	-2.00	1.0
92.0	0.59	1.51	0.90	-0.44	4.49	4.50	16.0	-2.60	1.0
92.0	0.59	1.51	0.90	-0.59	3.67	3.71	20.0	+4.72	1.0
92.0	0.48	1.51	0.90	-0.52	4.02	4.09	16.0	+1.00	1.0
92.0	0.72	1.51	0.90	-0.52	4.92	4.93	16.0	-5.39	1.0
93.0									
93.0	0.40	1.51	1.10	-1.00	4.50	4.60	16.0	-5.60	1.0
93.0	0.42	1.51	1.10	-0.60	4.49	4.51	12.0	+2.00	1.0
93.0	0.54	1.51	1.10	-1.12	3.11	3.20	16.0	+1.72	1.0
93.0	0.39	1.51	1.10	-0.91	4.33	4.45	12.0	+0.00	1.0
93.0	0.46	1.51	1.10	-1.16	4.16	4.34	24.0	-7.88	1.0
93.0	0.46	1.51	1.10	-0.78	3.44	3.53	20.0	+7.71	1.0

93.0	0.45	1.51	1.10	-0.70	3.72	3.80	12.0	+2.78	1.0
93.0	0.45	1.51	1.10	-0.78	3.80	3.89	12.0	+3.25	1.0
93.0	0.50	1.51	1.10	-1.46	3.15	3.45	12.0	-11.07	1.0
93.0	0.55	1.51	1.10	-0.58	4.29	4.41	16.0	+5.53	1.0
93.0	0.55	1.51	1.10	-0.56	4.21	4.29	16.0	+5.20	1.0
93.0	0.65	1.51	1.10	-0.55	4.46	4.50	20.0	-0.50	1.0
93.0	0.65	1.51	1.10	-0.77	4.28	4.32	20.0	-0.35	1.0

Figure-A2-4

Analysis of View B Recordings

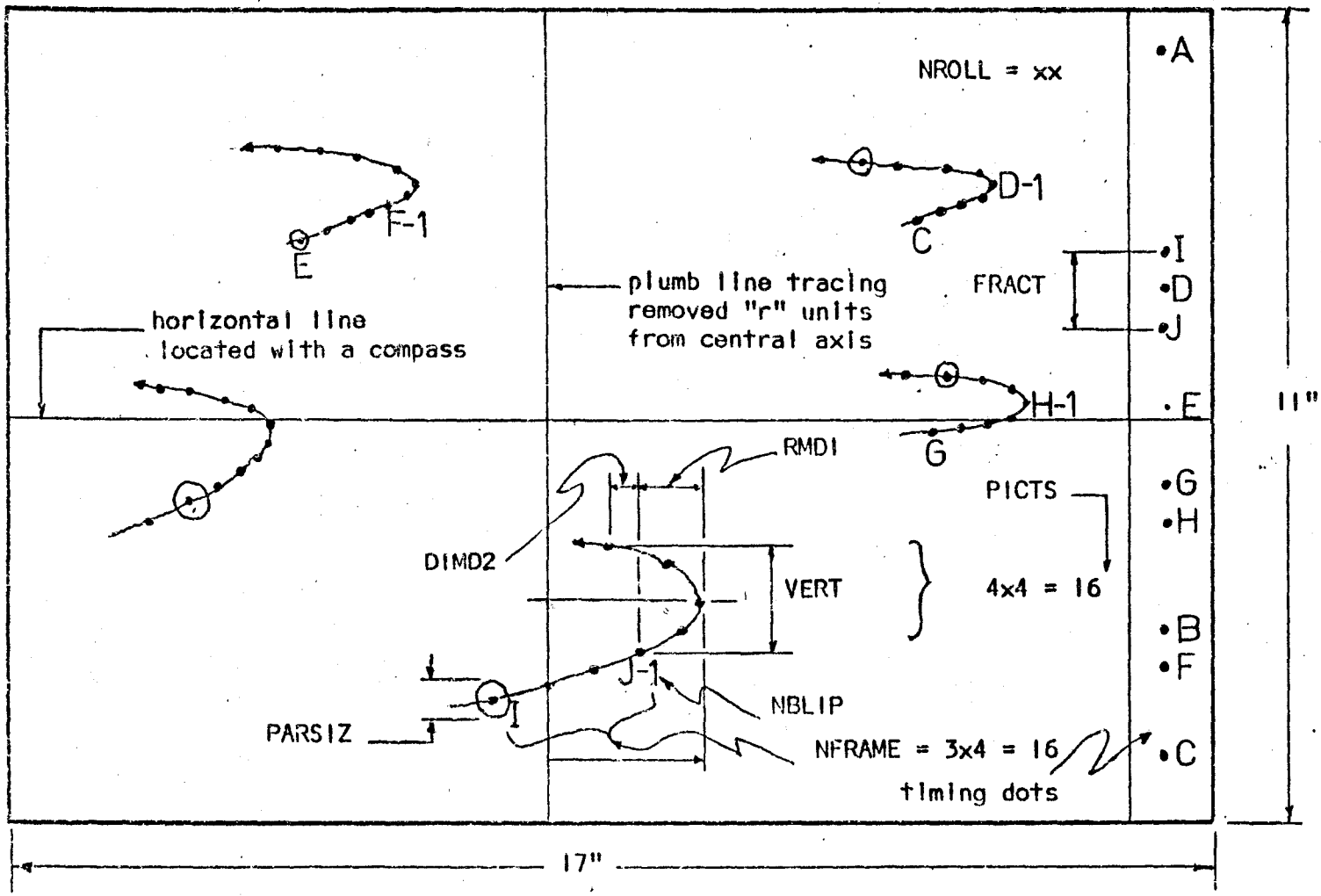

shown in Figure-A2-2 was analyzed.

The distances VERT, DIMD2, RMD1, PARSIZ and RADCOR were measured as described above. The latter quatity was used to determine "r" exactly. The quatities NFRAME and FRACT were measured to determine film-speed. The term picts was measured to calculate Δt.

The above procedure was carried out for all films and the data collected is given in Table-A2-2.

TABLE-A2-2

DATA FROM VIEW R SCREEN RECORDINGS

HEIGHT		RADCOR		VERT		RMD1		NFRAME		NBLIP
NROLL		RADCL		PARSIZ		PICTS		DIMD2		FRACT	
--	IN	IN	S.U.	S.U.	S.U.	--	S.U.	S.U.	--	S.U.	-
33	-2.49	0.10	+3.89	0.31	+1.46	11.03	0.65	-0.14	24	-1.78	1
33	-2.49	0.10	+1.58	0.43	+2.73	10.92	0.72	-0.19	24	-0.82	1
33	-2.49	0.10	+0.31	0.54	+1.19	12.00	1.69	-0.07	20	+3.99	1
33	-2.49	0.10	+0.12	0.48	+1.69	20.00	2.27	-0.09	20	+7.02	1
33	-2.49	0.10	+0.35	0.39	+1.50	16.00	1.97	+0.32	20	+8.82	1
33	-2.49	0.10	+0.61	0.47	+1.60	16.00	2.04	-0.34	20	+3.03	1
34											
34	-2.49	0.20	+0.18	0.40	+0.82	32.00	2.05	+0.88	20	+3.85	1
34	-2.49	0.20	+0.95	0.67	+0.75	28.00	1.45	+0.22	44	+0.00	2
34	-2.49	0.20	+0.15	0.44	+0.62	32.00	1.60	+0.14	44	-5.15	2
34	-2.49	0.20	+0.19	0.58	+1.19	36.00	2.30	-0.09	20	+0.20	1
35											
35	-2.49	0.30	-0.37	0.69	+2.98	24.00	0.25	+0.51	20	+3.30	1
35	-2.49	0.30	+0.56	0.45	+1.89	16.00	0.16	+0.02	20	+3.10	2
35	-2.49	0.30	-0.24	0.44	+1.95	24.00	0.55	+0.00	20	+6.30	2
35	-2.49	0.30	+0.52	0.65	+2.96	24.00	0.61	+0.22	20	+3.35	1
36											
36	-2.49	0.50	-5.85	0.59	+1.79	20.00	0.34	-0.08	20	+3.60	1
36	-2.49	0.50	-4.32	0.40	+1.65	28.00	0.51	+0.00	20	-2.76	1
36	-2.49	0.50	-4.78	0.50	+2.36	44.00	1.10	-0.22	20	+3.64	1
36	-2.49	0.50	-5.00	0.57	+2.11	40.00	0.70	-0.09	44	-6.36	2
37											
37	-2.49	0.75	+8.62	0.65	-1.82	36.00	3.12	+0.44	20	+7.10	1
37	-2.49	0.75	+7.59	0.54	-1.35	28.00	2.56	+0.19	44	-3.95	2
37	-2.49	0.75	+8.58	0.64	-1.35	20.00	2.70	+0.52	16	-7.84	1
38											
38	-2.49	1.00	+8.71	0.75	-1.50	32.00	0.57	+0.36	20	-2.45	1
38	-2.49	1.00	+8.20	0.92	-0.74	24.00	2.30	+0.41	20	-7.11	1
38	-2.49	1.00	+8.55	0.91	-0.55	16.00	0.81	+0.12	44	-1.50	2
43											
43	-2.02	0.05	+4.72	0.56	+1.90	6.54	0.44	-0.15	20	-10.60	1
43	-2.02	0.05	+5.15	0.56	+2.49	8.00	1.20	-0.61	16	+2.60	1
43	-2.02	0.05	+5.85	0.50	+2.02	8.00	0.59	-0.26	16	+8.40	1
44											
44	-2.02	0.10	+3.53	0.38	+1.41	12.00	1.25	-0.21	16	+3.92	1
44	-2.02	0.10	+11.78	0.48	+1.45	24.00	0.56	+0.60	20	+0.35	1
44	-2.02	0.10	+8.55	0.67	+0.70	16.00	0.70	+0.73	20	+7.70	1
44	-2.02	0.10	+4.36	0.32	+0.71	8.00	0.16	+0.00	16	+0.00	1
45											
45	-2.02	0.17	+6.61	0.29	+1.59	18.67	0.67	+0.29	16	+7.20	1
45	-2.02	0.17	-1.66	0.67	+2.21	8.00	0.59	-0.20	16	+6.35	1
45	-2.02	0.17	+5.68	0.26	+1.72	21.52	1.00	+0.27	16	+6.35	1
45	-2.02	0.17	+5.99	0.51	+0.91	16.00	0.52	+0.19	16	+7.43	1
46											
46	-2.02	0.20	+4.85	0.20	+2.32	10.28	1.21	+0.11	12	+6.89	1
46	-2.02	0.20	+5.60	0.38	+2.16	16.00	0.51	+0.16	16	-0.50	1
46	-2.02	0.20	+3.36	0.30	+0.69	16.00	0.50	+0.09	20	+4.35	1

46	-2.02	0.20	+4.32	0.48	+1.41	16.00	0.59	+0.23	28	+7.92	2
46	-2.02	0.20	-3.69	0.40	+2.81	13.04	1.50	-0.16	20	+0.60	1
46	-2.02	0.20	-3.88	0.23	+1.18	10.72	0.81	-0.03	20	+4.02	1
47											
47	-2.02	0.30	+9.23	0.43	+1.69	20.00	0.22	+0.06	20	-5.30	1
47	-2.02	0.30	-1.98	0.31	+2.05	16.00	0.86	+0.25	12	+4.71	1
47	-2.02	0.30	+1.11	0.71	+2.71	20.96	0.66	+0.06	20	-7.25	1
47	-2.02	0.30	-2.49	0.52	+1.92	16.00	0.71	+0.32	16	-7.75	1
48											
48	-2.02	0.50	+8.69	0.36	+0.95	36.00	0.69	+0.00	16	-5.45	1
48	-2.02	0.50	+5.85	0.25	+1.18	32.00	1.16	-0.29	12	-6.17	1
48	-2.02	0.50	+4.95	0.50	+1.19	36.00	0.69	-0.38	28	-3.00	2
48	-2.02	0.50	-1.20	0.57	+1.18	16.00	0.29	+0.00	12	+0.92	1
48	-2.02	0.50	-2.70	0.40	+2.29	28.00	0.86	+0.16	28	-0.90	2
48	-2.02	0.50	-4.36	0.52	+2.30	18.64	0.59	+0.10	12	+1.60	1
49											
49	-2.02	0.75	-8.10	0.31	+0.94	48.00	0.85	-0.06	20	-10.20	1
49	-2.02	0.75	-1.41	0.22	+0.82	48.00	0.49	+0.10	36	-8.40	2
49	-2.02	0.75	+2.93	0.48	+0.28	16.00	0.18	+0.45	16	+3.75	2
50											
50	-2.02	1.00	-2.36	0.39	-0.65	48.00	0.76	+0.04	16	-6.72	1
50	-2.02	1.00	+9.45	0.61	-1.01	16.00	1.12	+0.20	20	-6.27	1
50	-2.02	1.00	+12.38	0.52	-0.52	24.00	1.70	+0.50	16	-3.01	1
55											
55	-3.00	0.05	+5.25	0.44	+2.64	10.56	0.93	-0.21	24	+0.00	1
55	-3.00	0.05	+6.61	0.65	+2.30	14.24	1.41	-0.19	20	+6.78	1
55	-3.00	0.05	10.85	0.44	+1.02	12.00	1.00	+0.00	20	-12.80	1
56											
56	-3.00	0.10	+2.70	0.70	+1.60	9.36	0.77	-0.18	20	+4.48	1
56	-3.00	0.10	+0.42	0.40	+2.18	24.00	1.15	+0.31	20	-8.15	1
56	-3.00	0.10	+8.95	0.45	+1.60	24.00	0.98	+0.20	20	+3.55	1
57											
57	-3.00	0.15	-4.38	0.46	+1.20	11.60	0.76	-0.14	24	-8.40	1
57	-3.00	0.15	-4.26	0.64	+1.74	12.88	0.64	-0.41	16	+2.00	1
57	-3.00	0.15	+2.86	0.40	+0.35	32.00	1.74	+0.09	20	+8.40	1
58											
58	-3.00	0.20	+4.17	0.51	+2.65	32.00	0.91	+0.19	20	+7.02	1
58	-3.00	0.20	+3.19	0.40	+0.92	32.00	1.46	+0.20	24	-10.75	1
58	-3.00	0.20	+1.75	0.42	+0.75	28.00	1.50	+0.24	20	-1.14	1
58	-3.00	0.20	+10.25	0.86	+0.80	32.00	1.86	+0.29	40	-1.52	2
59											
59	-3.00	0.25	-5.85	0.50	+1.55	12.00	0.47	-0.30	20	+4.30	1
59	-3.00	0.25	-0.40	0.60	+1.56	20.00	0.42	+0.15	44	-1.51	2
59	-3.00	0.25	-1.04	0.71	+1.15	24.00	0.80	+0.12	44	-6.58	2
59	-3.00	0.25	+9.30	0.53	+2.43	32.00	0.65	-0.02	20	+0.18	1
59	-3.00	0.25	+1.66	0.51	+1.39	24.00	0.70	+0.19	20	+9.10	1
59	-3.00	0.25	+4.15	0.32	+1.80	18.96	0.32	+0.19	24	-9.30	1
60											
60	-3.00	0.50	-6.19	0.59	+2.33	40.00	0.71	-0.27	24	-8.48	1
60	-3.00	0.50	-2.49	0.31	+1.93	48.00	1.05	-0.49	44	+1.57	2
60	-3.00	0.50	-2.67	0.48	+1.77	48.00	1.09	-0.59	20	+8.18	1
60	-3.00	0.50	+2.81	0.61	+0.62	56.00	1.10	-0.01	44	+1.07	2
60	-3.00	0.50	+6.10	0.30	+0.59	56.00	1.05	-0.04	44	+1.22	2
60	-3.00	0.50	+9.32	0.46	-0.60	72.00	1.30	-0.14	20	+6.32	1
61											
61	-3.00	1.00	-3.11	0.31	-1.49	24.00	0.72	+0.69	20	-7.30	1
61	-3.00	1.00	-7.78	0.53	-0.81	128.0	1.05	+0.44	44	-3.88	2

61	-3.00	1.00	+2.19	0.36	-0.90	20.00	0.61	+0.31	20	+4.65	1
66											
66	-3.51	0.05	+3.87	0.49	+1.70	8.00	0.61	+0.00	24	-10.68	1
66	-3.51	0.05	+3.69	0.46	+0.85	6.88	0.30	+0.00	20	+9.43	1
66	-3.51	0.05	+11.38	0.53	+0.82	28.00	1.22	+0.01	44	+1.39	1
66	-3.51	0.05	+3.49	0.60	+1.41	8.00	0.31	-0.22	24	-12.85	1
67											
67	-3.51	0.10	+8.24	0.58	+1.46	24.00	0.80	+0.02	20	+8.50	1
67	-3.51	0.10	+8.30	0.68	+1.42	24.00	0.73	+0.19	20	+9.30	1
67	-3.51	0.10	+9.52	0.85	+1.30	20.00	0.62	-0.09	20	+4.39	1
67	-3.51	0.10	10.50	0.66	+2.15	20.80	1.07	+0.30	36	-4.30	2
67	-3.51	0.10	+6.70	0.50	+1.02	28.00	1.28	+0.18	20	+0.60	1
68											
68	-3.51	0.15	+6.64	0.56	+1.84	24.00	0.69	+0.08	44	-0.71	2
68	-3.51	0.15	+3.80	0.30	+1.80	28.00	1.00	+0.00	44	+1.92	2
68	-3.51	0.15	+8.88	0.65	+2.28	28.00	0.89	-0.07	44	+1.86	2
68	-3.51	0.15	+4.93	0.45	+1.21	28.00	1.30	+0.33	44	+2.00	2
68	-3.51	0.15	+4.32	0.39	+0.98	24.00	1.15	+0.33	44	-1.37	2
70											
70	-3.51	0.25	+11.18	0.49	+1.80	36.00	0.70	-0.13	20	+5.40	1
70	-3.51	0.25	+3.19	0.39	+1.81	19.04	0.35	+0.20	20	+4.50	1
70	-3.51	0.25	+0.18	0.59	+1.72	20.00	0.46	+0.15	20	+1.21	1
70	-3.51	0.25	+0.61	0.52	+1.65	24.00	0.39	+0.19	44	-1.28	2
70	-3.51	0.25	-2.03	0.89	+0.75	20.00	0.98	-0.10	20	-7.60	1
71											
71	-3.51	0.50	-11.94	0.32	+1.90	20.00	0.48	+0.05	20	+2.93	1
71	-3.51	0.50	-6.39	0.27	+1.40	32.00	0.59	-0.14	24	-8.45	1
71	-3.51	0.50	-1.00	0.50	+0.96	48.00	0.52	-0.15	24	-8.50	1
71	-3.51	0.50	+1.84	0.70	+0.82	64.00	1.66	-0.75	44	+1.20	2
71	-3.51	0.50	+5.97	0.78	+0.00	64.00	0.80	+0.31	44	-6.51	2
71	-3.51	0.50	+9.09	0.28	-0.47	96.00	1.31	+0.95	44	-4.12	2
71	-3.51	0.50	+3.91	0.19	+0.24	96.00	2.51	-0.10	44	-4.56	2
72											
72	-3.51	0.75	-10.69	0.31	+0.22	96.00	1.59	+0.16	20	+2.30	1
72	-3.51	0.75	-9.34	0.51	+0.44	96.00	2.03	+0.50	44	-0.51	2
72	-3.51	0.75	+0.77	0.60	-0.41	128.0	1.64	+0.30	24	-9.29	1
72	-3.51	0.75	-4.48	0.31	+0.71	96.00	1.20	+0.30	44	+0.45	2
72	-3.51	0.75	+1.29	0.44	-0.81	160.0	2.57	+0.70	44	-1.92	2
72	-3.51	0.75	+2.45	0.39	-0.26	112.0	1.20	+0.30	88	-2.79	4
73											
73	-3.51	1.00	-8.87	0.60	-1.00	160.0	1.80	+0.50	44	+1.55	2
73	-3.51	1.00	-4.22	0.33	-1.82	80.00	0.50	+0.49	20	+5.14	1
73	-3.51	1.00	-4.84	0.36	-1.84	112.0	1.29	+0.69	44	+1.92	2
78											
78	-1.00	0.60	+5.63	0.40	-0.51	22.67	1.46	-0.45	44	-6.93	2
78	-1.00	0.60	+12.19	0.60	-1.59	20.00	0.70	-0.10	24	-11.24	1
78	-1.00	0.60	+12.70	0.37	-1.71	24.00	1.05	+0.05	40	-11.29	2
78	-1.00	0.60	+15.56	0.59	-1.87	20.00	0.81	+0.13	20	+6.07	1
79											
79	-1.00	0.80	-1.15	0.40	-0.93	80.00	1.39	+0.10	16	+1.21	1
79	-1.00	0.80	+3.89	0.34	-2.71	96.00	0.71	+0.26	20	+1.22	1
79	-1.00	0.80	-0.40	0.47	-2.60	64.00	0.65	+0.18	20	-10.60	1
79	-1.00	0.80	+10.75	0.64	-1.92	105.9	1.18	+0.65	16	+2.08	1
80											
80	-1.00	1.00	-0.58	0.61	-0.93	64.00	0.40	+0.20	44	+9.31	3
80	-1.00	1.00	-3.18	0.36	-2.56	112.0	1.00	+0.27	44	-6.80	2
80	-1.00	1.00	-0.58	0.39	-2.19	80.00	0.60	+0.33	16	+2.21	1

85									
85	-1.51	0.10+10.45	0.66	+1.79	20.00	0.80	+0.58	12	+0.16	1
85	-1.51	0.10+13.05	0.47	+2.11	18.08	0.50	+0.00	20	+0.63	1
85	-1.51	0.10+11.45	0.43	+2.14	20.00	0.80	+0.18	20	-6.58	1
85	-1.51	0.10+12.92	0.54	+1.21	16.00	1.18	-0.50	28	-2.22	2
85	-1.51	0.10 14.86	0.61	+2.02	20.00	0.56	-0.20	24	-8.41	1
85	-1.51	0.10 +0.06	0.56	+1.50	12.00	0.33	-0.22	24	-1.93	1
85	-1.51	0.10 +2.71	0.58	+2.00	24.00	0.54	-0.20	24	-1.61	1
85	-1.51	0.10 +2.06	0.71	+2.14	12.00	0.61	-0.22	20	+12.92	1
85	-1.51	0.10+11.75	0.49	+2.18	24.00	0.73	-0.20	16	+3.42	1
86									
86	-1.51	0.20 +3.53	0.40	+1.37	24.00	2.23	-0.62	16	-3.92	1
86	-1.51	0.20+10.86	0.49	+3.05	16.00	0.62	+0.20	12	+3.91	1
86	-1.51	0.20 16.43	0.48	+1.87	10.40	0.27	-0.07	16	-0.25	1
86	-1.51	0.20 -0.74	0.62	+0.55	8.00	1.35	-1.00	12	-4.34	1
86	-1.51	0.20 +7.11	0.56	+1.17	8.00	0.10	-0.00	16	-1.20	1
86	-1.51	0.20 +5.19	0.59	+0.59	5.44	0.18	-0.10	32	+3.22	2
87									
87	-1.51	0.30 10.66	0.48	+2.62	19.68	0.89	-0.31	12	-3.80	1
87	-1.51	0.30 -2.65	0.79	+1.05	12.00	0.78	-0.21	8	+2.78	1
87	-1.51	0.30 +1.08	0.56	+2.03	16.00	0.65	+0.07	12	+7.02	1
87	-1.51	0.30 11.14	0.70	+2.01	16.00	0.35	-0.13	12	+6.35	1
87	-1.51	0.30 +5-89	0.50	+2.75	17.12	0.29	-0.20	12	-6.00	1
87	-1.51	0.30+11.00	0.94	+1.43	8.00	0.20	+0.00	8	+1.48	1
88									
88	-1.51	0.30+12.28	0.78	+1.70	24.00	0.55	+0.08	16	-7.22	1
88	-1.51	0.30 +9.41	0.46	+1.64	16.00	0.25	+0.07	12	+5.30	1
88	-1.51	0.30 -0.12	0.65	+1.83	12.00	0.30	+0.30	16	-7.85	1
88	-1.51	0.30 -0.33	0.43	+2.25	12.00	0.63	+0.38	8	+4.95	1
88	-1.51	0.30 -2.35	0.71	+1.36	20.00	0.61	-0.41	20	-5.12	1
88	-1.51	0.30 -4.41	0.65	+0.84	20.00	0.97	-0.26	20	-5.40	1
89									
89	-1.51	0.50 -5.72	0.45	+1.82	16.00	0.23	+0.10	12	+3.07	1
89	-1.51	0.50 -0.01	0.60	+1.65	16.00	0.26	+0.21	16	-2.85	1
89	-1.51	0.50 +1.33	0.51	+2.00	24.00	0.95	-0.32	12	-4.65	1
89	-1.51	0.50 +3.27	0.47	+0.61	16.00	0.04	+0.21	36	-2.16	2
89	-1.51	0.50 +8.99	0.44	+0.79	48.00	0.80	+0.38	12	+5.96	1
90									
90	-1.51	0.70 -3.63	0.46	+1.19	48.00	0.57	+0.42	16	+6.07	1
90	-1.51	0.70 -1.94	0.37	+1.20	64.00	1.55	-0.55	36	10.00	2
90	-1.51	0.70 +5.11	0.71	+1.61	40.00	0.24	+0.00	8	+6.13	1
90	-1.51	0.70 +9.71	0.38	+0.51	60.00	0.72	+0.09	16	+2.20	1
90	-1.51	0.70 +3.93	0.52	+2.05	64.00	0.85	+0.18	16	-1.11	1
91									
91	-1.51	0.70 +0.45	0.43	+0.62	24.00	0.21	+0.14	16	+6.65	1
91	-1.51	0.70+14.70	0.79	+1.18	72.00	1.61	-0.29	12	+3.70	1
91	-1.51	0.70+12.51	0.30	+0.91	48.00	0.41	+0.29	12	+1.88	1
91	-1.51	0.70 +7.72	0.48	+1.03	24.00	0.20	+0.00	12	+0.00	1
91	-1.51	0.70 -0.84	0.43	+1.30	64.00	2.13	+0.19	12	+0.00	1
92									
92	-1.51	0.90 -4.09	0.49	+1.32	96.00	1.07	-0.60	20	+6.45	1
92	-1.51	0.90 -1.06	0.48	+1.75	64.00	1.01	-0.49	16	+0.89	1
92	-1.51	0.90 +9.92	0.33	-1.30	128.0	1.52	+0.34	20	-1.30	1
92	-1.51	0.90 +5.00	0.46	+0.70	96.00	0.65	-0.08	44	-1.90	2
92	-1.51	0.90 +1.52	0.78	+2.65	96.00	1.05	+0.11	16	+5.30	1
92	-1.51	0.90 +6.15	0.54	+1.41	91.20	0.86	+0.28	20	-7.75	1
93									

93	-1.51	1.10	-1.89	0.69	-3.07	72.00	0.69	+0.09	16	+5.98	1
93	-1.51	1.10	-3.36	0.50	-2.11	96.00	0.85	+0.59	16	-7.92	1
93	-1.51	1.10	+1.18	0.31	-0.77	96.00	0.78	+0.31	36	-1.16	2
93	-1.51	1.10	-1.52	0.20	-1.56	72.00	0.85	+0.23	16	+1.40	1

Appendix A3

Computations

A3.1 Computation of Final Velocities

There are no special calculations required to calculate velocity components from the data obtained from recordings of droplet movement in views A and B.

In general, the calculations involve conversion of distances measured on the screen to distances inside the cyclone by using the screen calibration as described in section A4.1. By calculating the film speed, time intervals can be measured. All velocities and co-ordinates have been calculated in dimensionless form in accordance with the scheme discussed in section 3. Two FORTRAN IV programs were divised for the data from the two types of screen recordings, to facilitate handling all the data in Tables A2-1 and A2-2.

The listing of the two FORTRAN programs is given on the following pages along with the entire output from each program.

```
      PROGRAM TST (INPUT,OUTPUT,TAPE5=INPUT,TAPE6=OUTPUT)
C
C
C     THIS PROGRAM CALCULATES TANGENTIAL AND VERTICAL VELOCITIES
C     FROM THE DATA FROM VIEW A SCREEN RECORDINGS.
C
C
C
000003      A=33.0
000004      HTCYC=15.0
000006      RADCYC=1.50
000007      VINLET=4.34
000011      VOVER=2.37
000012      SUMTAN=0.0
000013      SUMVER=0.0
000014      I=0
000016   24 WRITE(6,5)
000022    5 FORMAT(35X,7HDROPLET,2X,8HVERTICAL,1X,10HTANGENTIAL,1X,4HFILM)
000022      WRITE(6,10)
000026   10 FORMAT(16X,4HROLL,1X,6HRADIUS,1X,6HHEIGHT,1X,8HDIAMETER,1X,8HVELOC
     1ITY,2X,8HVELOCITY,2X,5HSPEED,8X,3HVZR)
000026      WRITE(6,11)
000032   11 FORMAT(36X,7HMICRONS,21X,6HFR/SEC,4X,9HFT.IN/SEC//)
000032   25 READ(5,30) ROLL,PARSIZ,HEIGHT,RADIUS,VERT,HORIZ,VECT,FRAME,FRACT,B
     1LIP
000062   30 FORMAT(10F7.2)
000062      IF(ROLL.EQ.0.0) GO TO 77
000063      IF(A.NE.ROLL) GO TO 92
000065      RADIUS=RADIUS/RADCYC
000066      HEIGHT=-HEIGHT/HTCYC
000070      PARSIZ=(PARSIZ/2.61)*1000.0
000073      FRAMES=FRAME+FRACT/4.31
000076      CAMSPD=(1000.0*FRAMES)/BLIP
000100      HORIZF=HORIZ/(2.61*304.8)
000102      VERTF=VERT/(2.61*304.8)
000104      HPICSP=HORIZF/FRAME
000106      VPICSP=VERTF/FRAME
000110      TANGV=CAMSPD*HPICSP/VINLET
000112      VERTV=CAMSPD*VPICSP/VOVER
000115      I=I+1
000117      RI=I
000120      SUMTAN=SUMTAN+TANGV
000122      SUMVER=SUMVER+VERTV
000124      A=ROLL
000125      NPARSI=PARSIZ
000127      NROLL=ROLL
000131      WRITE(6,40) NROLL,RADIUS,HEIGHT,NPARSI,VERTV,TANGV,CAMSPD
000152   40 FORMAT(16X,I3,1X,F6.3,1X,F6.3,3X,I4,5X,F6.3,4X,F6.3,2X,F8.1)
000152      B=RADIUS*1.5
000154      GO TO 25
000155   92 AVTAN=SUMTAN/RI
000157      AVVERT=SUMVER/RI
000160      VZR=AVVERT*B*2.37
000163      WRITE(6,90)
000166   90 FORMAT(49X,8HAVERAGES,/)
000166      WRITE(6,91) AVVERT,AVTAN,VZR
000200   91 FORMAT(45X,F6.3,4X,F6.3,14X,F7.4//)
```

```
000200            A=ROLL
000201            SUMTAN=0.0
000202            SUMVER=0.0
000203            I=0
000205            GO TO 24
000205         77 CONTINUE
000205            STOP
000207            END

UNUSED COMPILER SPACE
006400
```

ROLL	RADIUS	HEIGHT	DROPLET DIAMETER MICRONS	VERTICAL VELOCITY	TANGENTIAL VELOCITY	FILM SPEED FR/SEC	VZR FT.IN/SEC
33	.067	-.166	122	1.369	2.131	19276.1	
33	.067	-.166	302	1.191	2.090	22232.0	
33	.067	-.166	210	1.365	1.853	19337.6	
				AVERAGES			
				1.308	2.024		.3100

ROLL	RADIUS	HEIGHT	DROPLET DIAMETER MICRONS	VERTICAL VELOCITY	TANGENTIAL VELOCITY	FILM SPEED FR/SEC	VZR FT.IN/SEC
34	.133	-.166	210	.523	1.886	18487.2	
34	.133	-.166	195	.833	2.472	19624.1	
34	.133	-.166	195	.823	2.148	19512.8	
34	.133	-.166	195	.638	1.992	21102.1	
				AVERAGES			
				.704	2.125		.3337

ROLL	RADIUS	HEIGHT	DROPLET DIAMETER MICRONS	VERTICAL VELOCITY	TANGENTIAL VELOCITY	FILM SPEED FR/SEC	VZR FT.IN/SEC
35	.200	-.166	329	.781	2.160	19628.8	
35	.200	-.166	329	.764	2.044	19600.9	
35	.200	-.166	256	.966	2.060	18322.5	
35	.200	-.166	298	.541	2.033	10649.7	
35	.200	-.166	191	.863	2.302	19600.9	
				AVERAGES			
				.783	2.120		.5567

ROLL	RADIUS	HEIGHT	DROPLET DIAMETER MICRONS	VERTICAL VELOCITY	TANGENTIAL VELOCITY	FILM SPEED FR/SEC	VZR FT.IN/SEC
36	.333	-.166	195	.734	2.042	20433.9	
36	.333	-.166	183	.655	.541	21744.8	
36	.333	-.166	268	.836	2.062	21872.4	
36	.333	-.166	111	.572	1.982	18157.8	
				AVERAGES			
				.699	1.657		.8286

ROLL	RADIUS	HEIGHT	DROPLET DIAMETER MICRONS	VERTICAL VELOCITY	TANGENTIAL VELOCITY	FILM SPEED FR/SEC	VZR FT.IN/SEC

37	.500	-.166	172	.075	1.326	21698.4
37	.500	-.166	199	.073	1.285	21032.5
37	.500	-.166	199	.073	1.274	21150.8
37	.500	-.166	199	.073	1.283	21002.3
37	.500	-.166	187	.057	1.235	19603.2
37	.500	-.166	187	.047	1.230	19487.2
37	.500	-.166	153	.044	1.296	17395.6
37	.500	-.166	153	.070	1.607	17475.6
37	.500	-.166	245	.047	1.470	19570.8
				AVERAGES		
				.062	1.334	.1100

ROLL	RADIUS	HEIGHT	DROPLET DIAMETER MICRONS	VERTICAL VELOCITY	TANGENTIAL VELOCITY	FILM SPEED FR/SEC	VZR FT.IN/SEC
38	.667	-.166	111	-.231	1.199	21280.7	
38	.667	-.166	111	-.197	1.266	21466.4	
38	.667	-.166	298	-.078	1.145	18468.7	
38	.667	-.166	298	-.136	1.219	18450.1	
38	.667	-.166	264	-.239	1.188	20000.0	
38	.667	-.166	264	-.198	1.179	20155.5	
38	.667	-.166	183	-.116	1.154	21828.3	
38	.667	-.166	183	-.116	1.121	21814.4	
38	.667	-.166	149	-.209	1.172	21881.7	
38	.667	-.166	149	-.135	1.150	21747.1	
38	.667	-.166	149	-.160	1.172	21816.7	
				AVERAGES			
				-.165	1.179		-.3909

ROLL	RADIUS	HEIGHT	DROPLET DIAMETER MICRONS	VERTICAL VELOCITY	TANGENTIAL VELOCITY	FILM SPEED FR/SEC	VZR FT.IN/SEC
39	.833	-.166	325	-.279	1.115	16204.2	
39	.833	-.166	325	-.141	.571	16337.6	
39	.833	-.166	114	-.337	.993	16670.5	
39	.833	-.166	114	-.171	.520	16609.0	
39	.833	-.166	153	-.323	1.148	18389.8	
				AVERAGES			
				-.250	.869		-.7412

ROLL	RADIUS	HEIGHT	DROPLET DIAMETER MICRONS	VERTICAL VELOCITY	TANGENTIAL VELOCITY	FILM SPEED FR/SEC	VZR FT.IN/SEC
43	.033	-.135	183	1.166	2.217	12935.0	
43	.033	-.135	187	1.471	2.353	19000.0	
43	.033	-.135	172	1.325	2.632	21716.9	
43	.033	-.135	153	1.164	2.159	12250.6	
43	.033	-.135	344	1.666	3.511	23554.5	
43	.033	-.135	390	1.226	2.193	16967.5	

43	.033	-.135	210	.789	2.070	12744.8
43	.033	-.135	314	.968	2.071	13807.4
43	.033	-.135	233	.873	2.443	18909.5
				AVERAGES		
				1.183	2.405	.1402

ROLL	RADIUS	HEIGHT	DROPLET DIAMETER MICRONS	VERTICAL VELOCITY	TANGENTIAL VELOCITY	FILM SPEED FR/SEC	VZR FT.IN/SEC
44	.067	-.135	310	1.217	2.027	15234.3	
44	.067	-.135	306	1.400	2.252	20225.1	
44	.067	-.135	298	1.284	1.729	16700.7	
44	.067	-.135	134	1.392	2.290	19814.4	
44	.067	-.135	145	1.254	2.175	12893.3	
44	.067	-.135	141	1.451	2.223	18930.4	
44	.067	-.135	157	1.600	2.101	13816.7	
44	.067	-.135	229	1.605	1.968	15554.5	
				AVERAGES			
				1.325	2.096		.3141

ROLL	RADIUS	HEIGHT	DROPLET DIAMETER MICRONS	VERTICAL VELOCITY	TANGENTIAL VELOCITY	FILM SPEED FR/SEC	VZR FT.IN/SEC
45	.113	-.135	191	1.129	1.953	18424.6	
45	.113	-.135	229	1.063	2.058	16693.7	
45	.113	-.135	249	1.400	2.219	19547.6	
45	.113	-.135	260	1.347	2.089	16652.0	
45	.113	-.135	279	1.308	1.858	14396.8	
45	.113	-.135	172	1.442	1.669	15317.9	
45	.113	-.135	134	1.654	1.705	16816.7	
45	.113	-.135	237	1.427	1.989	20464.0	
				AVERAGES			
				1.271	1.943		.5121

ROLL	RADIUS	HEIGHT	DROPLET DIAMETER MICRONS	VERTICAL VELOCITY	TANGENTIAL VELOCITY	FILM SPEED FR/SEC	VZR FT.IN/SEC
46	.133	-.135	233	.876	1.722	18350.3	
46	.133	-.135	191	1.040	2.076	13440.8	
46	.133	-.135	80	.908	2.142	13345.7	
46	.133	-.135	176	.939	2.033	12352.7	
46	.133	-.135	199	.956	2.333	18972.2	
46	.133	-.135	191	1.093	1.802	16904.9	
				AVERAGES			
				.969	2.018		.4591

ROLL	RADIUS	HEIGHT	DROPLET	VERTICAL	TANGENTIAL	FILM

ROLL	RADIUS	HEIGHT	DIAMETER MICRONS	VELOCITY	VELOCITY	SPEED FR/SEC	VZR FT.IN/SEC
47	.200	-.135	249	.357	1.475	20371.2	
47	.200	-.135	268	.332	1.373	9031.3	
47	.200	-.135	260	.360	1.457	20870.1	
47	.200	-.135	352	.348	1.442	10501.2	
47	.200	-.135	275	.284	1.468	11916.5	
47	.200	-.135	137	.553	1.416	19478.0	
47	.200	-.135	275	.590	1.782	18529.0	
				AVERAGES			
				.403	1.488		.2868

ROLL	RADIUS	HEIGHT	DROPLET DIAMETER MICRONS	VERTICAL VELOCITY	TANGENTIAL VELOCITY	FILM SPEED FR/SEC	VZR FT.IN/SEC
48	.333	-.135	379	.757	2.031	19178.7	
48	.333	-.135	379	.796	2.060	19756.4	
48	.333	-.135	214	.507	2.044	14329.5	
48	.333	-.135	272	.585	2.001	17299.3	
48	.333	-.135	291	.301	1.831	17438.5	
48	.333	-.135	291	.420	1.926	17993.0	
				AVERAGES			
				.561	1.982		.6646

ROLL	RADIUS	HEIGHT	DROPLET DIAMETER MICRONS	VERTICAL VELOCITY	TANGENTIAL VELOCITY	FILM SPEED FR/SEC	VZR FT.IN/SEC
49	.500	-.135	268	.108	1.320	12211.1	
49	.500	-.135	160	.075	1.491	16083.5	
49	.500	-.135	191	.079	1.181	14828.3	
49	.500	-.135	210	.049	1.570	16422.3	
49	.500	-.135	122	.140	1.419	14547.6	
				AVERAGES			
				.090	1.396		.1600

ROLL	RADIUS	HEIGHT	DROPLET DIAMETER MICRONS	VERTICAL VELOCITY	TANGENTIAL VELOCITY	FILM SPEED FR/SEC	VZR FT.IN/SEC
50	.667	-.135	153	.056	1.350	9348.0	
50	.667	-.135	153	.066	1.340	9071.9	
50	.667	-.135	187	-.036	1.252	15723.9	
50	.667	-.135	210	.056	1.460	12654.3	
50	.667	-.135	233	.054	1.435	13484.9	
50	.667	-.135	164	.049	1.360	10983.8	
50	.667	-.135	183	-.055	1.594	13784.2	
50	.667	-.135	111	.059	1.350	12211.1	
				AVERAGES			

				.031	1.393		.0735
ROLL	RADIUS	HEIGHT	DROPLET DIAMETER MICRONS	VERTICAL VELOCITY	TANGENTIAL VELOCITY	FILM SPEED FR/SEC	VZR FT.IN/SEC
51	.887	-.135	306	-.236	1.269	18559.2	
51	.887	-.135	176	-.368	1.215	17978.0	
51	.887	-.135	379	-.339	1.287	17440.8	
51	.887	-.135	383	-.331	1.310	17225.1	
51	.887	-.135	176	-.191	1.131	17978.0	
51	.887	-.135	214	-.163	1.330	11879.4	
51	.887	-.135	145	-.372	.900	13851.5	
51	.887	-.135	145	-.307	.891	13628.8	
51	.887	-.135	145	-.251	.921	13787.7	
				AVERAGES			
				-.284	1.139		-.8959
ROLL	RADIUS	HEIGHT	DROPLET DIAMETER MICRONS	VERTICAL VELOCITY	TANGENTIAL VELOCITY	FILM SPEED FR/SEC	VZR FT.IN/SEC
52	.967	-.135	360	-.506	1.184	18353.8	
52	.967	-.135	183	-.588	1.230	18834.1	
52	.967	-.135	222	-.441	1.154	18581.2	
52	.967	-.135	333	-.612	1.392	18918.8	
52	.967	-.135	157	-.396	1.316	13846.9	
52	.967	-.135	157	-.308	1.283	14944.3	
52	.967	-.135	222	-.404	1.179	18406.0	
52	.967	-.135	183	-.488	1.208	16728.5	
				AVERAGES			
				-.468	1.243		-1.6078
ROLL	RADIUS	HEIGHT	DROPLET DIAMETER MICRONS	VERTICAL VELOCITY	TANGENTIAL VELOCITY	FILM SPEED FR/SEC	VZR FT.IN/SEC
53	1.000	-.135	199	-.449	1.157	19051.0	
53	1.000	-.135	352	-.586	1.184	20860.8	
53	1.000	-.135	149	-.427	1.199	20907.2	
53	1.000	-.135	210	-.441	1.180	20777.3	
53	1.000	-.135	272	-.295	1.319	17426.9	
53	1.000	-.135	145	-.550	1.175	19187.9	
53	1.000	-.135	229	-.552	1.291	21020.9	
				AVERAGES			
				-.471	1.215		-1.6756
ROLL	RADIUS	HEIGHT	DROPLET DIAMETER MICRONS	VERTICAL VELOCITY	TANGENTIAL VELOCITY	FILM SPEED FR/SEC	VZR FT.IN/SEC

ROLL	RADIUS	HEIGHT	DROPLET DIAMETER MICRONS	VERTICAL VELOCITY	TANGENTIAL VELOCITY	FILM SPEED FR/SEC	VZR FT.IN/SEC
55	.033	-.200	268	.905	2.089	18758.7	
55	.033	-.200	145	1.308	2.276	15911.8	
55	.033	-.200	145	1.343	2.246	21276.1	
55	.033	-.200	314	1.099	2.142	18749.4	
55	.033	-.200	199	.966	2.094	19385.2	
55	.033	-.200	164	1.437	2.142	14696.1	
55	.033	-.200	214	.660	1.676	14030.2	
55	.033	-.200	363	1.436	2.321	21229.7	
55	.033	-.200	229	1.228	2.265	20580.0	
				AVERAGES			
				1.154	2.139		.1367

ROLL	RADIUS	HEIGHT	DROPLET DIAMETER MICRONS	VERTICAL VELOCITY	TANGENTIAL VELOCITY	FILM SPEED FR/SEC	VZR FT.IN/SEC
56	.067	-.200	252	1.144	2.409	21577.7	
56	.067	-.200	249	1.160	1.942	20345.7	
56	.067	-.200	249	1.252	2.222	22213.5	
56	.067	-.200	199	1.240	2.298	16923.4	
56	.067	-.200	302	1.197	2.111	21183.3	
56	.067	-.200	172	1.422	2.376	21705.3	
56	.067	-.200	195	1.261	2.292	22320.2	
56	.067	-.200	214	1.370	2.410	22143.9	
				AVERAGES			
				1.256	2.258		.2976

ROLL	RADIUS	HEIGHT	DROPLET DIAMETER MICRONS	VERTICAL VELOCITY	TANGENTIAL VELOCITY	FILM SPEED FR/SEC	VZR FT.IN/SEC
57	.100	-.200	187	1.177	2.237	16902.6	
57	.100	-.200	260	1.380	2.110	18181.0	
57	.100	-.200	264	1.250	2.123	15849.2	
57	.100	-.200	279	1.302	2.459	17002.3	
57	.100	-.200	421	.760	2.152	19891.0	
57	.100	-.200	214	.979	2.263	20290.0	
57	.100	-.200	260	.933	1.825	18051.0	
				AVERAGES			
				1.112	2.167		.3952

ROLL	RADIUS	HEIGHT	DROPLET DIAMETER MICRONS	VERTICAL VELOCITY	TANGENTIAL VELOCITY	FILM SPEED FR/SEC	VZR FT.IN/SEC
58	.133	-.200	260	1.024	2.037	22183.3	
58	.133	-.200	287	1.114	2.230	16000.0	
58	.133	-.200	137	.752	2.152	20993.0	
58	.133	-.200	245	1.236	2.307	21672.9	
58	.133	-.200	183	1.254	1.721	22095.1	

58	.133	-.200	222	1.099	1.931	21134.6
58	.133	-.200	260	1.051	1.838	20742.5
				AVERAGES		
				1.075	2.031	.5098

ROLL	RADIUS	HEIGHT	DROPLET DIAMETER MICRONS	VERTICAL VELOCITY	TANGENTIAL VELOCITY	FILM SPEED FR/SEC	VZR FT.IN/SEC
59	.167	-.200	260	.537	1.549	18069.6	
59	.167	-.200	160	1.100	2.371	21603.2	
59	.167	-.200	229	1.001	2.464	20399.1	
59	.167	-.200	283	.915	2.228	20649.7	
59	.167	-.200	275	.615	2.416	22095.1	
59	.167	-.200	249	1.076	2.368	20700.7	
59	.167	-.200	264	.498	1.413	11278.4	
59	.167	-.200	172	.551	1.551	16607.9	
				AVERAGES			
				.787	2.045		.4660

ROLL	RADIUS	HEIGHT	DROPLET DIAMETER MICRONS	VERTICAL VELOCITY	TANGENTIAL VELOCITY	FILM SPEED FR/SEC	VZR FT.IN/SEC
60	.333	-.200	229	.342	2.002	17886.3	
60	.333	-.200	210	.392	1.991	20794.7	
60	.333	-.200	210	.137	.953	8460.6	
60	.333	-.200	268	.485	2.009	22167.1	
60	.333	-.200	160	.268	1.758	20232.0	
60	.333	-.200	191	.426	1.961	20329.5	
60	.333	-.200	229	.206	1.823	22185.6	
60	.333	-.200	318	.485	2.155	10967.5	
60	.333	-.200	302	.504	2.129	19187.9	
				AVERAGES			
				.360	1.864		.4271

ROLL	RADIUS	HEIGHT	DROPLET DIAMETER MICRONS	VERTICAL VELOCITY	TANGENTIAL VELOCITY	FILM SPEED FR/SEC	VZR FT.IN/SEC
61	.667	-.200	191	-.106	1.195	20861.9	
61	.667	-.200	199	-.171	1.259	22171.7	
61	.667	-.200	199	-.098	1.256	22199.5	
61	.667	-.200	199	-.201	1.351	17355.0	
61	.667	-.200	195	-.089	1.214	22457.1	
61	.667	-.200	195	-.110	1.214	21765.7	
61	.667	-.200	222	-.123	1.284	15420.0	
61	.667	-.200	191	-.098	1.210	22234.3	
61	.667	-.200	226	-.120	1.234	21577.7	
61	.667	-.200	298	-.158	1.248	18136.9	
				AVERAGES			

				-.127	1.246		-.3018

ROLL	RADIUS	HEIGHT	DROPLET DIAMETER MICRONS	VERTICAL VELOCITY	TANGENTIAL VELOCITY	FILM SPEED FR/SEC	VZR FT.IN/SEC
62	.833	-.200	329	-.284	1.263	22171.7	
62	.833	-.200	249	-.276	.994	18556.8	
62	.833	-.200	210	-.379	1.158	19554.5	
62	.833	-.200	183	-.333	1.097	22016.2	
62	.833	-.200	260	-.258	1.096	15563.8	
62	.833	-.200	260	-.292	1.136	15452.4	
62	.833	-.200	260	-.319	1.182	15545.2	
62	.833	-.200	287	-.301	1.090	21257.5	
				AVERAGES			
				-.305	1.127		-.9040

ROLL	RADIUS	HEIGHT	DROPLET DIAMETER MICRONS	VERTICAL VELOCITY	TANGENTIAL VELOCITY	FILM SPEED FR/SEC	VZR FT.IN/SEC
63	.900	-.200	249	-.400	1.328	17473.3	
63	.900	-.200	233	-.361	1.316	22181.0	
63	.900	-.200	210	-.266	1.152	21791.2	
63	.900	-.200	222	-.305	1.069	21650.8	
63	.900	-.200	249	-.295	.948	19201.9	
63	.900	-.200	287	-.265	1.063	21278.4	
63	.900	-.200	114	-.303	1.111	20740.1	
63	.900	-.200	233	-.430	1.184	20280.7	
63	.900	-.200	249	-.398	1.264	18768.0	
63	.900	-.200	183	-.340	1.163	14440.8	
				AVERAGES			
				-.336	1.160		-1.0761

ROLL	RADIUS	HEIGHT	DROPLET DIAMETER MICRONS	VERTICAL VELOCITY	TANGENTIAL VELOCITY	FILM SPEED FR/SEC	VZR FT.IN/SEC
64	.933	-.200	298	-.600	1.148	21361.9	
64	.933	-.200	252	-.382	1.127	20000.0	
64	.933	-.200	306	-.197	1.160	21754.1	
64	.933	-.200	229	-.236	.934	22232.0	
64	.933	-.200	195	-.475	1.086	22000.0	
64	.933	-.200	226	-.294	1.002	18491.9	
64	.933	-.200	275	-.293	1.047	21271.5	
64	.933	-.200	203	-.411	.889	22132.3	
64	.933	-.200	229	-.438	.956	20631.1	
64	.933	-.200	222	-.345	1.214	21712.3	
64	.933	-.200	302	-.403	.973	22213.5	
				AVERAGES			
				-.370	1.049		-1.2289

ROLL	RADIUS	HEIGHT	DROPLET DIAMETER MICRONS	VERTICAL VELOCITY	TANGENTIAL VELOCITY	FILM SPEED FR/SEC	VZR FT.IN/SEC
66	.033	-.234	226	1.071	2.190	21921.1	
66	.033	-.234	245	1.190	2.320	19345.7	
66	.033	-.367	226	.884	2.272	16554.5	
66	.033	-.234	379	.932	2.271	22187.9	
66	.033	-.234	325	1.128	2.103	21703.0	
				AVERAGES			
				1.041	2.231		.1233

ROLL	RADIUS	HEIGHT	DROPLET DIAMETER MICRONS	VERTICAL VELOCITY	TANGENTIAL VELOCITY	FILM SPEED FR/SEC	VZR FT.IN/SEC
67	.067	-.234	229	1.203	2.327	21392.1	
67	.067	-.234	199	1.290	2.163	16779.6	
67	.067	-.234	367	1.265	1.941	21582.4	
67	.067	-.234	229	1.263	1.867	11665.9	
67	.067	-.234	229	1.046	2.062	21904.9	
67	.067	-.234	268	1.309	2.029	16055.7	
67	.067	-.234	153	.926	1.802	21830.6	
67	.067	-.234	367	1.191	2.247	21280.7	
67	.067	-.234	260	1.312	2.181	19793.5	
67	.067	-.234	340	1.278	2.050	21710.0	
				AVERAGES			
				1.208	2.067		.2864

ROLL	RADIUS	HEIGHT	DROPLET DIAMETER MICRONS	VERTICAL VELOCITY	TANGENTIAL VELOCITY	FILM SPEED FR/SEC	VZR FT.IN/SEC
68	.100	-.234	153	1.188	1.793	21498.8	
68	.100	-.234	195	.920	1.419	18450.1	
68	.100	-.234	229	.739	1.829	13837.6	
68	.100	-.234	199	1.157	1.787	22032.5	
68	.100	-.234	214	.994	1.758	20712.3	
68	.100	-.234	222	1.071	1.905	21923.4	
68	.100	-.234	237	.689	1.918	21287.7	
68	.100	-.234	145	1.091	1.737	19403.7	
				AVERAGES			
				.981	1.768		.3487

ROLL	RADIUS	HEIGHT	DROPLET DIAMETER MICRONS	VERTICAL VELOCITY	TANGENTIAL VELOCITY	FILM SPEED FR/SEC	VZR FT.IN/SEC
70	.167	-.234	233	.397	1.604	22128.8	
70	.167	-.234	210	.435	1.645	20243.6	

70	.167	-.234	145	.286	1.376	21995.4
70	.167	-.234	268	.699	1.739	21953.6
70	.167	-.234	275	.743	1.859	22264.5
70	.167	-.234	183	.361	1.401	13150.8
				AVERAGES		
				.487	1.604	

.2884

ROLL	RADIUS	HEIGHT	DROPLET DIAMETER MICRONS	VERTICAL VELOCITY	TANGENTIAL VELOCITY	FILM SPEED FR/SEC
71	.333	-.234	226	.749	2.068	21447.8
71	.333	-.234	295	.262	1.847	18979.1
71	.333	-.234	180	.306	1.911	19262.2
71	.333	-.234	344	.187	1.368	19839.9
71	.333	-.234	191	.258	1.882	20301.6
71	.333	-.234	229	0.000	1.696	21686.8
71	.333	-.234	210	.094	1.740	22208.8
71	.333	-.234	134	.204	1.838	20742.5
71	.333	-.234	134	.143	1.802	20670.5
				AVERAGES		
				.245	1.795	

VZR FT.IN/SEC

.2900

ROLL	RADIUS	HEIGHT	DROPLET DIAMETER MICRONS	VERTICAL VELOCITY	TANGENTIAL VELOCITY	FILM SPEED FR/SEC
72	.500	-.234	153	.059	1.396	20081.2
72	.500	-.234	153	.154	1.369	20065.0
72	.500	-.234	172	.117	1.308	17714.6
72	.500	-.234	172	.106	1.332	17809.7
72	.500	-.234	264	.023	1.293	21355.0
72	.500	-.234	306	.048	1.425	21863.1
72	.500	-.234	153	.074	1.298	21930.4
72	.500	-.234	172	.069	1.329	21916.5
72	.500	-.234	164	.105	1.236	19802.8
72	.500	-.234	164	.145	1.286	20276.1
72	.500	-.234	229	.109	1.281	21686.8
				AVERAGES		
				.092	1.323	

VZR FT.IN/SEC

.1633

ROLL	RADIUS	HEIGHT	DROPLET DIAMETER MICRONS	VERTICAL VELOCITY	TANGENTIAL VELOCITY	FILM SPEED FR/SEC
73	.667	-.234	187	-.344	1.227	22145.0
73	.667	-.234	195	-.315	1.176	22161.3
73	.667	-.234	210	-.236	1.153	22213.5
73	.667	-.234	210	-.183	1.122	22201.9
73	.667	-.234	210	-.142	1.183	22222.7
73	.667	-.234	256	-.194	1.164	21925.8
73	.667	-.234	256	-.234	1.247	22085.8

73	.667	-.234	237	-.323	1.191	22113.7	
73	.667	-.234	306	-.369	1.176	22034.8	
73	.667	-.234	153	-.268	1.146	22197.2	
73	.667	-.234	183	-.174	1.223	21849.2	
73	.667	-.234	233	-.335	1.141	22043.3	
73	.667	-.234	226	-.243	1.186	22027.8	
				AVERAGES			
				-.258	1.180		-.6126

ROLL	RADIUS	HEIGHT	DROPLET DIAMETER MICRONS	VERTICAL VELOCITY	TANGENTIAL VELOCITY	FILM SPEED FR/SEC	VZR FT.IN/SEC
74	.833	-.234	160	-.290	1.114	22262.2	
74	.833	-.234	172	-.377	1.255	21552.2	
74	.833	-.234	195	-.405	1.162	22157.8	
74	.833	-.234	195	-.412	1.116	21884.0	
74	.833	-.234	237	-.288	1.173	22097.4	
74	.833	-.234	210	-.430	.872	22039.4	
74	.833	-.234	210	-.419	.874	22069.6	
74	.833	-.234	187	-.303	1.135	21526.7	
74	.833	-.234	210	-.457	1.118	22213.5	
74	.833	-.234	210	-.482	1.124	22181.0	
74	.833	-.234	310	-.514	1.224	21788.9	
74	.833	-.234	226	-.562	1.165	22186.8	
74	.833	-.234	302	-.375	1.105	20870.1	
				AVERAGES			
				-.409	1.110		-1.2111

ROLL	RADIUS	HEIGHT	DROPLET DIAMETER MICRONS	VERTICAL VELOCITY	TANGENTIAL VELOCITY	FILM SPEED FR/SEC	VZR FT.IN/SEC
75	.900	-.234	210	-.446	.991	15821.3	
75	.900	-.234	172	-.472	1.126	20953.6	
75	.900	-.234	195	-.352	1.229	19515.1	
75	.900	-.234	195	-.409	1.214	19545.2	
75	.900	-.234	306	-.385	1.195	22000.0	
75	.900	-.234	298	-.340	1.131	21684.5	
75	.900	-.234	187	-.368	1.151	21930.4	
75	.900	-.234	187	-.428	1.179	22116.0	
75	.900	-.234	172	-.416	1.220	21874.7	
75	.900	-.234	210	-.607	1.121	21809.7	
75	.900	-.234	160	-.549	1.152	21786.5	
75	.900	-.234	210	-.292	1.200	21993.0	
75	.900	-.234	214	-.692	1.241	21610.2	
75	.900	-.234	210	-.352	1.224	22123.0	
				AVERAGES			
				-.436	1.170		-1.3962

ROLL	RADIUS	HEIGHT	DROPLET DIAMETER MICRONS	VERTICAL VELOCITY	TANGENTIAL VELOCITY	FILM SPEED FR/SEC	VZR FT.IN/SEC

78	.427	-.067	321	-.146	.741	22009.3
78	.427	-.067	321	-.112	.807	22199.5
78	.427	-.067	321	-.151	.635	22030.2
78	.427	-.067	222	-.106	.786	22162.4
78	.427	-.067	310	-.247	.881	21647.3
78	.427	-.067	233	-.325	.963	22306.3
				AVERAGES		
				-.181	.802	-.2747

ROLL	RADIUS	HEIGHT	DROPLET DIAMETER MICRONS	VERTICAL VELOCITY	TANGENTIAL VELOCITY	FILM SPEED FR/SEC	VZR FT.IN/SEC
79	.533	-.067	214	-.384	.980	22007.0	
79	.533	-.067	214	-.423	.927	22146.2	
79	.533	-.067	245	-.344	.744	14835.3	
79	.533	-.067	245	-.308	.749	13114.8	
79	.533	-.067	390	-.554	1.273	20487.2	
79	.533	-.067	390	-.500	1.307	20512.8	
79	.533	-.067	390	-.602	1.417	20464.0	
				AVERAGES			
				-.445	1.057		-.8441

ROLL	RADIUS	HEIGHT	DROPLET DIAMETER MICRONS	VERTICAL VELOCITY	TANGENTIAL VELOCITY	FILM SPEED FR/SEC	VZR FT.IN/SEC
80	.667	-.067	180	-.710	1.192	22301.6	
80	.667	-.067	180	-.537	1.112	21888.6	
80	.667	-.067	153	-.484	1.195	15196.1	
80	.667	-.067	187	-.722	1.127	12656.6	
80	.667	-.067	363	-.542	1.121	9614.8	
80	.667	-.067	145	-.770	1.164	20459.4	
80	.667	-.067	226	-.450	.942	13988.4	
80	.667	-.067	226	-.417	.979	14090.5	
80	.667	-.067	252	-.773	1.006	21113.7	
80	.667	-.067	360	-.812	.924	18225.1	
80	.667	-.067	360	-.676	.991	18366.6	
				AVERAGES			
				-.627	1.068		-1.4849

ROLL	RADIUS	HEIGHT	DROPLET DIAMETER MICRONS	VERTICAL VELOCITY	TANGENTIAL VELOCITY	FILM SPEED FR/SEC	VZR FT.IN/SEC
81	.800	-.067	310	-.482	1.040	16508.1	
81	.800	-.067	321	-.954	1.293	17331.8	
81	.800	-.067	149	-1.062	1.285	12645.0	
81	.800	-.067	214	-.638	.961	14584.7	
81	.800	-.067	310	-.418	1.313	18928.1	

81	.800	-.067	275	-.573	1.044	11525.1
81	.800	-.067	291	-.346	1.388	15580.0
81	.800	-.067	302	-.404	1.139	15619.5
81	.800	-.067	302	-.315	1.059	15559.2
81	.800	-.067	291	-.474	.898	18914.2
				AVERAGES		
				-.567	1.142	-1.6111

ROLL	RADIUS	HEIGHT	DROPLET DIAMETER MICRONS	VERTICAL VELOCITY	TANGENTIAL VELOCITY	FILM SPEED FR/SEC	VZR FT.IN/SEC
82	.933	-.067	337	-.547	1.213	20979.1	
82	.933	-.067	260	-.394	1.168	16986.1	
82	.933	-.067	260	-.490	1.110	16988.4	
82	.933	-.067	314	-.596	1.038	13911.8	
82	.933	-.067	314	-.593	.909	13763.3	
82	.933	-.067	275	-.595	1.228	16923.4	
82	.933	-.067	275	-.653	1.199	16983.8	
82	.933	-.067	218	-.396	.959	18194.9	
82	.933	-.067	218	-.305	.914	18032.5	
82	.933	-.067	275	-.712	1.200	16531.3	
82	.933	-.067	172	-.867	1.142	14538.3	
82	.933	-.067	268	-.732	1.199	16000.0	
82	.933	-.067	268	-.663	1.173	16118.3	
				AVERAGES			
				-.580	1.112		-1.9253

ROLL	RADIUS	HEIGHT	DROPLET DIAMETER MICRONS	VERTICAL VELOCITY	TANGENTIAL VELOCITY	FILM SPEED FR/SEC	VZR FT.IN/SEC
83	1.000	-.067	245	-.476	1.238	16932.7	
83	1.000	-.067	199	-.481	1.284	21111.4	
83	1.000	-.067	226	-.588	1.524	13438.5	
83	1.000	-.067	233	-.796	1.366	22234.3	
83	1.000	-.067	272	-.719	1.119	22129.9	
83	1.000	-.067	229	-.977	1.498	13150.8	
				AVERAGES			
				-.673	1.338		-2.3919

ROLL	RADIUS	HEIGHT	DROPLET DIAMETER MICRONS	VERTICAL VELOCITY	TANGENTIAL VELOCITY	FILM SPEED FR/SEC	VZR FT.IN/SEC
85	.067	-.101	157	.368	1.765	13640.4	
85	.067	-.101	157	.280	1.774	14083.5	
85	.067	-.101	157	.239	1.730	14626.5	
85	.067	-.101	233	.408	1.685	13197.2	
85	.067	-.101	233	.409	1.811	13208.8	
85	.067	-.101	233	.427	1.685	12895.6	
85	.067	-.101	383	1.137	2.021	14352.7	

85	.067	-.101	130	.309	1.644	22000.0
85	.067	-.101	229	.252	1.525	11385.2
85	.067	-.101	229	.208	1.663	11484.9
85	.067	-.101	229	.219	1.650	11510.4
85	.067	-.101	275	.335	1.656	16280.7
85	.067	-.101	275	.348	1.756	16385.2
85	.067	-.101	268	.933	1.855	17368.9
85	.067	-.101	402	.695	1.773	20000.0
				AVERAGES		
				.438	1.733	.1037

ROLL	RADIUS	HEIGHT	DROPLET DIAMETER MICRONS	VERTICAL VELOCITY	TANGENTIAL VELOCITY	FILM SPEED FR/SEC	VZR FT.IN/SEC
86	.133	-.101	260	.525	1.706	21735.5	
86	.133	-.101	287	.183	1.347	16685.6	
86	.133	-.101	287	.204	1.324	16626.5	
86	.133	-.101	287	.200	1.322	16747.1	
86	.133	-.101	275	.365	1.413	16677.5	
86	.133	-.101	275	.376	1.424	16661.3	
86	.133	-.101	114	.653	1.777	16417.6	
86	.133	-.101	114	.632	1.895	15624.1	
86	.133	-.101	191	.130	1.552	19559.2	
86	.133	-.101	191	.130	1.641	19605.6	
86	.133	-.101	229	.204	1.444	17082.4	
86	.133	-.101	191	.206	1.618	19433.9	
86	.133	-.101	191	.229	1.343	18758.7	
86	.133	-.101	191	.331	1.288	15136.9	
86	.133	-.101	191	.287	1.297	15183.3	
86	.133	-.101	149	.625	1.700	15967.5	
				AVERAGES			
				.330	1.506	.1563	

ROLL	RADIUS	HEIGHT	DROPLET DIAMETER MICRONS	VERTICAL VELOCITY	TANGENTIAL VELOCITY	FILM SPEED FR/SEC	VZR FT.IN/SEC
87	.200	-.101	237	.221	1.404	12812.1	
87	.200	-.101	237	.206	1.451	12928.1	
87	.200	-.101	237	.177	1.441	12946.6	
87	.200	-.101	256	.198	1.553	18654.3	
87	.200	-.101	256	.271	1.722	18909.5	
87	.200	-.101	333	.067	1.371	12626.5	
87	.200	-.101	333	.056	1.372	12631.1	
87	.200	-.101	199	.164	1.568	19329.5	
87	.200	-.101	199	.165	1.659	19387.5	
87	.200	-.101	287	.305	1.230	15071.9	
87	.200	-.101	352	.171	1.336	11113.7	
87	.200	-.101	352	.246	1.387	11113.7	
87	.200	-.101	237	.155	1.487	15083.5	
87	.200	-.101	268	.216	1.687	19879.4	
87	.200	-.101	268	.281	1.804	19965.2	
87	.200	-.101	191	.219	1.338	17911.8	
87	.200	-.101	191	.223	1.386	18141.5	

AVERAGES

.196 1.482 .1396

ROLL	RADIUS	HEIGHT	DROPLET DIAMETER MICRONS	VERTICAL VELOCITY	TANGENTIAL VELOCITY	FILM SPEED FR/SEC	VZR FT.IN/SEC
88	.200	-.101	268	.177	1.411	20259.9	
88	.200	-.101	268	.169	1.422	19953.6	
88	.200	-.101	268	.239	1.486	20044.1	
88	.200	-.101	176	.303	1.311	13314.4	
88	.200	-.101	268	.193	1.346	22248.3	
88	.200	-.101	199	.204	1.488	15359.6	
88	.200	-.101	199	.215	1.571	15445.5	
88	.200	-.101	199	.264	1.623	15594.0	
88	.200	-.101	306	.352	1.341	15150.8	
88	.200	-.101	306	.347	1.308	15048.7	
88	.200	-.101	306	.235	1.285	11095.1	
88	.200	-.101	306	.221	1.277	11118.3	
88	.200	-.101	306	.246	1.328	11290.0	
88	.200	-.101	260	.311	1.592	19561.5	
88	.200	-.101	260	.313	1.705	19652.0	
88	.200	-.101	191	.266	1.450	21349.2	

AVERAGES

.253 1.434 .1802

ROLL	RADIUS	HEIGHT	DROPLET DIAMETER MICRONS	VERTICAL VELOCITY	TANGENTIAL VELOCITY	FILM SPEED FR/SEC	VZR FT.IN/SEC
89	.333	-.101	222	.157	1.276	18473.3	
89	.333	-.101	222	.217	1.312	18721.6	
89	.333	-.101	222	.186	1.313	18464.0	
89	.333	-.101	222	.256	1.305	18538.3	
89	.333	-.101	252	.155	1.268	15563.8	
89	.333	-.101	252	.207	1.244	15577.7	
89	.333	-.101	252	.284	1.283	15573.1	
89	.333	-.101	291	.223	1.286	12621.8	
89	.333	-.101	291	.265	1.290	12487.2	
89	.333	-.101	149	.140	1.295	11345.7	
89	.333	-.101	149	.131	1.292	11415.3	
89	.333	-.101	145	.103	1.118	14839.9	
89	.333	-.101	237	.220	1.258	11846.9	
89	.333	-.101	237	.209	1.253	11849.2	
89	.333	-.101	237	.220	1.234	11858.5	
89	.333	-.101	237	.220	1.255	11872.4	
89	.333	-.101	279	.107	1.230	18259.9	
89	.333	-.101	279	.110	1.267	18417.6	
89	.333	-.101	279	.130	1.293	18218.1	
89	.333	-.101	157	.108	1.214	12893.3	
89	.333	-.101	157	.170	1.178	12839.9	
89	.333	-.101	157	.173	1.197	13048.7	
89	.333	-.101	157	.166	1.232	12873.5	

AVERAGES

				.181	1.256		.2142
ROLL	RADIUS	HEIGHT	DROPLET DIAMETER MICRONS	VERTICAL VELOCITY	TANGENTIAL VELOCITY	FILM SPEED FR/SEC	VZR FT.IN/SEC
90	.467	-.101	229	.034	1.230	16951.3	
90	.467	-.101	229	0.000	1.255	16931.6	
90	.467	-.101	229	.045	1.215	17034.8	
90	.467	-.101	172	.132	1.261	17373.5	
90	.467	-.101	172	.120	1.281	17343.4	
90	.467	-.101	172	.233	1.209	17174.0	
90	.467	-.101	172	.229	1.256	17303.9	
90	.467	-.101	153	.144	1.245	17618.7	
90	.467	-.101	153	.139	1.181	17420.0	
90	.467	-.101	199	.039	1.329	20849.2	
90	.467	-.101	199	.033	1.234	20788.9	
90	.467	-.101	199	.222	1.243	22016.2	
90	.467	-.101	329	.246	1.218	14266.8	
90	.467	-.101	157	.140	1.216	15095.1	
90	.467	-.101	157	.174	1.214	15037.1	
90	.467	-.101	157	.117	1.233	15066.1	
				AVERAGES			
				.128	1.239		.2123

ROLL	RADIUS	HEIGHT	DROPLET DIAMETER MICRONS	VERTICAL VELOCITY	TANGENTIAL VELOCITY	FILM SPEED FR/SEC	VZR FT.IN/SEC
91	.467	-.101	214	.111	1.226	18787.7	
91	.467	-.101	134	.118	1.191	14781.9	
91	.467	-.101	229	.114	1.247	21480.3	
91	.467	-.101	222	.231	1.190	16990.7	
91	.467	-.101	222	.160	1.139	20761.0	
91	.467	-.101	306	.113	1.216	12784.2	
91	.467	-.101	306	.120	1.240	12904.9	
91	.467	-.101	195	.158	1.253	19234.3	
91	.467	-.101	287	.256	1.294	20071.9	
91	.467	-.101	287	.258	1.224	19837.6	
91	.467	-.101	287	.326	1.265	20127.6	
				AVERAGES			
				.178	1.226		.2960

ROLL	RADIUS	HEIGHT	DROPLET DIAMETER MICRONS	VERTICAL VELOCITY	TANGENTIAL VELOCITY	FILM SPEED FR/SEC	VZR FT.IN/SEC
92	.600	-.101	118	-.258	1.335	21628.8	
92	.600	-.101	229	-.553	1.319	18148.5	
92	.600	-.101	126	-.348	1.322	21860.8	
92	.600	-.101	157	-.290	1.155	17652.0	
92	.600	-.101	241	-.134	1.297	15536.0	
92	.600	-.101	226	-.225	1.251	15396.8	

92	.600	-.101	226	-.330	1.121	21095.1
92	.600	-.101	183	-.280	1.181	16232.0
92	.600	-.101	275	-.254	1.314	14749.4
				AVERAGES		
				-.297	1.255	

-.6333

ROLL	RADIUS	HEIGHT	DROPLET DIAMETER MICRONS	VERTICAL VELOCITY	TANGENTIAL VELOCITY	FILM SPEED FR/SEC
93	.733	-.101	153	-.487	1.198	14700.7
93	.733	-.101	160	-.381	1.353	12484.9
93	.733	-.101	206	-.609	.923	16399.1
93	.733	-.101	149	-.483	1.254	12000.0
93	.733	-.101	176	-.568	1.113	22171.7
93	.733	-.101	176	-.451	1.085	21788.9
93	.733	-.101	172	-.391	1.135	12645.0
93	.733	-.101	172	-.440	1.170	12754.1
93	.733	-.101	191	-.609	.717	9431.6
93	.733	-.101	210	-.332	1.373	17283.1
93	.733	-.101	210	-.319	1.311	17206.5
93	.733	-.101	249	-.290	1.284	19884.0
93	.733	-.101	249	-.407	1.235	19918.8
				AVERAGES		
				-.444	1.166	

VZR FT.IN/SEC: -1.1564

ROLL	RADIUS	HEIGHT	DROPLET DIAMETER MICRONS	VERTICAL VELOCITY	TANGENTIAL VELOCITY	FILM SPEED FR/SEC
94	.867	-.101	191	-.626	.882	1686.8
94	.867	-.101	214	-.989	1.569	15698.4
94	.867	-.101	180	-1.048	1.286	21658.9
94	.867	-.101	122	-.843	1.089	14524.4
94	.867	-.101	229	-1.088	1.092	21598.6
94	.867	-.101	172	-1.268	1.376	12417.6
94	.867	-.101	187	-.645	1.210	20788.9
94	.867	-.101	187	-.732	1.414	11835.3
94	.867	-.101	195	-.737	1.580	20591.6
94	.867	-.101	137	-.497	1.329	12928.1
94	.867	-.101	172	-.372	1.088	19505.8
94	.867	-.101	191	-.446	1.158	13290.0
				AVERAGES		
				-.774	1.256	

VZR FT.IN/SEC: -2.3859

ROLL	RADIUS	HEIGHT	DROPLET DIAMETER MICRONS	VERTICAL VELOCITY	TANGENTIAL VELOCITY	FILM SPEED FR/SEC
95	.867	-.101	195	-.743	1.419	16000.0
95	.867	-.101	218	-.442	1.167	19371.2
95	.867	-.101	222	-.752	1.251	21647.3

95	.867	-.101	226	-.494	1.404	9906.0
95	.867	-.101	229	-.576	1.191	13793.5
95	.867	-.101	199	-.421	1.212	17658.9
95	.867	-.101	245	-.917	1.330	11227.4
95	.867	-.101	210	-.529	1.286	22153.1
				AVERAGES		
				-.609	1.278	

-1.8770

ROLL	RADIUS	HEIGHT	DROPLET DIAMETER MICRONS	VERTICAL VELOCITY	TANGENTIAL VELOCITY	FILM SPEED FR/SEC	VZR FT.IN/SEC
96	1.000	-.101	233	-.732	1.185	18239.0	
96	1.000	-.101	272	-.424	1.118	19740.1	
96	1.000	-.101	168	-.546	1.183	19078.9	
96	1.000	-.101	191	-.985	1.408	20638.1	
96	1.000	-.101	229	-.733	.982	19891.0	
96	1.000	-.101	226	-.691	1.369	19287.7	
96	1.000	-.101	210	-.480	1.329	20348.0	
				AVERAGES			
				-.656	1.225		-2.3317

ROLL	RADIUS	HEIGHT	DROPLET DIAMETER MICRONS	VERTICAL VELOCITY	TANGENTIAL VELOCITY	FILM SPEED FR/SEC	VZR FT.IN/SEC

```
      PROGRAM TST (INPUT,OUTPUT,TAPE5=INPUT,TAPE6=OUTPUT)
C
C     THIS PROGRAM CALCULATES   VERTICAL AND RADIAL FLUID VELOCITIES
C     FROM THE DATA FROM VIEW B RECORDINGS.
C
C
C
000003      NA=33
000004      HTCYC=15.0
000005      RADCYC=1.50
000007      VINLET=4.34
000010      VOVER=2.37
000012      GO TO 15
000013   10 NA=NPOLL
000015   15 WRITE(6,20)
000021   20 FORMAT(//,46X,9HCORRECTED)
000021      WRITE(6,30)
000025   30 FORMAT(29X,7HDROPLET,1X,8HVERTICAL,3X,6HRADIAL,4X,10HCORRECTION,3X
     1,4HFILM)
000025      WRITE(6,40)
000031   40 FORMAT(10X,4HROLL,1X,6HHEIGHT,1X,6HRADIUS,3X,4HSIZE,2X,8HVELOCITY,
     12X,8HVELOCITY,5X,6HDBAR/R,5X,5HSPEED,7X,3HVZR)
000031      WRITE(6,50)
000035   50 FORMAT(29X,7HMICRONS,34X,6HFR/SEC,4X,9HFT.IN/SEC//)
000035   55 READ(5,60) NROLL,HEIGHT,RADCL,RADCOR,PARSIZ,VERT,PICTS,RMD1,D1MD2,
     1NFRAME,FRACT,NBLIP
000071   60 FORMAT(I2,8F6.2,2X,I2,2X,F6.2,2X,I1)
000071      IF(NPOLL.EQ.0) GO TO 77
000072      IF(NROLL.NE.NA) GO TO 10
000074      PARSIZ=(PARSIZ*1000.0)/2.555
000076      NPARSI=PARSIZ
000100      R=RADCL/12.0 + RADCOR/(2.555*304.8)
000104      DELZ=VERT/(2.555*304.8)
000106      BLIP=NBLIP
000107      FRAME=NFRAME
000111      ADDIT=FRACT/4.31
000113      FRAMES=FRAME+ADDIT
000114      FILSPD=FRAMES*1000.0/BLIP
000117      DELTAT=PICTS/FILSPD
000120      D1=R-RMD1/(2.555*304.8)
000123      D2=D1-D1MD2/(2.555*304.8)
000126      DBAR=(D1+D2)/2.0
000131      CORN=DBAR/R
000133      RADVEL=(((D1-D2)/CORN)/DELTAT)/VINLET
000137      VERTV=(DELZ/DELTAT)/VOVER
000142      RADIN=R*12.0/RADCYC
000144      HEIGHT=HEIGHT/HTCYC
000146      VZR=RADIN*VERTV*1.50*2.37
000151      WRITE(6,70) NROLL,HEIGHT,RADIN,NPARSI,VERTV,RADVEL,CORN,FILSPD,VZR
000177   70 FORMAT(10X,I3,1X,F6.3,2X,F6.3,2X,I4,4X,F6.3,3X,F7.4,3X,F10.7,2X,F8
     1.1,5X,F7.4)
000177      NA=NROLL
000201      GO TO 55
000201   77 CONTINUE
000201      STOP
000203      END
```

ROLL	HEIGHT	RADIUS	DROPLET SIZE MICRONS	VERTICAL VELOCITY	CORRECTED RADIAL VELOCITY	CORRECTION DBAR/R	FILM SPEED FR/SEC	VZR FT.IN/SEC
33	-.166	.107	121	1.692	-.0938	.9441217	23587.0	.6412
33	-.166	.083	168	3.225	-.1329	.9225498	23809.7	.9504
33	-.166	.070	211	1.124	-.0477	.7566069	20925.8	.2792
33	-.166	.068	187	.990	-.0434	.6633735	21628.8	.2390
33	-.166	.070	152	1.120	.1895	.6885828	22046.4	.2797
33	-.166	.073	183	1.122	-.1767	.7366086	20703.0	.2908

ROLL	HEIGHT	RADIUS	DROPLET SIZE MICRONS	VERTICAL VELOCITY	CORRECTED RADIAL VELOCITY	CORRECTION DBAR/R	FILM SPEED FR/SEC	VZR FT.IN/SEC
34	-.166	.135	156	.290	.2097	.8107816	20893.3	.1394
34	-.166	.143	252	.319	.0576	.8880067	22000.0	.1624
34	-.166	.135	172	.225	.0317	.8728045	21402.6	.1077
34	-.166	.135	227	.359	-.0179	.8286396	20046.4	.1725

ROLL	HEIGHT	RADIUS	DROPLET SIZE MICRONS	VERTICAL VELOCITY	CORRECTED RADIAL VELOCITY	CORRECTION DBAR/R	FILM SPEED FR/SEC	VZR FT.IN/SEC
35	-.166	.196	270	1.397	.1341	.9735590	20765.7	.9744
35	-.166	.206	176	.663	.0039	.9915123	10359.6	.4850
35	-.166	.198	172	.472	0.0000	.9713975	10730.9	.3317
35	-.166	.205	254	1.388	.0585	.9639804	20777.3	1.0135

ROLL	HEIGHT	RADIUS	DROPLET SIZE MICRONS	VERTICAL VELOCITY	CORRECTED RADIAL VELOCITY	CORRECTION DBAR/R	FILM SPEED FR/SEC	VZR FT.IN/SEC
36	-.166	.273	230	1.010	-.0249	.9887212	20835.3	.9814
36	-.166	.289	191	.618	0.0000	.9818689	19359.6	.6349
36	-.166	.284	195	.606	-.0320	.9642192	20844.5	.6121
36	-.166	.282	223	.608	-.0145	.9761371	21262.2	.6091

ROLL	HEIGHT	RADIUS	DROPLET SIZE MICRONS	VERTICAL VELOCITY	CORRECTED RADIAL VELOCITY	CORRECTION DBAR/R	FILM SPEED FR/SEC	VZR FT.IN/SEC
37	-.166	.589	254	-.593	.0831	.9417029	21647.3	-1.2406
37	-.166	.578	211	-.563	.0430	.9528996	21541.8	-1.1562
37	-.166	.588	250	-.519	.1150	.9482994	14181.0	-1.0844

ROLL	HEIGHT	RADIUS	DROPLET SIZE MICRONS	VERTICAL VELOCITY	CORRECTED RADIAL VELOCITY	CORRECTION DBAR/R	FILM SPEED FR/SEC	VZR FT.IN/SEC
38	-.166	.756	293	-.494	.0653	.9898108	19431.6	-1.3266
38	-.166	.751	360	-.307	.0960	.9657305	18350.3	-.8183
38	-.166	.754	317	-.407	.0490	.9881547	21826.0	-1.0903

ROLL	HEIGHT	RADIUS	DROPLET SIZE MICRONS	VERTICAL VELOCITY	CORRECTED RADIAL VELOCITY	CORRECTION DBAR/R	FILM SPEED FR/SEC	VZR FT.IN/SEC
43	-.135	.082	219	2.892	-.1247	.9541737	17540.6	.8411
43	-.135	.086	219	2.800	-.4193	.8933870	16603.2	.8584
43	-.135	.093	195	2.456	-.1818	.9494219	17949.0	.8156

ROLL	HEIGHT	RADIUS	DROPLET SIZE MICRONS	VERTICAL VELOCITY	CORRECTED RADIAL VELOCITY	CORRECTION DBAR/R	FILM SPEED FR/SEC	VZR FT.IN/SEC
44	-.135	.103	148	1.077	-.0988	.8857251	16909.5	.3939
44	-.135	.188	187	.657	.1559	.9529275	20081.2	.4386
44	-.135	.165	262	.516	.3150	.9336022	21786.5	.3025
44	-.135	.111	125	.769	0.0000	.9852530	16000.0	.3048

ROLL	HEIGHT	RADIUS	DROPLET SIZE MICRONS	VERTICAL VELOCITY	CORRECTED RADIAL VELOCITY	CORRECTION DBAR/R	FILM SPEED FR/SEC	VZR FT.IN/SEC
45	-.135	.181	113	.815	.0851	.9538047	17670.5	.5253
45	-.135	.096	262	2.615	-.1364	.9477193	17473.3	.8952
45	-.135	.172	101	.757	.0696	.9320867	17473.3	.4618
45	-.135	.175	199	.546	.0646	.9638713	17723.9	.3395

ROLL	HEIGHT	RADIUS	DROPLET SIZE MICRONS	VERTICAL VELOCITY	CORRECTED RADIAL VELOCITY	CORRECTION DBAR/R	FILM SPEED FR/SEC	VZR FT.IN/SEC
46	-.135	.183	78	.887	.0247	.9290498	13598.6	.5773
46	-.135	.191	148	1.162	.0485	.9682444	15884.0	.7883
46	-.135	.173	117	.491	.0361	.9676354	21009.3	.3019
46	-.135	.178	187	.712	.0661	.9592471	14918.8	.4500
46	-.135	.095	156	2.351	-.0863	.8471376	20139.2	.7977
46	-.135	.093	129	1.248	-.0190	.9126316	20932.7	.4149

ROLL	HEIGHT	RADIUS	DROPLET SIZE MICRONS	VERTICAL VELOCITY	CORRECTED RADIAL VELOCITY	CORRECTION DBAR/R	FILM SPEED FR/SEC	VZR FT.IN/SEC
47	-.135	.295	168	.859	.0168	.9912889	18770.3	.9007
47	-.135	.180	121	.909	.0641	.9436792	13092.8	.5805
47	-.135	.211	277	1.283	.0161	.9664708	18317.9	.9644
47	-.135	.174	203	.923	.0886	.9487605	14201.9	.5725

ROLL	HEIGHT	RADIUS	DROPLET SIZE MICRONS	VERTICAL VELOCITY	CORRECTED RADIAL VELOCITY	CORRECTION DBAR/R	FILM SPEED FR/SEC	VZR FT.IN/SEC
48	-.135	.423	140	.211	0.0000	.9832274	14735.5	.3165
48	-.135	.393	136	.211	-.0291	.9734977	10568.4	.2953
48	-.135	.384	195	.243	-.0429	.9866305	13547.6	.3314
48	-.135	.321	223	.571	0.0000	.9907196	14301.6	.6521
48	-.135	.306	191	.616	.0243	.9684018	13895.6	.6689
48	-.135	.289	203	.827	.0201	.9772149	12371.2	.8484

ROLL	HEIGHT	RADIUS	DROPLET SIZE MICRONS	VERTICAL VELOCITY	CORRECTED RADIAL VELOCITY	CORRECTION DBAR/R	FILM SPEED FR/SEC	VZR FT.IN/SEC
49	-.135	.417	121	.187	-.0067	.9797894	17633.4	.2772
49	-.135	.486	86	.158	.0106	.9885745	17025.5	.2720
49	-.135	.530	187	.080	.0707	.9921516	8435.0	.1507

ROLL	HEIGHT	RADIUS	DROPLET SIZE MICRONS	VERTICAL VELOCITY	CORRECTED RADIAL VELOCITY	CORRECTION DBAR/R	FILM SPEED FR/SEC	VZR FT.IN/SEC
50	-.135	.642	152	-.106	.0036	.9875274	14440.8	-.2420
50	-.135	.764	238	-.634	.0697	.9835905	18545.2	-1.7221
50	-.135	.794	203	-.180	.0968	.9747661	15301.6	-.5069

ROLL	HEIGHT	RADIUS	DROPLET SIZE MICRONS	VERTICAL VELOCITY	CORRECTED RADIAL VELOCITY	CORRECTION DBAR/R	FILM SPEED FR/SEC	VZR FT.IN/SEC
55	-.200	.087	172	3.251	-.1564	.9028823	24000.0	1.0085
55	-.200	.101	254	1.888	-.0983	.8665632	21573.1	.6794
55	-.200	.145	172	.784	0.0000	.8651990	17030.2	.4037

CORRECTED

ROLL	HEIGHT	RADIUS	DROPLET SIZE MICRONS	VERTICAL VELOCITY	RADIAL VELOCITY	CORRECTION DBAR/R	FILM SPEED FR/SEC	VZR FT.IN/SEC
56	-.200	.094	273	1.949	-.1293	.9260041	21039.4	.6540
56	-.200	.163	191	.891	.0754	.9179746	18109.0	.5178
56	-.200	.159	176	.752	.0552	.9300505	20823.7	.4241

ROLL	HEIGHT	RADIUS	DROPLET SIZE MICRONS	VERTICAL VELOCITY	CORRECTED RADIAL VELOCITY	CORRECTION DBAR/R	FILM SPEED FR/SEC	VZR FT.IN/SEC
57	-.200	.055	180	1.236	-.0904	.8711376	22051.0	.2417
57	-.200	.056	250	1.220	-.1706	.9205414	16672.9	.2440
57	-.200	.129	156	.316	.0213	.8582720	21949.0	.1453

ROLL	HEIGHT	RADIUS	DROPLET SIZE MICRONS	VERTICAL VELOCITY	CORRECTED RADIAL VELOCITY	CORRECTION DBAR/R	FILM SPEED FR/SEC	VZR FT.IN/SEC
58	-.200	.176	199	.971	.0404	.9413974	21631.1	.6078
58	-.200	.165	156	.335	.0440	.9029815	21505.8	.1967
58	-.200	.151	164	.286	.0562	.8900159	19735.5	.1541
58	-.200	.239	336	.269	.0582	.9136870	19823.7	.2278

ROLL	HEIGHT	RADIUS	DROPLET SIZE MICRONS	VERTICAL VELOCITY	CORRECTED RADIAL VELOCITY	CORRECTION DBAR/R	FILM SPEED FR/SEC	VZR FT.IN/SEC
59	-.200	.107	195	1.469	-.1603	.9691544	20997.7	.5567
59	-.200	.163	234	.922	.0500	.9687189	21824.8	.5330
59	-.200	.147	277	.551	.0334	.9397938	21236.7	.2876
59	-.200	.252	207	.911	-.0042	.9739034	22129.9	.8155
59	-.200	.184	199	.943	.0542	.9555475	22111.4	.6162
59	-.200	.209	125	1.180	.0347	.9818398	21842.2	.8778

ROLL	HEIGHT	RADIUS	DROPLET SIZE MICRONS	VERTICAL VELOCITY	CORRECTED RADIAL VELOCITY	CORRECTION DBAR/R	FILM SPEED FR/SEC	VZR FT.IN/SEC
60	-.200	.270	230	.695	-.0450	.9781023	22032.5	.6668
60	-.200	.308	121	.483	-.0688	.9731295	22182.1	.5287
60	-.200	.306	187	.438	-.0818	.9733029	21897.9	.4758
60	-.200	.362	238	.133	-.0012	.9689437	22124.1	.1709
60	-.200	.396	117	.126	-.0048	.9732804	22141.5	.1779
60	-.200	.429	180	-.097	-.0127	.9705520	21466.4	-.1478

ROLL	HEIGHT	RADIUS	DROPLET SIZE MICRONS	VERTICAL VELOCITY	CORRECTED RADIAL VELOCITY	CORRECTION DBAR/R	FILM SPEED FR/SEC	VZR FT.IN/SEC
61	-.200	.635	121	-.617	.1587	.9827634	18329.5	-1.3912
61	-.200	.587	207	-.074	.0224	.9777649	21548.7	-.1541
61	-.200	.689	140	-.514	.0978	.9885969	21078.9	-1.2591

ROLL	HEIGHT	RADIUS	DROPLET SIZE MICRONS	VERTICAL VELOCITY	CORRECTED RADIAL VELOCITY	CORRECTION DBAR/R	FILM SPEED FR/SEC	VZR FT.IN/SEC
66	-.234	.073	191	2.478	0.0000	.9142638	21522.0	.6438
66	-.234	.071	180	1.485	0.0000	.9567402	22187.9	.3761
66	-.234	.150	207	.703	.0051	.9162385	44322.5	.3756
66	-.234	.069	234	2.007	-.1763	.9703037	21018.6	.4937

ROLL	HEIGHT	RADIUS	DROPLET SIZE MICRONS	VERTICAL VELOCITY	CORRECTED RADIAL VELOCITY	CORRECTION DBAR/R	FILM SPEED FR/SEC	VZR FT.IN/SEC
67	-.234	.151	227	.724	.0057	.9450091	21972.2	.3896
67	-.234	.152	266	.710	.0550	.9442179	22157.8	.3836
67	-.234	.164	332	.740	-.0290	.9640843	21018.6	.4328
67	-.234	.175	258	.980	.0805	.9281918	17501.2	.6081
67	-.234	.135	195	.439	.0472	.8961311	22227.4	.2113

ROLL	HEIGHT	RADIUS	DROPLET SIZE MICRONS	VERTICAL VELOCITY	CORRECTED RADIAL VELOCITY	CORRECTION DBAR/R	FILM SPEED FR/SEC	VZR FT.IN/SEC
68	-.234	.168	219	.910	.0226	.9554186	21917.6	.5444
68	-.234	.139	117	.774	0.0000	.9261150	22222.7	.3826
68	-.234	.191	254	.980	-.0172	.9540682	22215.8	.6663
68	-.234	.151	176	.521	.0861	.9000992	22232.0	.2788
68	-.234	.144	152	.483	.0980	.9064360	21841.1	.2480

ROLL	HEIGHT	RADIUS	DROPLET SIZE MICRONS	VERTICAL VELOCITY	CORRECTED RADIAL VELOCITY	CORRECTION DBAR/R	FILM SPEED FR/SEC	VZR FT.IN/SEC
70	-.234	.282	191	.576	-.0232	.9768284	21252.9	.5762
70	-.234	.199	152	1.084	.0570	.9768211	21044.1	.7685
70	-.234	.169	230	.945	.0465	.9673865	20280.7	.5661
70	-.234	.173	203	.814	.0527	.9711897	21851.5	.5004
70	-.234	.146	348	.371	-.0289	.9344805	18236.7	.1921

ROLL	HEIGHT	RADIUS	DROPLET SIZE MICRONS	VERTICAL VELOCITY	CORRECTED RADIAL VELOCITY	CORRECTION DBAR/R	FILM SPEED FR/SEC	VZR FT.IN/SEC
71	-.234	.211	125	1.064	.0157	.9753761	20679.8	.7972
71	-.234	.268	105	.522	-.0291	.9800449	22039.4	.4972
71	-.234	.323	195	.239	-.0207	.9858499	22027.8	.2741
71	-.234	.352	273	.154	-.0798	.9625239	22139.2	.1924
71	-.234	.405	305	0.000	.0312	.9757728	21244.8	0.0000
71	-.234	.427	109	-.057	.0658	.9570278	21522.0	-.0866
71	-.234	.373	74	.029	-.0071	.9323404	21471.0	.0386

ROLL	HEIGHT	RADIUS	DROPLET SIZE MICRONS	VERTICAL VELOCITY	CORRECTED RADIAL VELOCITY	CORRECTION DBAR/R	FILM SPEED FR/SEC	VZR FT.IN/SEC
72	-.234	.390	121	.026	.0107	.9560327	20649.7	.0356
72	-.234	.404	238	.054	.0359	.9420330	21940.8	.0783
72	-.234	.508	234	-.038	.0157	.9637965	21844.5	-.0685
72	-.234	.454	121	.088	.0210	.9694520	22052.2	.1426
72	-.234	.513	172	-.060	.0299	.9415565	21777.3	-.1090
72	-.234	.525	152	-.027	.0178	.9735930	21838.2	-.0513

ROLL	HEIGHT	RADIUS	DROPLET SIZE MICRONS	VERTICAL VELOCITY	CORRECTED RADIAL VELOCITY	CORRECTION DBAR/R	FILM SPEED FR/SEC	VZR FT.IN/SEC
73	-.234	.576	234	-.075	.0213	.9634105	22179.8	-.1537
73	-.234	.623	129	-.261	.0389	.9877219	21192.6	-.5788
73	-.234	.617	140	-.198	.0416	.9727759	22222.7	-.4338

ROLL	HEIGHT	RADIUS	DROPLET SIZE MICRONS	VERTICAL VELOCITY	CORRECTED RADIAL VELOCITY	CORRECTION DBAR/R	FILM SPEED FR/SEC	VZR FT.IN/SEC
78	-.067	.458	156	-.258	-.1280	.9722897	21196.1	-.4205
78	-.067	.525	234	-.921	-.0321	.9872869	21392.1	-1.7205
78	-.067	.530	144	-.722	.0118	.9791821	18690.3	-1.3606
78	-.067	.560	230	-1.085	.0418	.9839444	21408.4	-2.1585

ROLL	HEIGHT	RADIUS	DROPLET SIZE MICRONS	VERTICAL VELOCITY	CORRECTED RADIAL VELOCITY	CORRECTION DBAR/R	FILM SPEED FR/SEC	VZR FT.IN/SEC
79	-.067	.522	156	-.103	.0062	.9716355	16280.7	-.1901
79	-.067	.573	133	-.310	.0165	.9849456	20283.1	-.6321

79	-.067	.529	183	-.386	.0148	.9856360	17540.6	-.7264
79	-.067	.644	250	-.162	.0307	.9759844	16482.6	-.3705

ROLL	HEIGHT	RADIUS	DROPLET SIZE MICRONS	VERTICAL VELOCITY	CORRECTED RADIAL VELOCITY	CORRECTION DBAR/R	FILM SPEED FR/SEC	VZR FT.IN/SEC
80	-.067	.661	238	-.121	.0143	.9922260	15386.7	-.2845
80	-.067	.634	140	-.263	.0154	.9816096	21211.1	-.5921
80	-.067	.661	152	-.245	.0204	.9881058	16512.8	-.5753

ROLL	HEIGHT	RADIUS	DROPLET SIZE MICRONS	VERTICAL VELOCITY	CORRECTED RADIAL VELOCITY	CORRECTION DBAR/R	FILM SPEED FR/SEC	VZR FT.IN/SEC
85	-.101	.176	258	.584	.1103	.9364050	12037.1	.3654
85	-.101	.201	183	1.274	0.0000	.9744111	20146.2	.9090
85	-.101	.184	168	1.071	.0520	.9453726	18473.3	.7016
85	-.101	.199	211	.563	-.1335	.9520858	13742.5	.3991
85	-.101	.219	238	1.207	-.0667	.9784540	22048.7	.9407
85	-.101	.067	219	1.595	-.1322	.9664107	23552.2	.3815
85	-.101	.105	227	1.067	-.0609	.9568615	23626.5	.3974
85	-.101	.088	277	3.260	-.1325	.9415184	22997.7	1.0180
85	-.101	.187	191	.826	-.0429	.9654600	16793.5	.5505

ROLL	HEIGHT	RADIUS	DROPLET SIZE MICRONS	VERTICAL VELOCITY	CORRECTED RADIAL VELOCITY	CORRECTION DBAR/R	FILM SPEED FR/SEC	VZR FT.IN/SEC
86	-.101	.170	156	.467	-.1305	.8837026	15090.5	.2814
86	-.101	.245	191	1.333	.0492	.9697979	12907.2	1.1606
86	-.101	.302	187	1.553	-.0320	.9920094	15942.0	1.6680
86	-.101	.126	242	.409	-.4369	.9305522	10993.0	.1830
86	-.101	.206	219	1.246	-.0525	.9972622	15721.6	.9140
86	-.101	.187	230	.962	-.0897	.9928451	16373.5	.6384

ROLL	HEIGHT	RADIUS	DROPLET SIZE MICRONS	VERTICAL VELOCITY	CORRECTED RADIAL VELOCITY	CORRECTION DBAR/R	FILM SPEED FR/SEC	VZR FT.IN/SEC
87	-.101	.310	187	.802	-.0531	.9756050	11118.3	.8824
87	-.101	.173	309	.410	-.0466	.9598671	8645.0	.2517
87	-.101	.211	219	.937	.0183	.9666652	13628.8	.7031
87	-.101	.314	273	.917	-.0327	.9906890	13473.3	1.0251
87	-.101	.200	195	.923	-.0372	.9856182	10607.9	.6564
87	-.101	.322	367	.808	0.0000	.9936243	8343.4	.9257

CORRECTED

ROLL	HEIGHT	RADIUS	DROPLET SIZE MICRONS	VERTICAL VELOCITY	RADIAL VELOCITY	CORRECTION DBAR/R	FILM SPEED FR/SEC	VZR FT.IN/SEC
88	-.101	.326	305	.550	.0144	.9814168	14324.8	.6374
88	-.101	.297	180	.735	.0174	.9866686	13229.7	.7749
88	-.101	.199	254	1.172	.1074	.9767431	14178.7	.8278
88	-.101	.197	168	1.342	.0658	.9597682	9148.5	.9383
88	-.101	.176	277	.693	-.1169	.9763422	18812.1	.4333
88	-.101	.155	254	.427	-.0764	.9442198	18747.1	.2346

ROLL	HEIGHT	RADIUS	DROPLET SIZE MICRONS	VERTICAL VELOCITY	CORRECTED RADIAL VELOCITY	CORRECTION DBAR/R	FILM SPEED FR/SEC	VZR FT.IN/SEC
89	-.101	.275	176	.796	.0241	.9895243	12921.1	.7773
89	-.101	.324	270	.779	.0550	.9852561	13946.6	.8975
89	-.101	.347	199	.493	-.0441	.9766123	10921.1	.6083
89	-.101	.367	183	.367	.0692	.9959405	17749.4	.4783
89	-.101	.426	172	.119	.0330	.9759885	13382.8	.1806

ROLL	HEIGHT	RADIUS	DROPLET SIZE MICRONS	VERTICAL VELOCITY	CORRECTED RADIAL VELOCITY	CORRECTION DBAR/R	FILM SPEED FR/SEC	VZR FT.IN/SEC
90	-.101	.429	180	.237	.0466	.9789463	17617.2	.3612
90	-.101	.447	144	.195	-.0502	.9706815	19170.5	.3093
90	-.101	.519	277	.205	0.0000	.9814001	9422.3	.3792
90	-.101	.566	148	.076	.0074	.9861257	16510.4	.1531
90	-.101	.507	203	.273	.0134	.9809554	15742.5	.4925

ROLL	HEIGHT	RADIUS	DROPLET SIZE MICRONS	VERTICAL VELOCITY	CORRECTED RADIAL VELOCITY	CORRECTION DBAR/R	FILM SPEED FR/SEC	VZR FT.IN/SEC
91	-.101	.471	168	.246	.0305	.9938968	17542.9	.4114
91	-.101	.618	309	.114	-.0157	.9756353	12858.5	.2507
91	-.101	.595	117	.114	.0224	.9904208	12436.2	.2406
91	-.101	.546	187	.279	0.0000	.9962369	12000.0	.5416
91	-.101	.458	168	.132	.0111	.9500986	12000.0	.2150

ROLL	HEIGHT	RADIUS	DROPLET SIZE MICRONS	VERTICAL VELOCITY	CORRECTED RADIAL VELOCITY	CORRECTION DBAR/R	FILM SPEED FR/SEC	VZR FT.IN/SEC
92	-.101	.558	191	.161	-.0403	.9858240	21496.5	.3201
92	-.101	.589	187	.240	-.0372	.9866602	16204.2	.5028
92	-.101	.702	129	-.108	.0159	.9752661	19698.4	-.2705

92	-.101	.651	180	.086	-.0054	.9903797	21791.2	.1994
92	-.101	.616	305	.258	.0060	.9815610	17229.7	.5640
92	-.101	.663	211	.152	.0168	.9845099	18201.9	.3595

ROLL	HEIGHT	RADIUS	DROPLET SIZE MICRONS	VERTICAL VELOCITY	CORRECTED RADIAL VELOCITY	CORRECTION DBAR/R	FILM SPEED FR/SEC	VZR FT. IN/SEC
93	-.101	.714	270	-.402	.0065	.9894240	17387.5	-1.0195
93	-.101	.699	195	-.169	.0262	.9831684	14162.4	-.4190
93	-.101	.745	121	-.078	.0173	.9871153	17865.4	-.2057
93	-.101	.718	117	-.192	.0157	.9861880	16345.7	-.4896

A3.2 Power Law Representation of Tangential Velocity Profiles

As discussed in section I, the tangential velocity, v_e, at distances away from the central axis, is proportional to $1/r^n$ for cyclones operating with an air core.

To test the above relationship for a cyclone operating without an air core, plots of $\log(v_e)$ versus $\log(r)$ were prepared for the five runs where the relationship could possibly apply. It has been shown, as discussed in section I, that close to the central axis a transition occurs in the tangential velocity. For this reason the data at $r < 0.10$ in. was not used in the plots in Figures A3-1 and A3-2.

The slope, n, was determined by the least square method of fitting straight lines. The values of n are 0.122, 0.229, 0.334, 0.300 and 0.217 for the vertical locations of $z^+ = -0.100, -0.135, -0.166, -0.200$ and -0.234 respectively.

Figure-A3-1

Log(v_θ) versus Log(r)

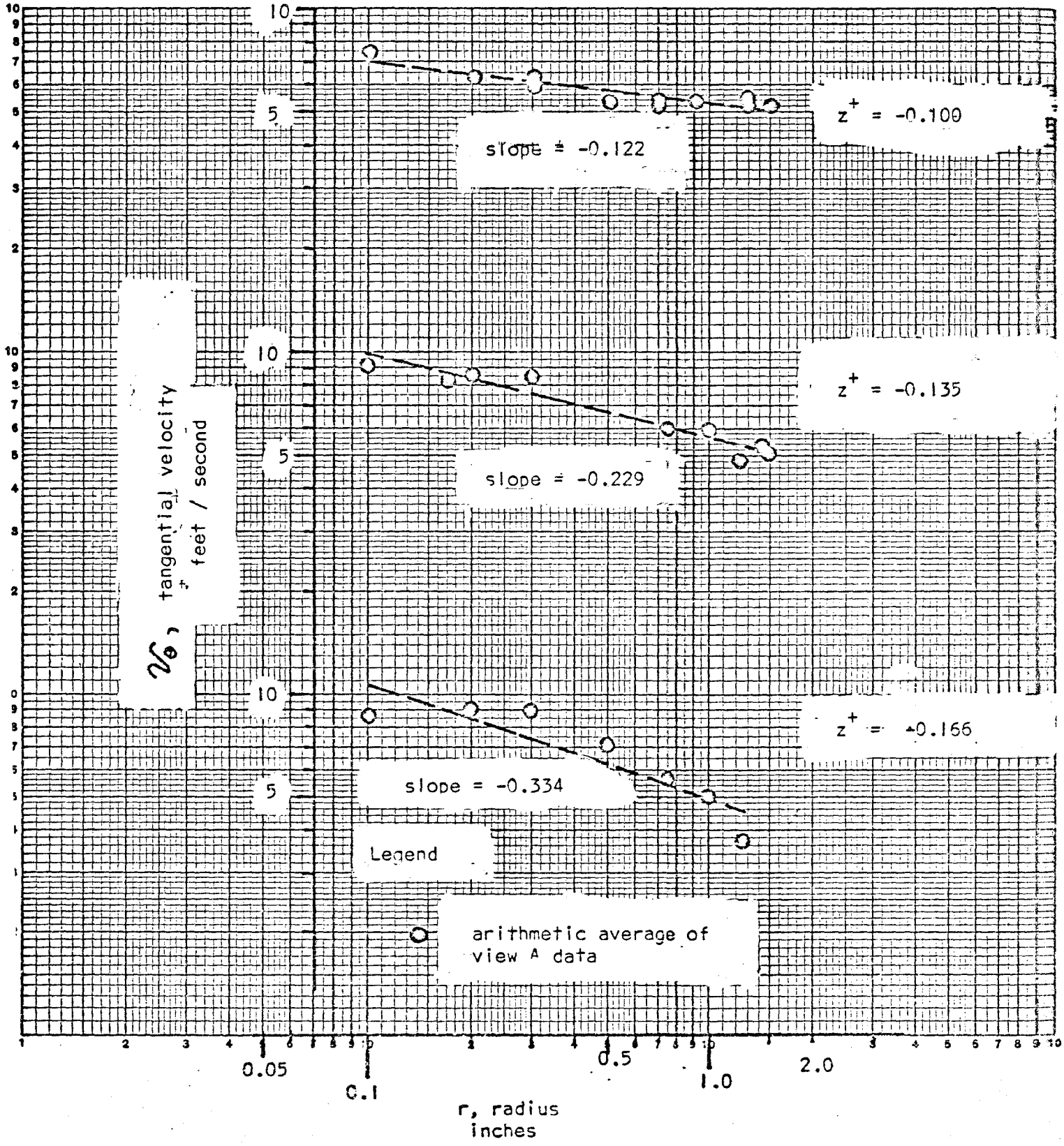

Figure-A3-2

Log(v_θ) versus Log(r)

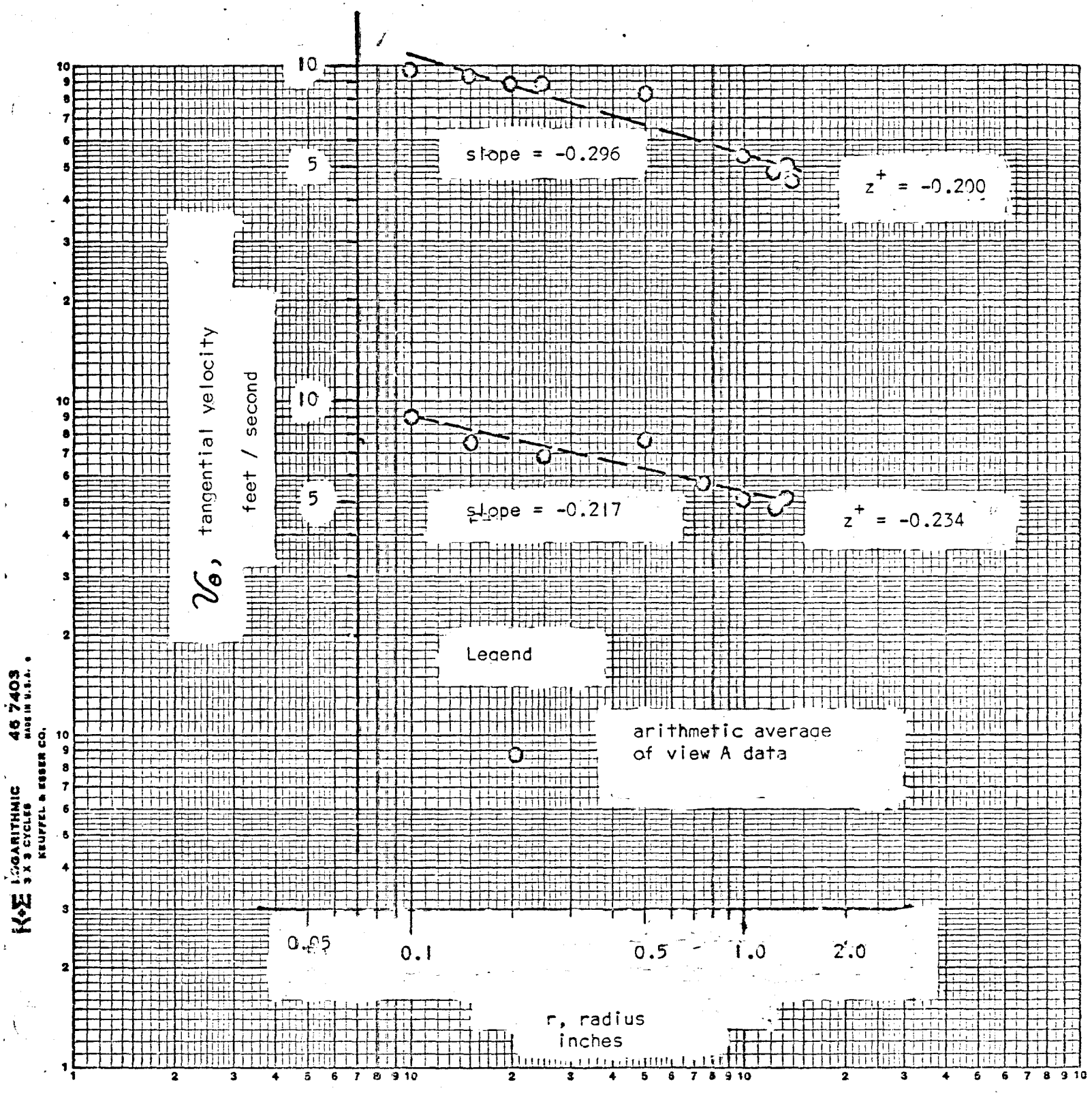

K+E LOGARITHMIC 46 7403
3 X 3 CYCLES MADE IN U.S.A.
KEUFFEL & ESSER CO.

A3.3 Vertical Velocity Integrations

The integrations were carried out using the curves in Figures 13 and 14.

At intervals of $r^+ = 0.05$, v_z^+ was determined and the $v_z^+ . r^+$ product calculated. This procedure was done for each of the six values of z^+. Table-A3-1 lists the results. The resulting dimensionles areas, proportional to the two vertical flows at each elevation are shown at the bottom of Table-A3-1. These areas were calculated using the trapazoidal rule. The areas were converted to flows in USGPM by using the conversion,

$$USGPM = area(2\pi)\langle v_z \rangle_2 (R)^2 (449 USGPM/ft^3/sec),$$

which has its basis in Equations (11) and (12). The converted flow rates are are given in Table-6 in section 3.

Table-A3-1

$v_z^+.r^+$ Values at All Vertical Elevations *

r^+ \ z^+ =	-0.067	-0.100	-0.134	-0.166	-0.200	-0.234
0.05		0.05	0.09	0.071	0.07	0.08
0.10		0.03	0.108	0.113	0.109	0.108
0.15		0.0315	0.120	0.138	0.125	0.129
0.20		0.232	0.122	0.154	0.136	0.134
0.25		0.308	0.125	0.158	0.133	0.130
0.30		0.246	0.120	0.150	0.126	0.114
0.35		0.165	0.105	0.130	0.109	0.105
0.40		0.125	0.0864	0.100	0.092	0.084
0.45	-0.108	0.113	0.081	0.0625	0.0675	0.0585
0.50	-0.195	0.120	0.060	0.0300	0.0400	0.0250
0.55	-0.270	0.110	0.044	-0.0165	0.0055	-0.0165
0.60	-0.348	0.072	0.0300	-0.0600	-0.0360	-0.0600
0.65	-0.403	-0.0975	0.0065	-0.104	-0.0780	-0.104
0.70	-0.434	-0.259	-0.0021	-0.140	-0.133	-0.154
0.75	-0.435	-0.353	-0.0675	-0.165	-0.180	-0.203
0.80	-0.456	-0.456	-0.0120	-0.192	-0.232	-0.248
0.85	-0.475	-0.561	-0.176	-0.230	-0.272	-0.289
0.90	-0.513	-0.630	-0.288	-0.261	-0.306	-0.324
0.95	-0.561	-0.665	-0.456	-0.295		
1.00	-0.670	-0.660	-0.470			
+ area	-	0.0794	0.0545	0.0553	0.0505	0.0481
- area	0.226	0.166	0.0672	0.0706	0.0648	0.0616

*Note: $v_z^+.r^+ = 0.00$ at all elevations for $r^+ = 0.00$

A3.4 Calculation of Radial Velocities from Vertical Velocity Data

The calculation of the radial velocities from the vertical velocity curves in Figures 13 and 14 involved using an r-z material balance and the assumption that the Flow was symmetric the central axis.

The area representing a small vertical flow segment, A_z is shown in Fig.A3-3. This area is converted to the flow, Q_z by

$$Q_z = 2\pi R^2 A_z \langle v_z \rangle_2.$$

This conversion has its basis in Equations (11 and(12). The area of each flow segment was calculated from the data in Table-A3-1, that is, an interval of $r^+ = 0.05$ was chosen. The individual areas were considered to be trapazoids. The areas are listed in Table-A3-2.

Using the assumption of circular symmetry, an r-z material balance between z_1^+ and z_2^+ shows the net radial flow is

$$Q_z\Big|_{z_1^+} - Q_z\Big|_{z_2^+}.$$

The area for this Flow, shown in Figure-A3-3 is $2\pi\bar{r}\Delta z$. Δz was chosen as 1.0 inch. The radial velocity at $\bar{z}^+$ and $\bar{r}^+$ is then

$$V_r = \frac{Q_z\Big|_{z_1^+} - Q_z\Big|_{z_2^+}}{2\pi\bar{r}\,\Delta z}$$

where $\bar{r}^+$ and $\bar{z}^+$ are the (arithmetic) average values of z and v as shown in Figure-A3-3.

Radial velocity profiles were determined using the above equation at $z^+ = -0.101$, -0.134, -0.166 and -0.200. The profiles at $z^+ = -0.067$ and -0.234 were not calculated as this would require extrapolation of the $v_z^+.r^+$ versus z^+ data and no criterion for extrapolation was available.

The calculated values of v_r presented in Table-A3-3, are also displayed in Figure-16 where they are compared with the experimental values.

Figure-A3-3

Calculation of Radial Velocities From Vertical Velocity Data

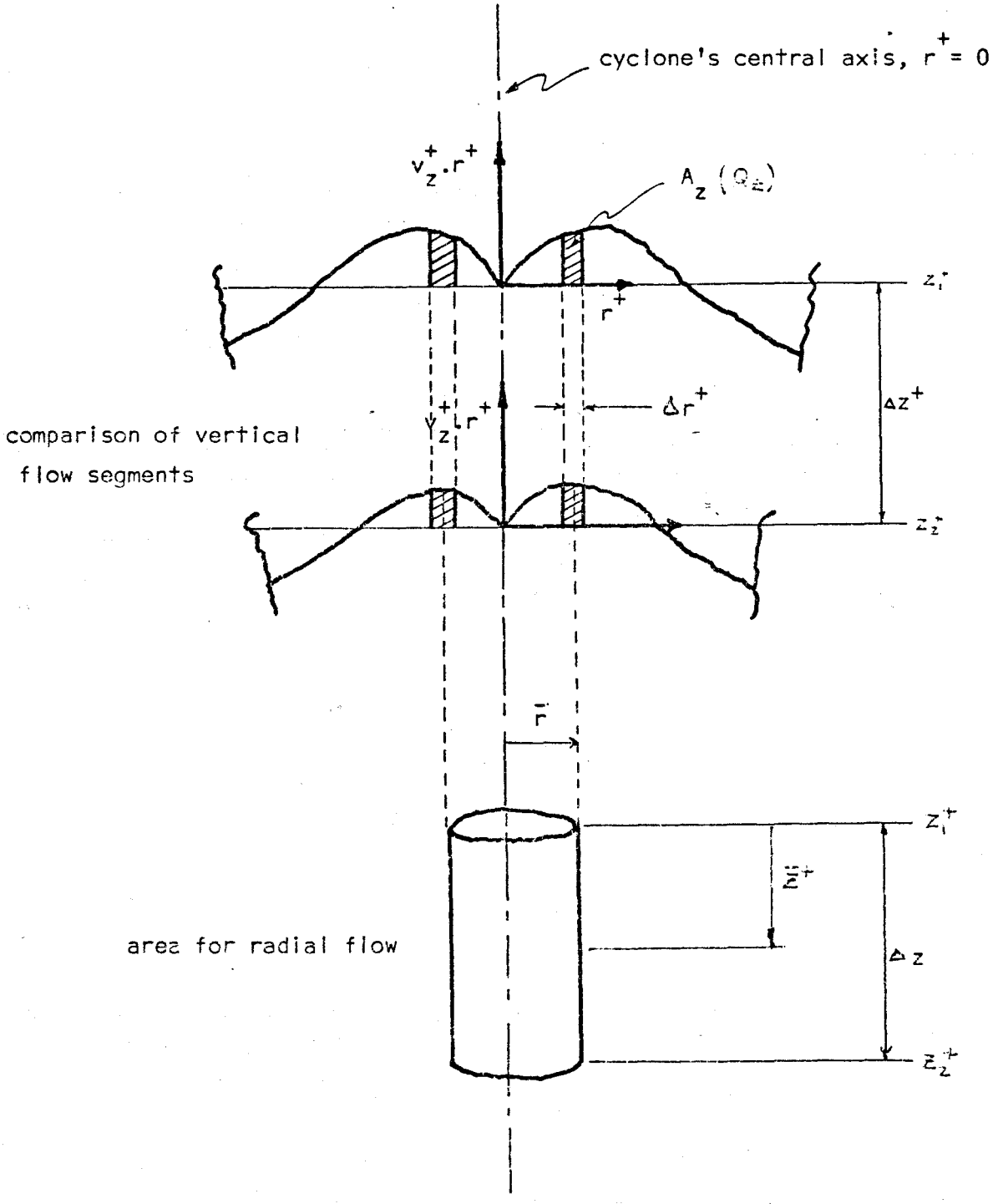

Table-A3-2

Vertical Flow Segments (areas)

$\bar{r}^+$ \ z^+ =	-0.067	-0.101	-0.134	-0.166	-0.200	-0.234
0.025		0.001250	0.002250	0.001775	0.001750	0.00200
0.075		0.00200	0.004950	0.004600	0.004475	0.004700
0.125		0.001538	0.005700	0.006275	0.005850	0.005925
0.175		0.006588	0.006050	0.007300	0.006525	0.006575
0.225		0.01350	0.006150	0.007800	0.006725	0.006600
0.275		0.01385	0.006150	0.007700	0.006100	0.005875
0.325		0.01028	0.005625	0.007000	0.005475	0.004550
0.375		0.007250	0.004725	0.005750	0.004725	0.002925
0.425		0.005950	0.004425	0.004063	0.003563	0.001225
0.475	-0.00758	0.005825	0.003525	0.002438	0.002088	-0.000525
0.525	-0.01163	0.005750	0.002600	0.000338	-0.000213	-0.002538
0.575	-0.01545	0.004550	0.001850	-0.001913	-0.001913	-0.004388
0.625	-0.01878	-0.0006375	0.000913	-0.004100	-0.004100	-0.006325
0.675	-0.02093	-0.008913	0.000111	-0.006100	-0.006450	-0.008625
0.725	-0.02173	-0.01530	-0.001740	-0.007625	-0.008925	-0.01053
0.775	-0.02228	-0.02023	-0.004688	-0.008925	-0.01128	-0.01203
0.825	-0.02328	-0.02543	-0.007400	-0.01055	-0.01343	-0.01363
0.875	-0.02470	-0.02978	-0.011600	-0.01228	-0.01533	-0.01510
0.925	-0.02685	-0.03238	-0.018600	-0.01390		
0.975	-0.03078	-0.03313	-0.02315			

Table-A3-3

Calculated Radial Velocities

feet / second

r^+ \ z^+ =	-0.101	-0.134	-0.166	-0.200
0.025		-0.0743	0.0708	-0.0319
0.075		-0.123	0.0224	-0.00472
0.125		-0.134	-0.00425	0.00991
0.175		-0.0144	-0.00961	0.0147
0.225		0.0897	-0.00905	0.0189
0.275		0.0747	-0.000644	0.0235
0.325		0.0357	0.00163	0.0267
0.375		0.0142	0.0	0.0267
0.425		0.0157	0.00718	0.0236
0.475	0.0842	0.0252	0.0107	0.0221
0.525	0.0252	0.0365	0.0190	0.0194
0.575	0.0209	0.0398	0.0232	0.0152
0.625	0.112	0.0196	0.0181	0.0126
0.675	0.110	0.0148	0.0344	0.0132
0.725	0.0490	0.0375	0.0351	0.0142
0.775	0.0805	0.0516	0.0301	0.0142
0.825	0.0684	0.0639	0.0259	0.0132
0.875	0.0530	0.0708	0.0151	0.0114
0.925	0.0310	0.0707		
0.975	0.0276			

Appendix A4

Calibrations

A4.1 Rotating Scale Screen Calibration

In order to relate the distance an image moved on the screen to the distance a droplet moved inside the hydrocyclone, it was necessary to calibrate the screen which was maintained at a fixed distance from the projector.

A transparent scale, divided into millimetre divisions, was attached to a thin plumbline (thread) which was hung along the centerline of the cyclone. Figure-A4-1 shows the arrangement used to view the scale.

The scale was set in motion by rotating the plumbline gently. Three rotations were then photographed using one prism at a time. The prisms wwere used separately in order to calibrate each view. When viewing the resulting film on a screen, the distance between two divisions was measured every few frames. The distance between these two divisions rose to a maximum and then decreased. At the maximum position, the plane of the scale was parallel to the face of the prism under consideration.

The actual distance between the two divisions mentioned above is 2.0 mm. The distance on the screen between these two divisions was measured in screen units (S.U.).(One screen unit is equal to 0.5 inch).Screen units were used in all film analysis, so that conversion factors in screen units/mm. were required for each view.

The conversion factors are given in Figures A4-2 and A4-3 which shows the results of the calibration procedure mentioned above. The calibrations were observed to be reproducible to within 0.2%.

Figure-A4-1

Rotating Scale Screen Calibration

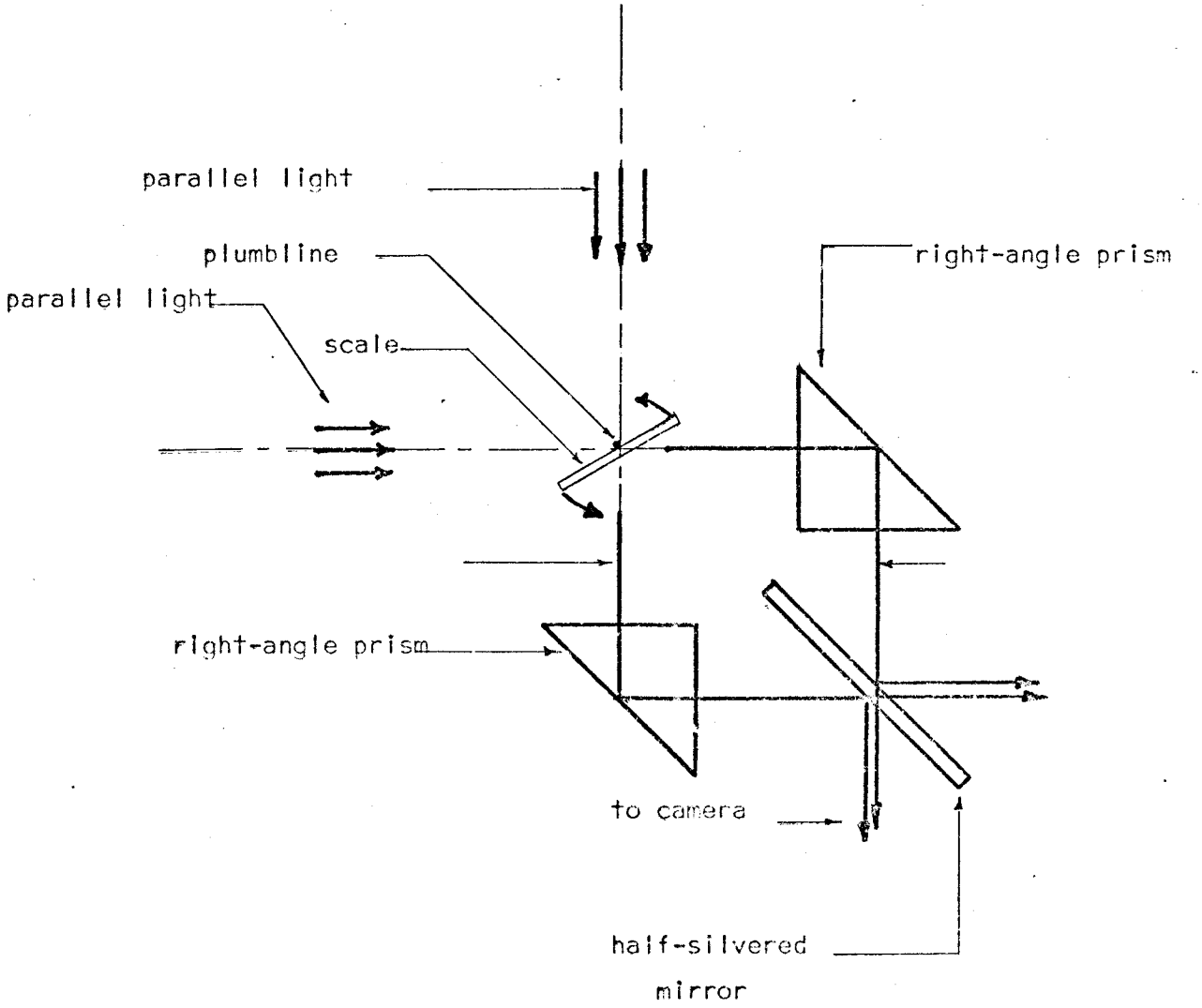

Figure-A4-2

View A Screen Calibration

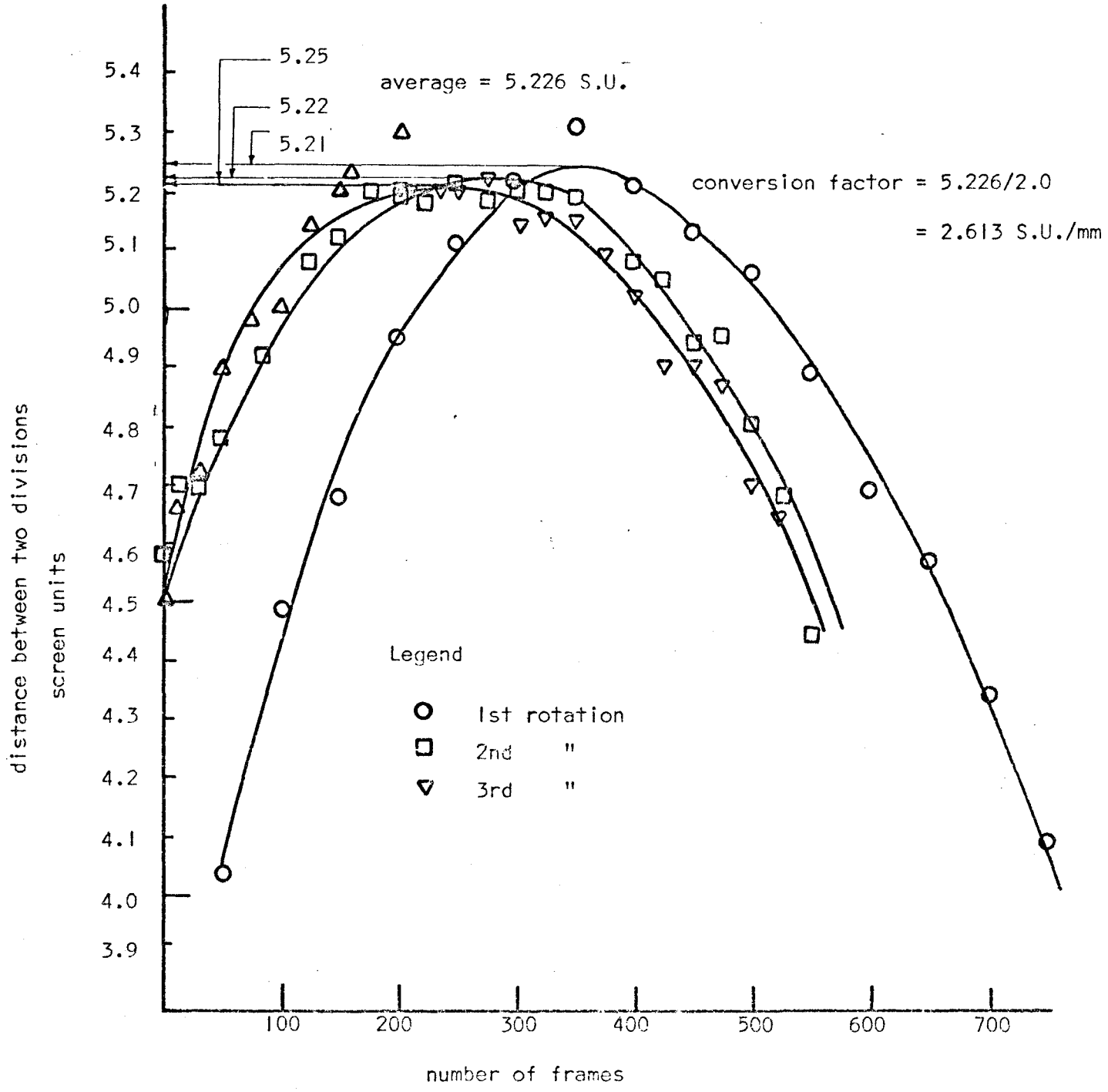

Figure-A4-3

View B Screen Calibration

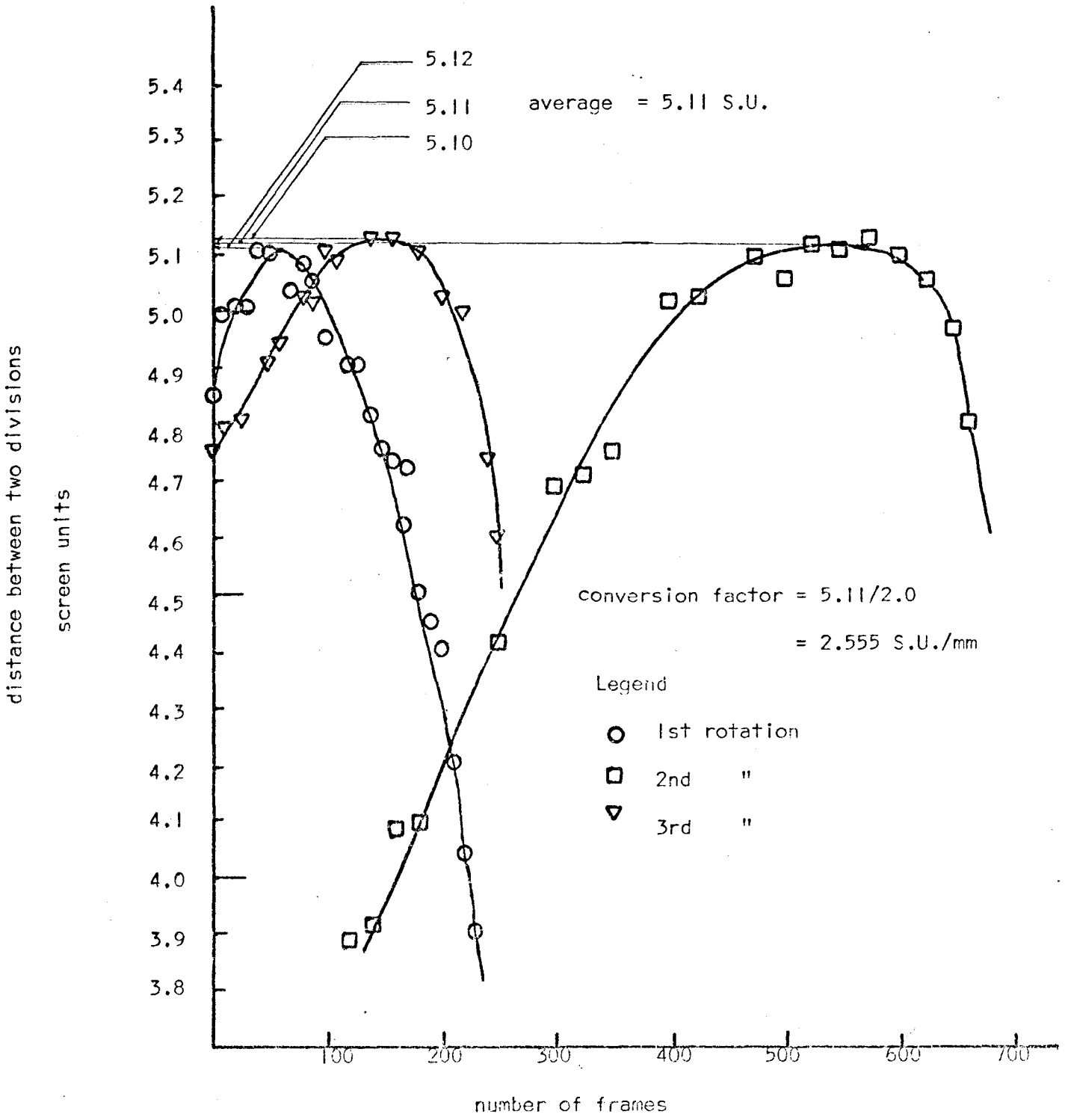

A4.2 Pulse Generator Calibration

The signal from the pulse generator was analyzed on an oscilloscope to find the time between successive peaks. The results are shown below. They indicated that no adjustment to the pulse generator was required.

Frequency of Pulse Generator Signal cycles/second	Time Between Successive Peaks milliseconds
1000	1.0
100	10.0

A4.3 Rotameter Calibrations

The feed and overflow rotameters were calibrated by the author by weighing volumes of water collected in a known time. The flowrates were computed in USGPM and the calibrations shown in Figures A4-4 and A4-5 prepared.

Figure-A4-4

Feed Rotameter Calibration

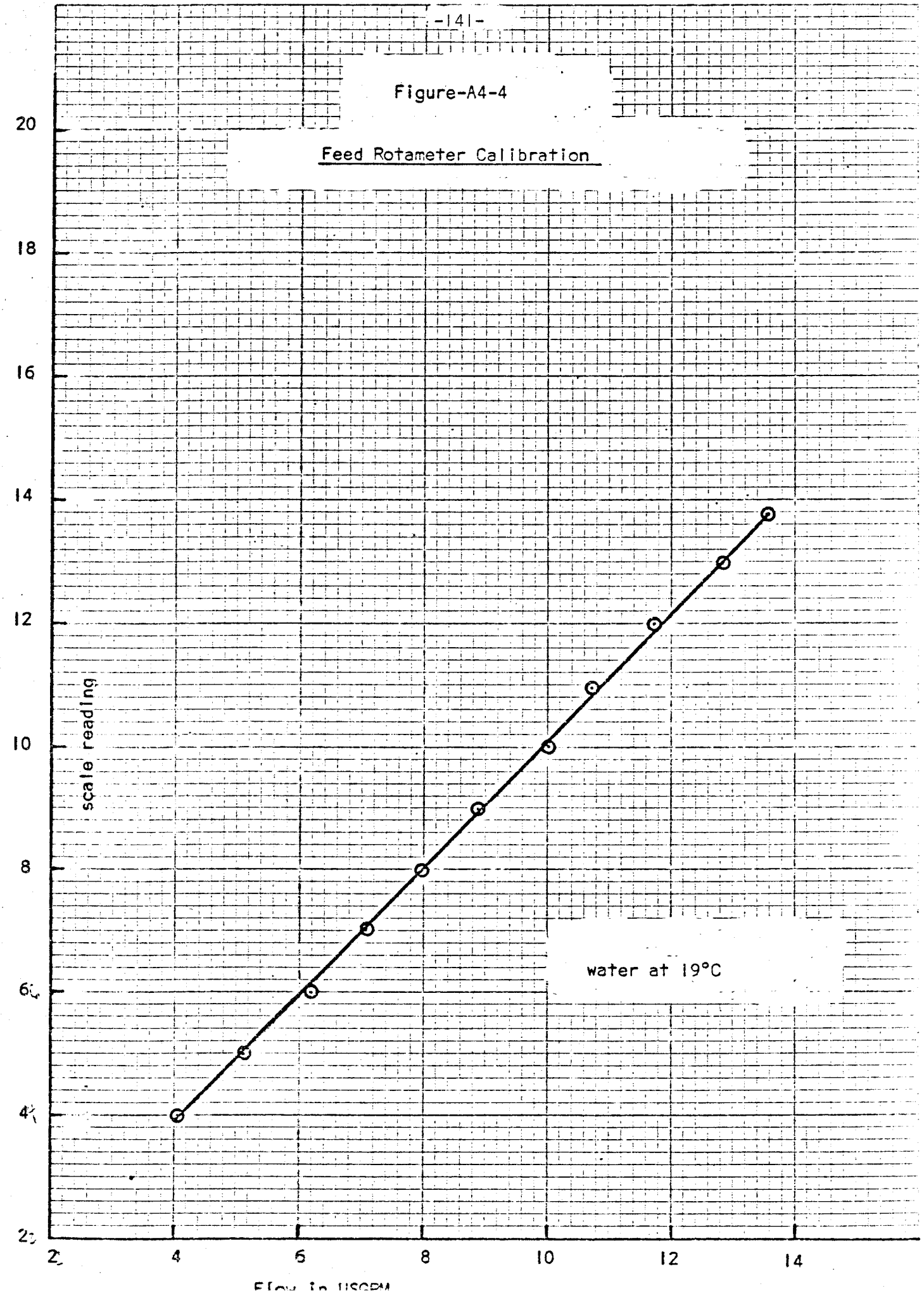

Figure-A4-5

Overflow Rotameter Calibration

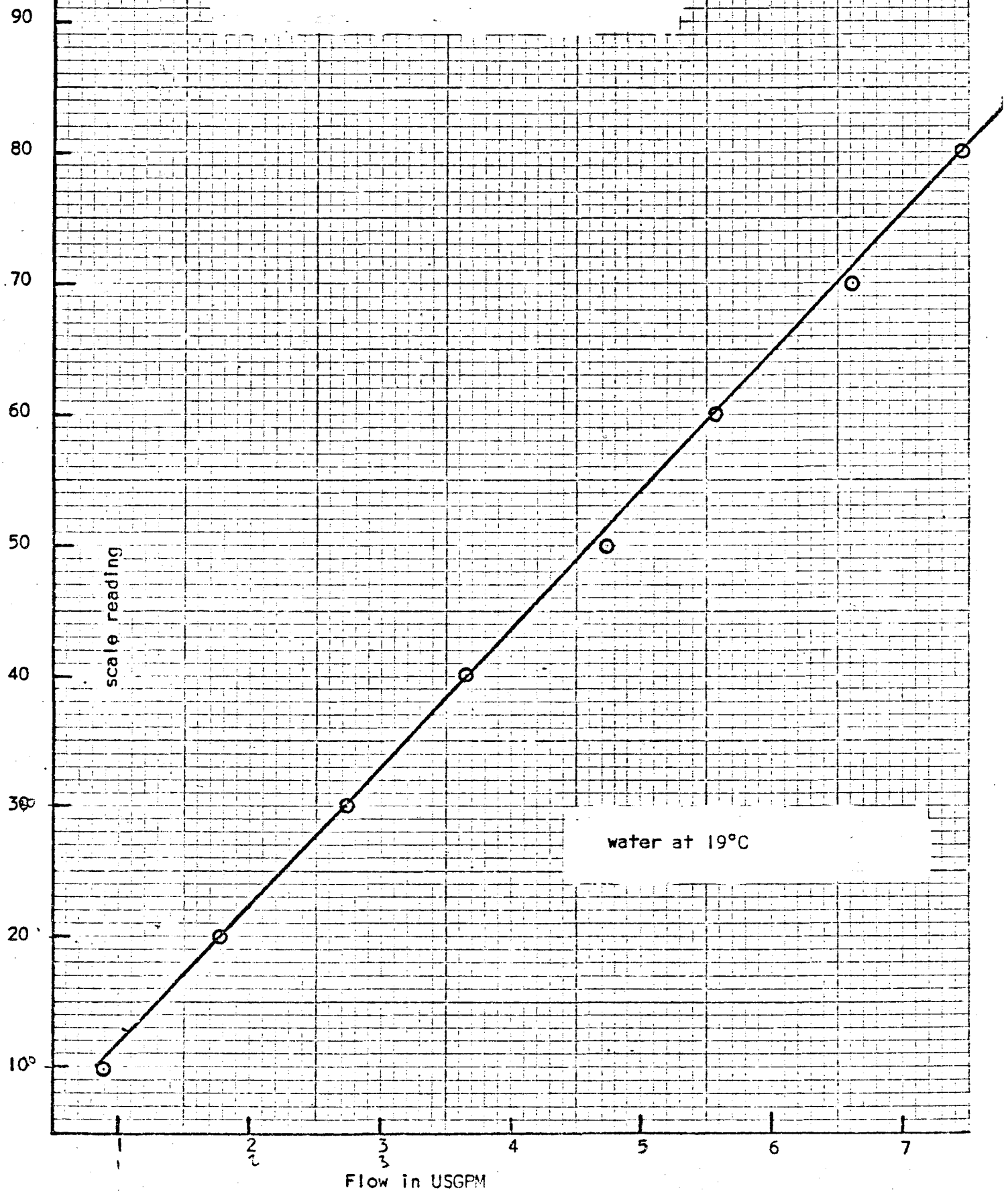

A4.4 Camera Characteristics

The characteristics presented in Figure-A4-6 have been provided by the manufacturer. Only the curve for model number K20SIBE is pertinent in this study.

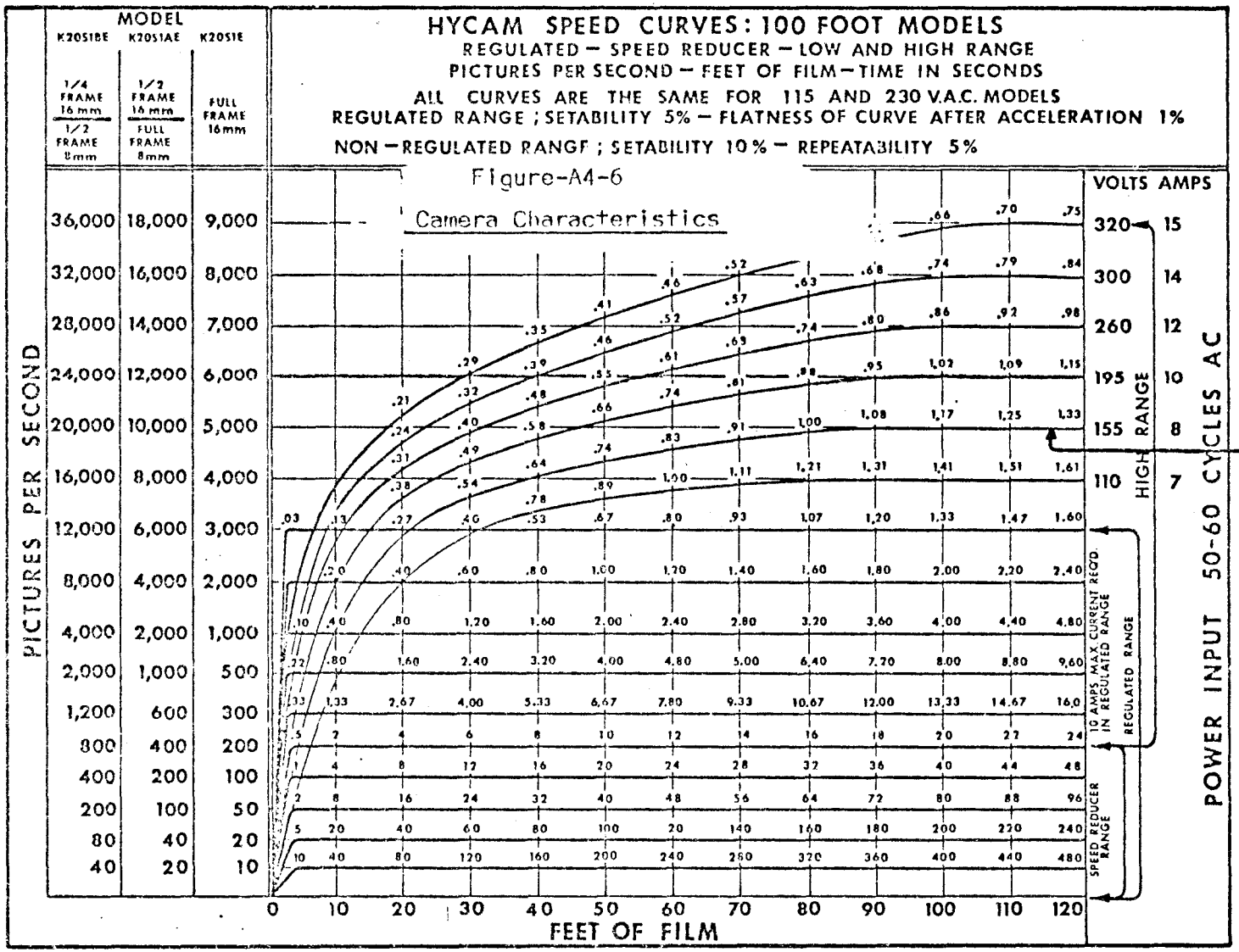

Red Lake Laboratories, Inc.
PHOTO INSTRUMENTATION EQUIPMENT
Products the User Likes
2971 CORVIN DRIVE
KIFER INDUSTRIAL PARK
SANTA CLARA, CALIFORNIA 95051
TELEPHONE (408)–739-3034
TWX 910-339-9241